The Slumgullion Earth Flow: A Large-Scale Natural Laboratory

U.S. GEOLOGICAL SURVEY BULLETIN 2130

AVAILABILITY OF BOOKS AND MAPS OF THE U.S. GEOLOGICAL SURVEY

Instructions on ordering publications of the U.S. Geological Survey, along with prices of the last offerings, are given in the current-year issues of the monthly catalog "New Publications of the U.S. Geological Survey." Prices of available U.S. Geological Survey publications released prior to the current year are listed in the most recent annual "Price and Availability List." Publications that may be listed in various U.S. Geological Survey catalogs (**see back inside cover**) but not listed in the most recent annual "Price and Availability List" may no longer be available.

Reports released through the NTIS may be obtained by writing to the National Technical Information Service, U.S. Department of Commerce, Springfield, VA 22161; please include NTIS report number with inquiry.

Order U.S. Geological Survey publications **by mail** or **over the counter** from the offices listed below.

BY MAIL

Books

Professional Papers, Bulletins, Water-Supply Papers, Techniques of Water-Resources Investigations, Circulars, publications of general interest (such as leaflets, pamphlets, booklets), single copies of Earthquakes & Volcanoes, Preliminary Determination of Epicenters, and some miscellaneous reports, including some of the foregoing series that have gone out of print at the Superintendent of Documents, are obtainable by mail from

U.S. Geological Survey, Information Services
Box 25286, Federal Center
Denver, CO 80225

Subscriptions to periodicals (Earthquakes & Volcanoes and Preliminary Determination of Epicenters) can be obtained ONLY from the

Superintendent of Documents
Government Printing Office
Washington, DC 20402

(Check or money order must be payable to Superintendent of Documents.)

Maps

For maps, address mail orders to

U.S. Geological Survey, Information Services
Box 25286, Federal Center
Denver, CO 80225

Residents of Alaska may order maps from

U.S. Geological Survey, Earth Science Information Center
101 Twelfth Ave., Box 12
Fairbanks, AK 99701

OVER THE COUNTER

Books and Maps

Books and maps of the U.S. Geological Survey are available over the counter at the following U.S. Geological Survey offices, all of which are authorized agents of the Superintendent of Documents.

- **ANCHORAGE, Alaska**–Rm. 101, 4230 University Dr.
- **LAKEWOOD, Colorado**–Federal Center, Bldg. 810
- **MENLO PARK, California**–Bldg. 3, Rm. 3128, 345 Middlefield Rd.
- **RESTON, Virginia**–USGS National Center, Rm. 1C402, 12201 Sunrise Valley Dr.
- **SALT LAKE CITY, Utah**–Federal Bldg., Rm. 8105, 125 South State St.
- **SPOKANE, Washington**–U.S. Post Office Bldg., Rm. 135, West 904 Riverside Ave.
- **WASHINGTON, D.C.**–Main Interior Bldg., Rm. 2650, 18th and C Sts., NW.

Maps Only

Maps may be purchased over the counter at the following U.S. Geological Survey offices:

- **FAIRBANKS, Alaska**–New Federal Bldg, 101 Twelfth Ave.
- **ROLLA, Missouri**–1400 Independence Rd.
- **STENNIS SPACE CENTER, Mississippi**–Bldg. 3101

The Slumgullion Earth Flow: A Large-Scale Natural Laboratory

Edited by D.J. Varnes *and* W.Z. Savage

U.S. GEOLOGICAL SURVEY BULLETIN 2130

UNITED STATES GOVERNMENT PRINTING OFFICE, WASHINGTON : 1996

U.S. DEPARTMENT OF THE INTERIOR
BRUCE BABBITT, Secretary

U.S. GEOLOGICAL SURVEY
Gordon P. Eaton, Director

For sale by U.S. Geological Survey, Information Services
Box 25286, Federal Center
Denver, CO 80225

Library of Congress Cataloging-in-Publication Data

The Slumgullion earth flow : A large-scale natural laboratory / edited by D.J. Varnes and W.Z. Savage.
p. cm. — (U.S. Geological Survey bulletin ; 2130)
Summaries of presentations at a meeting held in Golden, Colo., Jan. 26–27, 1994.
Includes bibliographical references.
Supt. of Docs. no.: I 19.2:2130
1. Earth flows—Colorado—Lake City Region. I. Varnes, David J. (David Joseph), 1919– . II. Savage, William Z. III. Series.
QE75.B9 no. 2130
[QE599.U5]
557.3 s—dc20
[551.3'07] 95–32788
CIP

CONTENTS

INTRODUCTION

By D.J. Varnes *and* W.Z. Savage

In 1990, the U.S. Geological Survey (USGS), with the assistance of scientists provided by a cooperative agreement between the USGS and the Istituto di Ricerca per la Protezione Idrogeologica (IRPI) of the Italian National Research Council, began a new study of the Slumgullion earth flow in the San Juan Mountains near Lake City, Colo. This famous landslide (figs. 1 and 2) has been described by numerous investigators (Endlich, 1876; Howe, 1909; Atwood and Mather, 1932; Burbank, 1947; Crandell and Varnes, 1960, 1961; Keefer and Johnson, 1983). It was chosen for a comprehensive study of landslide processes because part of it apparently has been moving continuously for the past 300 yr, transporting material hundreds of meters and repeatedly creating and destroying surface features such as folds and faults. Also, movement data have been collected periodically on the flow for more than 30 yr.

The Slumgullion earth flow occurs in altered Tertiary volcanic rocks and consists of a younger, active, upper part that moves on and over an older, much larger, inactive part. Based on radiocarbon and tree-ring dating, the younger, active part is about 300 yr old. The older, inactive part, which dammed the Lake Fork of the Gunnison River creating Lake San Cristobal, is about 700 yr old (Crandell and Varnes, 1960, 1961). The entire landslide is 6.8 km long and has an estimated volume of 170×10^6 m^3. The active part of the landslide is 3.9 km long and has an estimated volume of 20×10^6 m^3 (Parise and Guzzi, 1992).

On January 26–27, 1994, a meeting of many of the study participants was held in Golden, Colo., to review the progress of ongoing investigations. This Bulletin summarizes the presentations given at this meeting.

The first six chapters are concerned with the geological aspects of our investigations. Chapter 1 summarizes the chronology of the Slumgullion slide and presents some additional background on local surficial geology. This chapter is part of a larger study aimed at understanding geologic and climatic controls on landsliding and evaluating the interrelations between earth-flow movement and late Holocene climatic change. Chapter 2 presents the results of detailed field studies on the kinematics of the active part of the earth flow. The kinematic investigations are fundamental to understanding slide movement and determining what information about flow processes within the slide can be obtained from the study of features at the ground surface. Chapters 3 and 4 contain the results of field studies on the geology of the main scarp of the Slumgullion landslide and its retreat. As part of these studies, photogrammetric measurements are being made to establish the rate of retreat of the main scarp of the slide. These studies are of interest, because the main scarp provided material for the older, inactive slide and still provides material for the newer, active slide. Chapter 5 presents the results of recent field investigations of a newly identified Slumgullion landslide deposit. This deposit, which may be the result of a "spill-over" of Slumgullion landslide material, may be critical to understanding the slide's early history. Chapter 6 pertains to the 700-yr-old natural dam formed by the toe of the inactive slide. The continued stability of this dam, which created Lake San Cristobal, is of great importance to Lake City and the surrounding area.

Chapters 7 through 10 describe surveying, photogrammetric, and modeling efforts to understand movements in the newer and older parts of the Slumgullion earth flow. Chapter 7 discusses control and deformation surveys carried out on the landslide. The control surveys have established a coordinate system for all Slumgulllion studies, particularly the photogrammetric measurement of surface movement discussed in chapters 8 and 9. These measurements are the first to be done here, not only by standard analog and analytical photogrammetric methods, but also by a newly developed digital method. Aerial photographs were obtained in 1985 and 1990, precise survey control was established for the 1990 photography, and the same ground control was applied to the 1985 photography. As part of the deformation surveys discussed in chapter 7, leveling is being done to detect vertical movements in the inactive part of the earth flow in front of the advancing active toe.

The levelling work is of importance because, as mentioned previously, the Slumgullion earth flow consists of two parts, a lower, older inactive part and an upper, younger active part. The upper part is overriding the older part along a 40-m-high bulging and raveling front. The lower, older part is crossed by State Highway 149 connecting Lake City

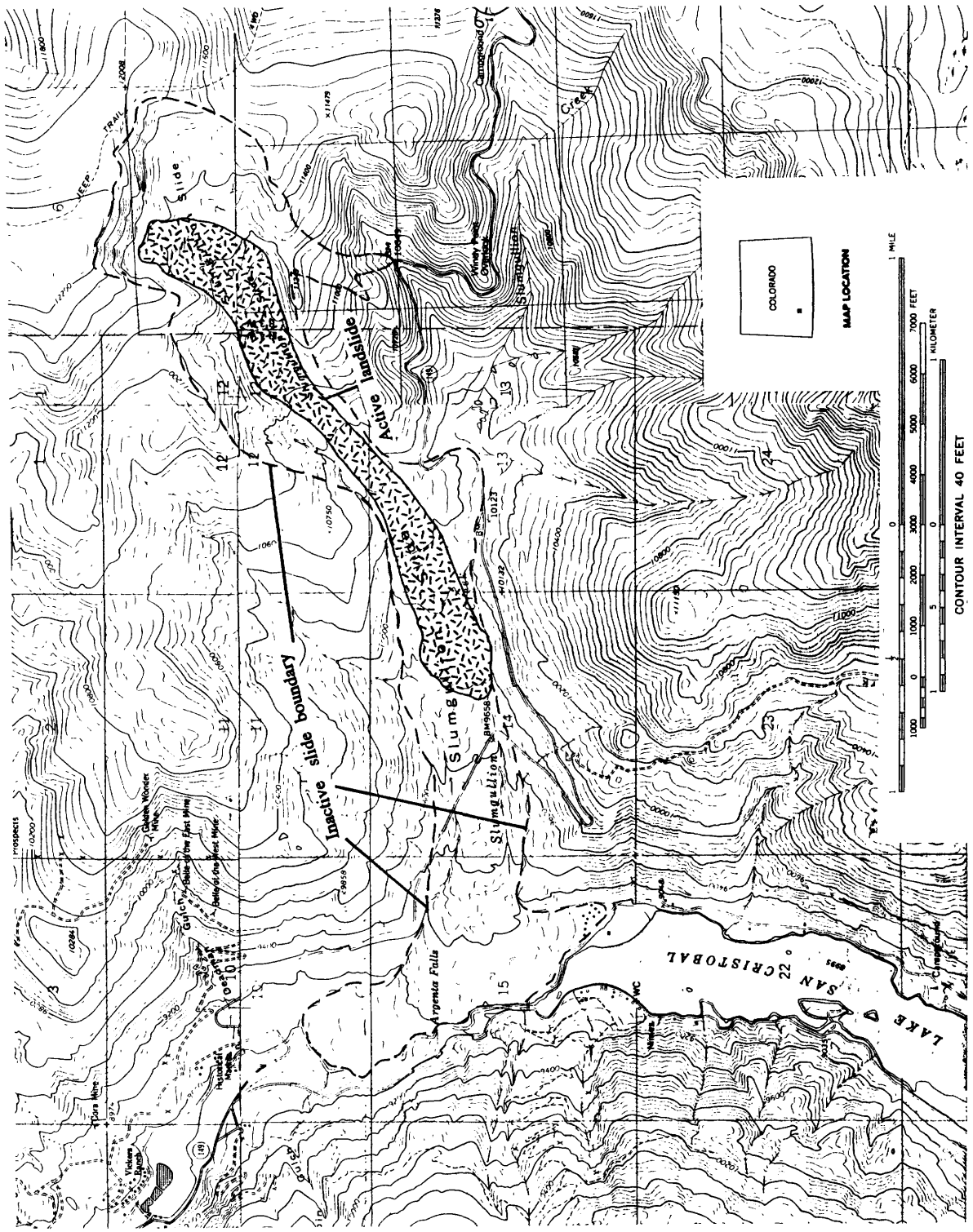

Figure 1. Topographic map and location of the Slumgullion earth flow.

Figure 2. Slumgullion earth flow. Lake San Cristobal is at lower right. The inactive landslide extends from the lake uphill to the active toe. Active toe is prominent light-colored bulge uphill from where Colorado State Highway 149 crosses the earth flow. Active flow extends from active toe to prominent main scarp at top of photograph.

and Creede, Colo., and is increasingly occupied by condominiums and other structures near Lake San Cristobal. We have assumed that the older slide mass is stable, but there is no direct evidence for stability other than verticality of trees on the older slide mass and absence of major distress on the highway. However, as will be described in chapter 7, the surcharge of the active part is causing minor deformation in older material at and near the base of the active front. The most general deformation is depression, which seems to decrease away from the active front. Because we do not know how far ahead of the advancing active front the effects of the surcharge may eventually be felt, or at what rate deformation over large areas, if any, is occurring, a theoretical model to supplement intermittent field measurements and to predict this deformation was developed. This model is described in chapter 10.

The remaining five chapters discuss the geophysical and geotechnical aspects of the Slumgullion research effort. Chapter 11 reports the geotechnical properties of materials collected from the surface of the landslide, and chapter 12 describes studies of fault creep at various locations on the slide using modified tide-gage wire extensometers. Chapter 13 records the seismic reflection and refraction survey that established the position of the base of the inactive slide in the area below the active toe. Chapter 14 describes measurements of fault creep and slidequakes along a major strike-slip fault bounding the active slide. This work supports the hypothesis that processes involved in landslide faulting are in many ways analogous to those that operate in crustal-scale faulting. Chapter 15 concerns an experiment conducted to measure horizontal velocities at a number of points on and off the slide using the Global Positioning System (GPS). This work confirms that modern GPS technology may permit the rapid assessment of velocity fields at the landslide surface.

Upon the completion of the studies reviewed here, further geotechnical, geophysical, and hydrologic studies will be made at selected sites on the earth flow to collect material-property data and ground-water flow data needed for quantitative models of earth-flow movement. The material-property data will include drained and undrained strengths and rheological parameters of the soils in the earth flow. Ground-water flow data will initially be collected from observation of stream levels, ponds, and seeps, and later from observation wells and piezometers.

Finally, the kinematic, geophysical, geotechnical, and hydrological data collected at the Slumgullion earth flow will be combined into quantitative models for hillslope stability. The objective of these studies is to develop better models for evaluation of slope stability, which then can be tested directly at the Slumgullion earth flow, a large-scale natural laboratory.

REFERENCES CITED

Atwood, W.W., and Mather, K.F., 1932, Physiography and Quaternary geology of the San Juan Mountains, Colorado: U.S. Geological Survey Professional Paper 166, 176 p.

Burbank, W.S., 1947, Lake City area, Hinsdale County, *in* Mineral Resources of Colorado: Colorado Mineral Resources Board, p. 439–443.

Crandell, D.R., and Varnes, D.J., 1960, Slumgullion earthflow and earthslide near Lake City, Colorado [abs.]: Geological Society of America Bulletin, v. 71, no. 12, pt. 2, p. 1846.

———1961, Movement of the Slumgullion earthflow near Lake City, Colorado, *in* Short Papers in the Geologic and Hydrologic Sciences: U.S. Geological Survey Professional Paper 424–B, p. B136–B139.

Endlich, F.M., 1876, Report of F.M. Endlich, *in* U.S. Geological and Geographical Survey (Hayden) of the Territories, Annual Report 1874, 203 p.

Howe, E., 1909, Landslides in the San Juan Mountains, Colorado: U.S. Geological Survey Professional Paper 67, 58 p.

Keefer, D.K., and Johnson, A.M., 1983, Earth flows: Morphology, mobilization, and movement: U.S. Geological Survey Professional Paper 1264, 56 p.

Parise, M., and Guzzi, R., 1992, Volume and shape of the active and inactive parts of the Slumgullion landslide, Hinsdale County, Colorado: U.S. Geological Survey Open-File Report 92-216, 29 p.

CHAPTER 1

PRELIMINARY CHRONOLOGY OF THE SLUMGULLION LANDSLIDE, HINSDALE COUNTY, COLORADO

By Richard F. Madole

INTRODUCTION

Twice during late Holocene time, large landslides (earth flows) dammed the Lake Fork Gunnison River in the San Juan Mountains near Lake City, Colo. (fig. 1). The river has since cut through the landslide deposits and into sediment of the pre-slide valley floor. Radiocarbon ages of wood from the base of the landslide deposits and soil humus from beneath the deposits show that the unnamed landslide at the north edge of Lake City dammed the Lake Fork about 3.5 ka and that the Slumgullion landslide probably dammed the Lake Fork between 0.9 and 0.8 ka (table 1). The lake that formed about 3.5 ka was apparently much shorter lived than Lake San Cristobal because lake deposits in the Lake City area are sparse. It probably lasted only as long as it took for water to overtop the low point on the landslide toe, which was near the east valley wall (fig. 1).

The Slumgullion landslide is the largest earth flow in the Lake City area and, on the basis of photogeologic analysis, appears to be the only one that includes continuously moving material. The size, complexity, accessibility, continued movement of the active part, and the many opportunities it offers for obtaining chronologic data are the reasons this landslide was selected for study. The study is part of a larger investigation aimed at understanding the geologic and climatic controls on landsliding and the distribution of landsliding in space and time. The following discussion is a progress report on efforts to reconstruct the history of the Slumgullion landslide.

SLUMGULLION LANDSLIDE STRATIGRAPHY

Landslide deposits of at least three different ages can be distinguished at Slumgullion on the basis of morphology, stratigraphy, and the differences in degree of weathering and soil formation (fig. 2). The few available radiocarbon ages indicate that all three landslide units are late Holocene (defined here as 3.5–0 ka).

The oldest landslide unit is distinguished by its position above or beyond the limits of the two younger units and by a greater degree of weathering and soil formation (fig. 3). The oldest unit is recognized only in the upper part of the slide area, where it forms flank ridges and lobes that are as much as 30 m higher than the flank ridges that bound the younger units. In most places, the soil developed in the oldest landslide unit has a B horizon, whereas the soils developed in the younger two units lack B horizons or, at most, show only incipient development of B-horizon characteristics in the form of slight color changes. Cambic horizons (Bw) are characteristic of the soils developed in the oldest unit (fig. 3).

Cambic B horizons are distinguished by the development of color or soil structure, or both, with little or no apparent accumulation of illuvial material (Soil Survey Staff, 1981). In the Slumgullion landslide deposits, the Bw horizon is defined both by soil structure and color. The Bw horizon has moderate, fine to medium blocky subangular structure and typically is light yellowish brown to yellowish brown (10YR 6/4 to 5/4, dry), whereas the C horizon (parent material) is structureless and typically brownish yellow (10YR 6/6, dry).

Soils developed in the oldest landslide unit also are thicker than those in the younger landslide units (fig. 3) and, in places, have incipient E horizons (also called A2 horizons in some classifications). The E horizons are distinguished by their gray color, which actually is grayish brown to brown (10YR 5/2–5/3) but looks gray because of the darker colors of the bounding horizons. The E horizon is lighter in color than the overlying A horizon because it has less organic matter. The E horizon is lighter than the underlying B horizon, mainly because coatings of organic matter and compounds of iron and aluminum on mineral grains have been removed and translocated from the E to the B horizon.

The radiocarbon age of the oldest wood found beneath deposits of the middle unit provides a minimum age of about 1.1 ka for the oldest landslide unit (fig. 4). Chleborad (1993 and this volume) describes deposits of the oldest unit on the upland south of the upper part of the main slide path. These deposits contain wood that yielded four radiocarbon ages ranging from 1,630±50 to 1,130±60 yr B.P.

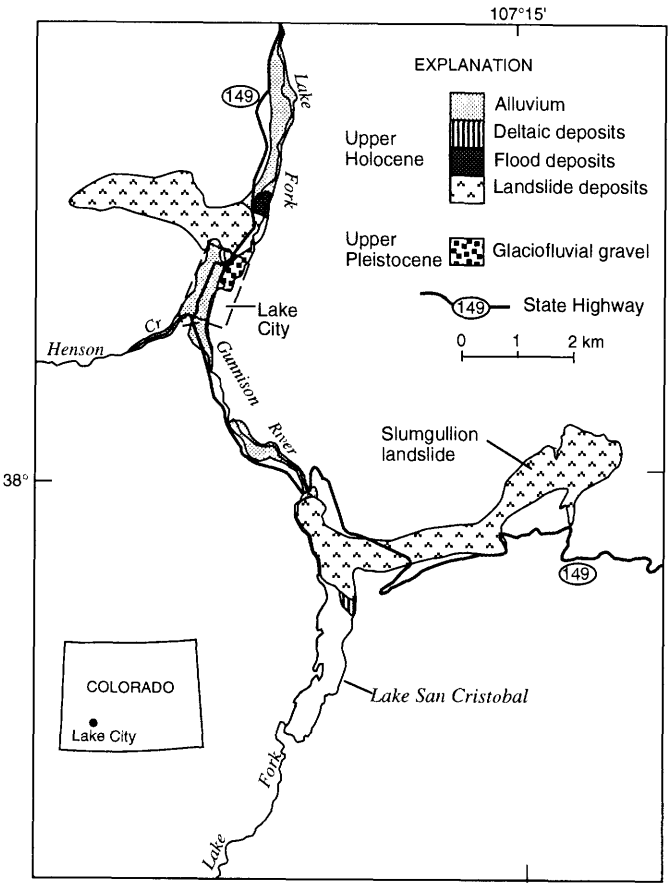

Figure 1. Geologic map of landslide and fluvial deposits on the valley floor of the Lake Fork Gunnison River in the vicinity of Lake City, Colo.

The middle unit crosscuts the oldest unit (Chleborad, 1993 and this volume) and is overlapped by the youngest unit (fig. 2). The middle unit apparently extended farther than the oldest unit; it reached the valley floor and dammed the Lake Fork Gunnison River, thereby forming Lake San Cristobal. The middle unit is more weathered than the youngest unit but is much less weathered than the oldest unit (fig. 3). Soil development in the middle unit is weak and limited to the formation and incorporation of humus into the mineral soil (A horizon). Oxidation of the parent material (Cox horizon) is slight but distinct because the light yellowish-brown oxidized color contrasts with the brownish-yellow to yellow color of the parent material (altered volcanic rock). In many places, variable amounts of soil appear to have been eroded, mainly by sheetwash, from the middle unit. Commonly, the roots of trees on the middle unit are exposed for 5–20 cm above the present soil surface, which is a measure of the amount of material removed since the trees germinated.

Table 1. Radiocarbon ages and $\delta^{13}C$ values.

[B.P., before present; leaders (--) indicate no data—$\delta^{13}C$ value assumed to be –25‰]

Locality[1]	Laboratory[2] sample no.	Material	Conventional ^{14}C age ± σ (yr B.P.)[3]	$\delta^{13}C$ (‰)
Slumgullion 1	W-822[4]	Wood	700±200	--
Slumgullion 2	Beta-66662	Wood	1,190±70	–25.3
Slumgullion 3	DIC-3184	Wood	860±50	--
Lake City earth flow	Beta-60562	Soil humus	3,540±80	–21.3

[1]Slumgullion localities 1, 2, and 3 are shown on figure 2.

[2]W, USGS laboratory; Beta, Beta Analytic Inc.; DIC, Dicarb Radioisotope Co.

[3]By definition, conventional ages are corrected for isotopic fractionation; however, the $\delta^{13}C$ values necessary for making this correction are not available for two samples, in which case the $\delta^{13}C$ value is assumed to be –25‰.

[4]Reported by Crandell and Varnes (1960).

Although not yet accurately dated, the middle unit of the Slumgullion landslide probably was deposited between 0.9 and 0.8 ka (fig. 4). The estimated date is based on three radiocarbon ages of wood from trees that were buried at or just above the base of the landslide deposit near the tip of the landslide toe (fig. 2). There is no way of knowing whether the wood was alive or dead at the time of burial. The two younger radiocarbon ages are probably a more reliable indicator of the date of landsliding than the oldest age because, at any given time, the age range of dead wood on the forest floor in this region is probably at least 200–300 yr. Also, tree-ring data reported by Crandell and Varnes (1961) provide a minimum age of 0.7 ka for the middle unit.

The youngest unit is the presently active part of the Slumgullion landslide and is morphologically distinct from the older landslide deposits (Crandell and Varnes, 1960, 1961). Soil is not developed in most places on the youngest unit, but relict soils do exist locally, which suggests that the youngest unit may include blocks of older landslide deposits. The possibility that some parts of the youngest unit were at the surface prior to initiation of the most recent landsliding may limit the use of dendrochronology and lichenometry in dating the active landslide. Also, the active landslide is so young that its age is difficult to determine accurately by radiocarbon dating. The production rate of atmospheric ^{14}C has so varied over the past few centuries that radiocarbon ages of this period have as many as three to five corresponding calendar dates, the combined standard deviations of which generally span several centuries.

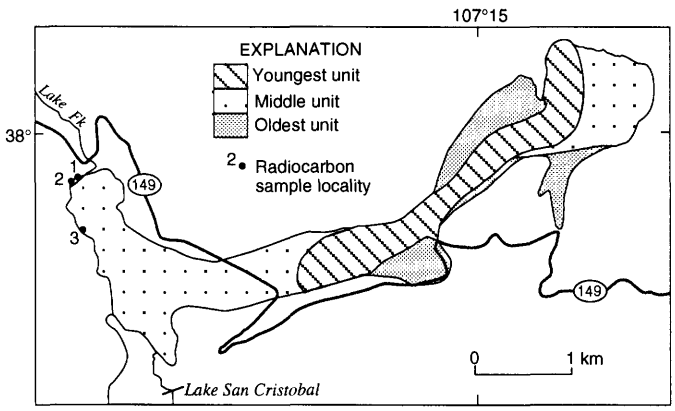

Figure 2. Geologic map of the Slumgullion landslide.

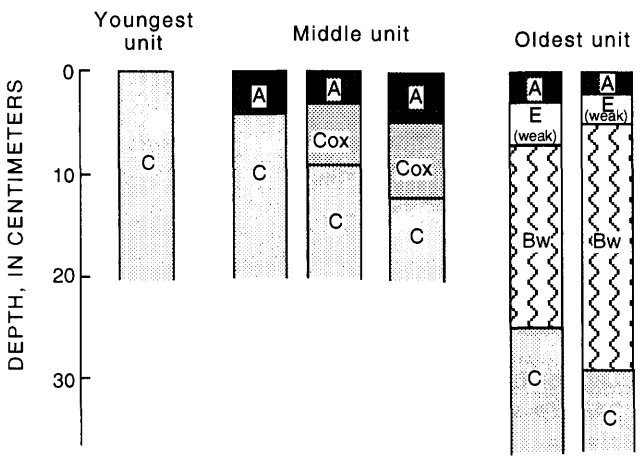

Distinguishing Features of Soil Horizons (Soil Survey Staff, 1981, chap. 4)

A–Characterized by an accumulation of humified organic matter intimately mixed with the mineral fraction and not dominated by properties characteristic of E or B horizons.

E–Characterized mainly by a loss of silicate, clay, iron, aluminum, or some combination of these, leaving a concentration of sand and silt particles of quartz or other resistant minerals; usually lighter in color than an underlying B horizon.

Bw–Characterized by the development of color or soil structure, or both, with little or no apparent accumulation of illuvial material.

C–Horizons or layers, excluding hard bedrock, that are little affected by pedogenic processes and lack properties of A, E, or B horizons.

Cox–An oxidized C horizon, see Birkeland (1984).

Figure 3. Schematic diagram showing differing degrees of soil development in landslide deposits of different ages in the Slumgullion area.

CONCLUSIONS

Clearly, the Slumgullion landslide has moved repeatedly during the last 2,000 yr. However, the total number of landslide movements, the causes of movement, and possible relations between climatic change and landsliding at Slumgullion are yet to be determined.

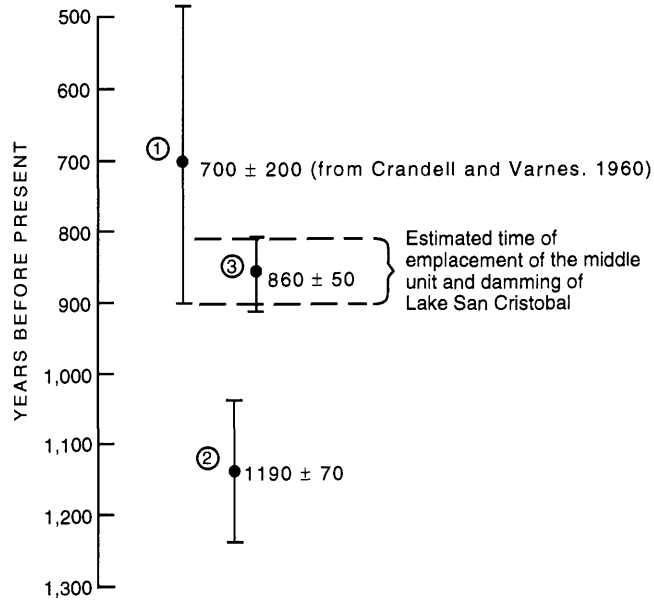

Figure 4. Diagram showing radiocarbon ages of wood obtained from just above basal contact of middle unit near toe of the Slumgullion landslide. Estimated time of emplacement of the middle unit is based on the younger radiocarbon ages because the age range of dead wood on the forest floor at any given time spans at least a few centuries. Circled numbers correspond to sample locations shown in figure 2. Vertical lines represent ±1 standard deviation of the error in counting the radioactive disintegration of the modern standard, background, and sample.

REFERENCES CITED

Birkeland, P.W., 1984, Soils and Geomorphology: New York, Oxford University Press, 372 p.

Chleborad, A.F., 1993, Description, origin, and implications of a newly identified Slumgullion landslide deposit, San Juan Mountains, southwestern Colorado: U.S. Geological Survey Open-File Report 93-548, 17 p.

Crandell, D.R., and Varnes, D.J., 1960, Slumgullion earth flow and earth slide near Lake City, Colorado [abs.]: Geological Society of America Bulletin, v. 71, no. 12, pt. 2, p. 1846.

———1961, Movement of the Slumgullion earthflow near Lake City, Colorado, art. 57, *in* Short Papers in the Geologic and Hydrologic Sciences: U.S. Geological Survey Professional Paper 424–B, p. B136–B139.

Soil Survey Staff, 1981, Examination and description of soils in the field, chap. 4 *of* Revised Soil Survey Manual, Agriculture Handbook no. 18, U.S. Department of Agriculture: Washington, D.C., U.S. Government Printing Office.

CHAPTER 2

KINEMATIC STUDIES OF THE SLUMGULLION LANDSLIDE, HINSDALE COUNTY, COLORADO

By Rex L. Baum *and* Robert W. Fleming

INTRODUCTION

During the past decade, we have mapped surface structures and monitored movement of several different slow-moving landslides to identify landslide-movement processes (Fleming and Johnson, 1989; Baum and others, 1993). In 1990, we began a field study of the Slumgullion landslide to compare its surface features and movement processes with those of landslides in Utah and Hawaii.

SLUMGULLION LANDSLIDE STRUCTURE AND MOVEMENT

The 3.7-km-long active part of the Slumgullion landslide moves 0.5 to 5.5 m annually, producing and destroying a variety of features on the landslide surface. The landslide boundaries define a sinuous, tabular slide mass, 120 m wide at the head and 420 m wide at the toe, that consists of two distinct landslides (fig. 1). A relatively small landslide that moves 0.2 to 0.5 m/yr extends south from the head of the slide at elevation 3,485 m to a poorly developed internal toe near elevation 3,430 m (shaded area, fig. 1). This 0.4-km-long landslide occupies the western part of a bowl-shaped scar at the south edge of Mesa Seco and apparently provides the driving force that triggered movement farther downslope. Near the internal toe, the slide begins to turn toward the southwest, and 0.2 km downslope from the internal toe, a zone of scarps near elevation 3,380 m forms the head of the remainder of the active landslide. The southwest-trending landslide is hour-glass-shaped and extends 3.1 km downslope to the active toe at elevation 2,960 m (fig. 1).

Strike-slip shear zones, cracks, scarps, and internal toes are the surface manifestations of structures that divide the landslide into a number of distinct elements; these elements are the product of irregular boundaries and rates of movement. Several structures facilitate the necessary convergence and acceleration in the top of the "hour glass," where slide width decreases from 370 m at the zone of scarps to 160 m at the neck of the hour glass. Displacement increases from 1 m/yr at the scarps to 5.5 m/yr at the neck (fig. 1). Internal right- or left-lateral shear zones coupled with transverse scarps isolate wedges along the flanks from faster moving blocks, and a hopper-like structure folds material from the edges toward the axis of the slide (fig. 1). The hopper-like structure is a steep-sided topographic basin within the landslide; its lowest point is near the axis of the landslide, and material appears to move toward the low point as in a hopper. Structures that accommodate distributed shearing at the flanks are well expressed near the neck. Most of the shear occurs on a surface or in a thin shear zone at the flank, and oblique cracks or listric faults (expressed by downhill-facing scarps) next to the flank carry the remainder. Downslope from the neck, the slide widens gradually, which results in a series of steps at the north flank. Right-lateral shear zones stepping to the right create small pull-apart basins at points of widening along the flank and cause the center of the slide to be higher than the edge (fig. 2). Shortening in the downslope direction below the neck has produced several groups of internal toes. Splaying of the right-lateral shear zone along the north flank accommodates further widening to 420 m at the toe. The most prominent part of the toe moves about 2 m/yr, and shear-zone-bounded wedges in the north part of the toe move 0–1 m/yr (fig. 1). A curious feature of the main segment of the slide is a ubiquitously higher rate of movement along the left (south) flank than at the right (north) flank. A discontinuous strip of longitudinal scarps and cracks along the axis of the slide appears to be a right-lateral shear zone that separates the faster moving left half from the right. Flank ridges occur at several places on both flanks. Field evidence is consistent with screw-like (forward with upward and inward rotation) movement at the shear zone where these

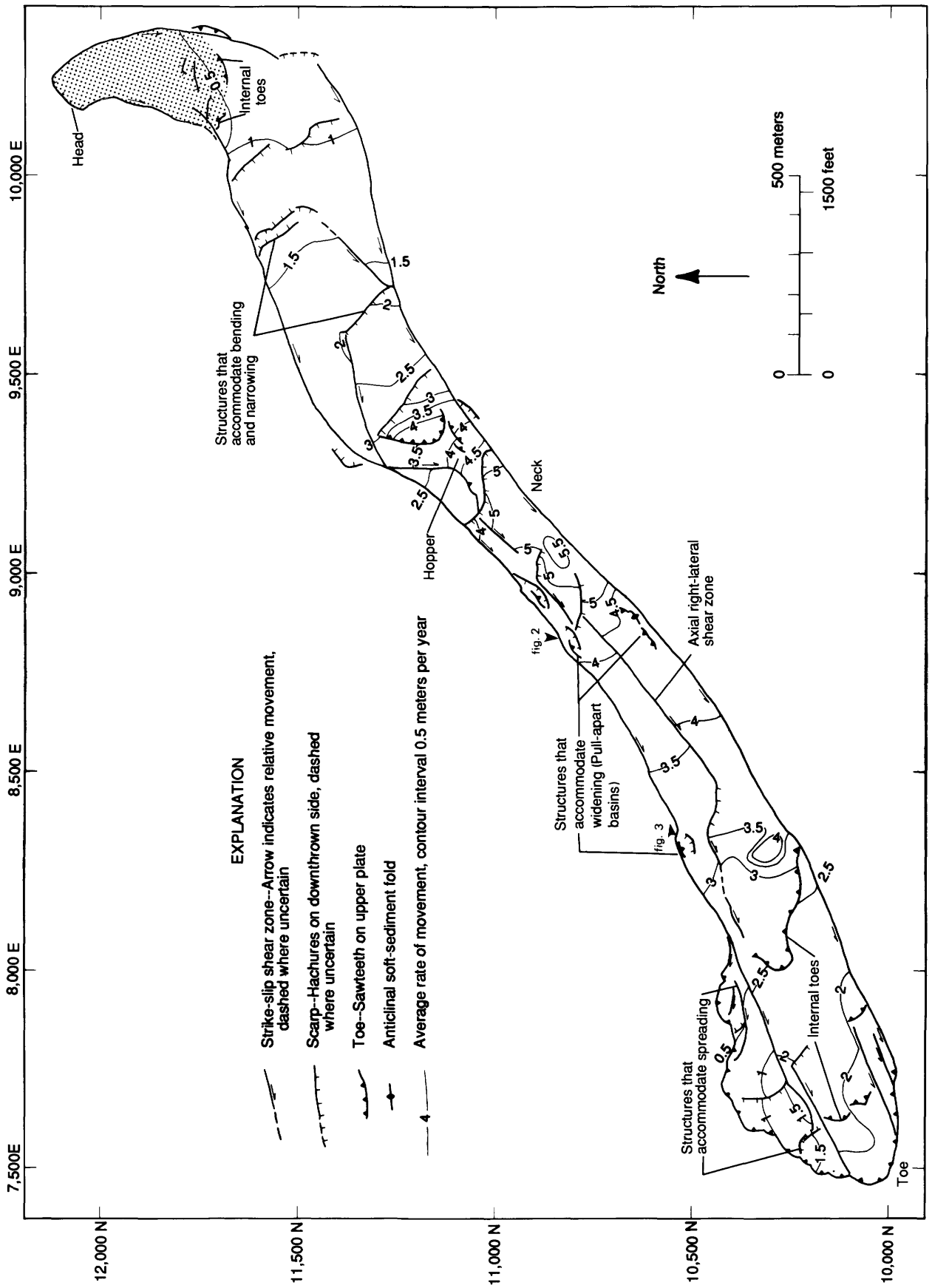

Figure 1. Primary surface features, kinematic elements, and mean annual rate of displacement of the Slumgullion landslide. Structures were mapped in the field, spring and autumn 1993, and simplified from our original 1:1,000-scale field maps. Rates were computed from our field measurements, 1991–93, and from photogrammetric measurements of aerial photographs made in 1985 and 1990 (Smith, 1993). Displacement changes abruptly across several of the scarps, shear zones, and internal toes, particularly near the narrowest part of the landslide. Local grid coordinates are from Varnes and others (1993).

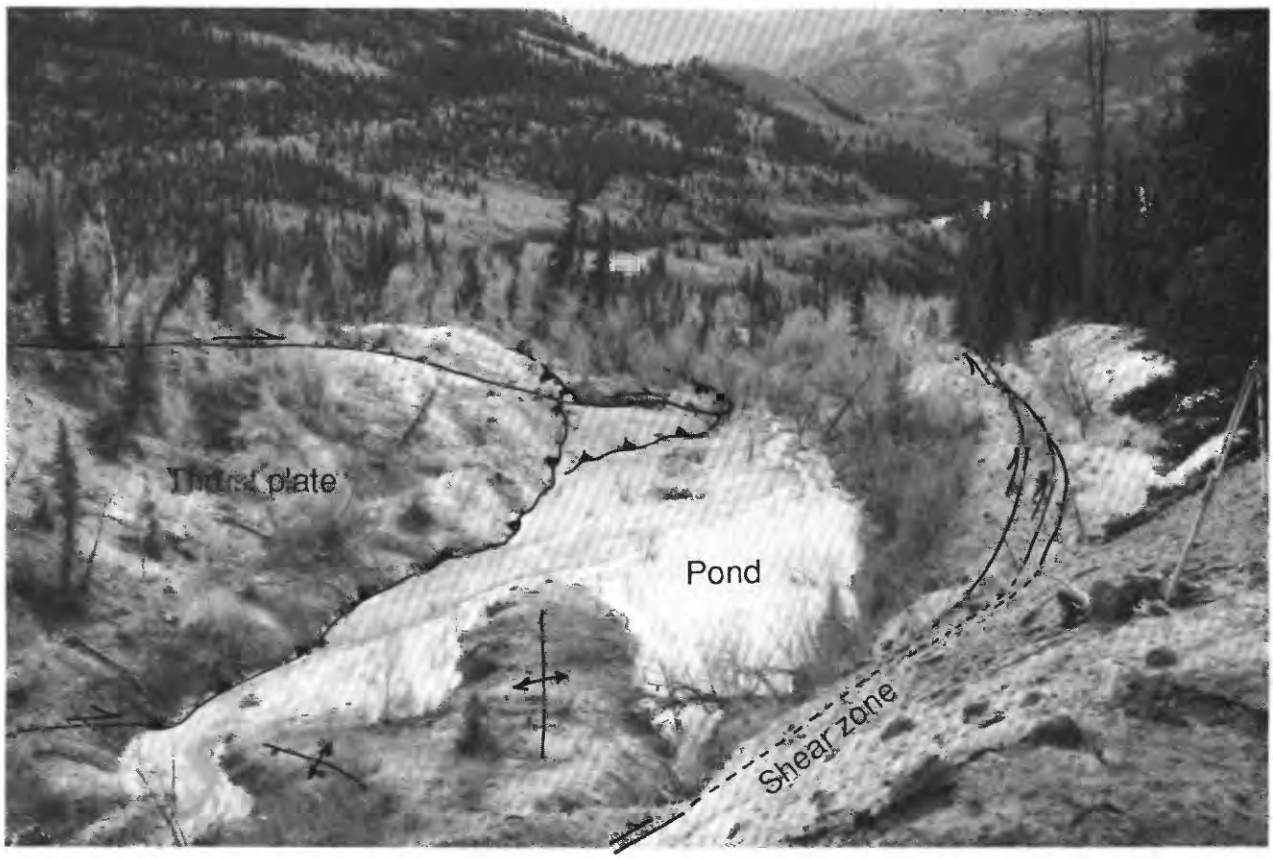

Figure 2. Pull-apart basin at step in right flank of the landslide (about 10850 N., 8850 E., see figure 1 for location). Annotated view looking downslope along right flank about 300 m below the narrowest part of the active landslide. Here, the landslide abruptly becomes wider. The right-lateral strike-slip shear zone on the landslide boundary is in the trough in the lower middle and curves along the right side of the view. The landslide widens at this step in the flank and others like it (fig. 1). Shown here are the typical structures formed in the downslope end of the widening section. We call the overall structure a pull-apart basin because of similarities to such basins in tectonic settings. Solid lines indicate visible active traces of the bounding faults, and dashed lines indicate projected traces where faults are obscured. The basin contains a pond, which is interrupted by two linear protrusions (shown by anticline symbols) that are apparently compressional features formed by movement of material into the pull-apart structure. The basin is filled in this lower (southwestern) part by material moving obliquely from left to right along strike-slip faults. The strike-slip faults in the interior of the slide are approximately parallel to the axis of the landslide near the upper (northeastern) part of the basin, but they curve toward the boundary in the lower part. These faults terminate in thrust faults that extend nearly to the landslide margin. Two of these strike-slip faults and some of the thrust faults are annotated. Note that the small trees on the thrust plate have been tilted toward the landslide flank; continued vertical growth of the tip of the trees has resulted in a bow shape convex toward the flank.

ridges are forming (fig. 3). Several flank ridges on other landslides are similar to the one shown in figure 3 (Fleming and Johnson, 1989); however, the processes of ridge formation might be more complicated than simple screw-like movement (Baum and others, 1993). Flank ridges and tilted fault blocks parallel to the flanks may be analogous to tectonic structures associated with strike-slip faults. Monitoring of displacement and deformation as well as detailed plane-table mapping in areas of distributed shearing, flank ridges, pull-apart basins, and tilted fault blocks are aimed at gaining a better understanding of these structures.

CONCLUSIONS

Our field studies have shown that the Slumgullion landslide has many features in common with other landslides. In addition, we have identified previously unrecognized mechanisms for changing width. The landslide becomes narrower by isolating wedges of material along its flanks and by transversely compressing material in a hopper-like basin. The landslide widens using a series of lateral steps in the flanks and by wedges that move obliquely from the main shear zone in the north flank.

Figure 3. Annotated view looking upslope at flank ridge on right flank of the landslide (about 10530 N., 8370 E. Tape is 2 m long. See figure 1 for location). A 1.5-m-wide transverse crack exposes a cross-sectional view of the ridge (dark area surrounded by clay dike and the hachured line). Landslide material in the exposed face is stony, heterogeneous, and has a blocky structure. Near the left side of the ridge, the fracture surfaces defining the blocky structure are iron stained. A scarp at the outboard side of ridge (light area at center) exposes an emergent part of the lateral shear surface. This shear surface is between the crest and the trace of the right-lateral shear zone (shown by a solid line where the trace is visible, dashed where obscured). The scarp tapers from a height of about 2 m in foreground to 0 m in the background (about 20 m upslope). The taper is consistent with screw-like movement along this part of the flank; the ridge growth is about 0.1 meter per meter of downslope of displacement. Annual movement here is about 3.5 m. The scarp is convex and is covered with sheared, highly plastic, blue-gray clay (liquid limit = 105, plasticity index = 77) that differs in color and texture from the stony, light-brown landslide material in the ridge. Movement at the shear zone has brought a tabular dike of blue-gray clay to the surface and injected the clay into the landslide materials. The double line on the light-colored side of the ridge shows the 5- to 10-cm thickness of blue-gray clay that has been intruded along the shear zone and into the ridge.

REFERENCES CITED

Baum, R.L., Fleming, R.W., and Johnson, A.M., 1993, Kinematics of the Aspen Grove landslide, Ephraim Canyon, central Utah: U.S. Geological Survey Bulletin 1842–F, p. F1–F34.

Fleming, R.W., and Johnson, A.M., 1989, Structures associated with strike-slip faults that bound landslide elements: Engineering Geology, v. 27, p. 39–114.

Smith, W.K., 1993, Photogrammetric determination of movement on the Slumgullion Slide, Hinsdale County, Colorado 1985–1990: U.S. Geological Survey Open-File Report 93-597, 17 p., 1 pl.

Varnes, D.J., Smith, W.K., Savage, W.Z., and Varnes, K.L., 1993, Control and deformation surveys at the Slumgullion Slide, Hinsdale County, Colorado—A progress report: U.S. Geological Survey Open-File Report 93-577, 15 p., 1 pl.

CHAPTER 3

PRELIMINARY GEOLOGIC MAP AND ALTERATION MINERALOGY OF THE MAIN SCARP OF THE SLUMGULLION LANDSLIDE

By Sharon F. Diehl *and* Robert L. Schuster

INTRODUCTION

The main scarp of the Slumgullion landslide lies near the eastern edge of the Uncompahgre–San Juan caldera complex and at the eastern edge of a regional limonitic alteration of rhyolitic volcanic rocks (Lipman, 1976; Sharp and others, 1983; Bove and Hon, 1992). In the San Cristobal quadrangle, hydrothermal alteration products such as alunite and smectite have long been known to be associated with weakening and failure of volcanic rock, with the resulting potential for landslides (Cross, 1909; Larsen, 1913). Larsen (1913) identified hydrothermal alteration products such as alunite and opal in the Slumgullion earth flow.

We investigated the geology of the main scarp because the geological characteristics and mineralogy of the hydrothermal alteration are important factors in the weakness of the rock and, therefore, in the initiation and intensity of landslide movement. The main scarp is composed of "pancake" stratigraphy: a series of relatively unaltered basaltic flows and ash-flow tuff overlying highly altered andesitic to rhyolitic flows. These units are intruded by porphyritic rhyolites and breccia pipes. Landslides caused by weakening of the rock by hydrothermal alteration were recognized and mapped in the Lake City area of the San Juan Mountains 85 yr ago by Howe (1909).

Preliminary investigations of the main scarp of the landslide indicate that faults (fig. 1) are important structural features that add to the instability of the main scarp. Faults and breccia pipes have been conduits for hydrothermal fluids, as evidenced by the association of alunite-altered rock with fault traces and breccia deposits.

METHODS OF STUDY

Because of the inaccessibility of units on the steep and unstable face of the main scarp, it was nearly impossible to collect in situ samples of all units. Thus, float material collected at the base of the scarp supplemented in situ samples that were collected from accessible outcrops along the sides of the scarp (fig. 1). The results of thin-section and bulk X-ray analyses of unaltered volcanic rock were compared with thin sections and X-ray traces of altered volcanic rock to determine the change in mineralogy caused by hydrothermal alteration (table 1). Powdered bulk samples were X-rayed using CuKθ radiation on a Philips-type 150-100-21 goniometer from 2° to 65° 2θ at a scan speed of 2° 2θ per minute. A Cambridge Mark 2 scanning electron microscope (SEM) with an attached energy-dispersive X-ray (EDX) was used to confirm the identity of the alteration mineralogy.

GEOLOGY

STRATIGRAPHY

Based on stratigraphic descriptions of Lipman (1976), Tertiary volcanic units exposed in the main scarp of the Slumgullion landslide, from youngest to oldest, are the Hinsdale Formation, the Sunshine Peak Tuff, and volcanic units of Uncompahgre Peak (fig. 1). The unaltered Miocene Hinsdale Formation is composed of vesicular basaltic lava flows that contain 5–15 percent phenocrysts of plagioclase, biotite, clinopyroxene, and opaque minerals (probably magnetite and (or) ilmenite). The Miocene Sunshine Peak Tuff is a welded ash-flow tuff. It was identified by float material, and this unit may also be present as a breccia deposit in the western portion of the main scarp. The underlying Uncompahgre Peak volcanics of Oligocene age are composed of andesitic flows that contain 10–20 percent phenocrysts of plagioclase, biotite, hornblende, clinopyroxene, and quartz. This unit has undergone acid-sulfate alteration. There is an erosional unconformity between the Oligocene Uncompahgre Peak volcanics and the younger Miocene formations.

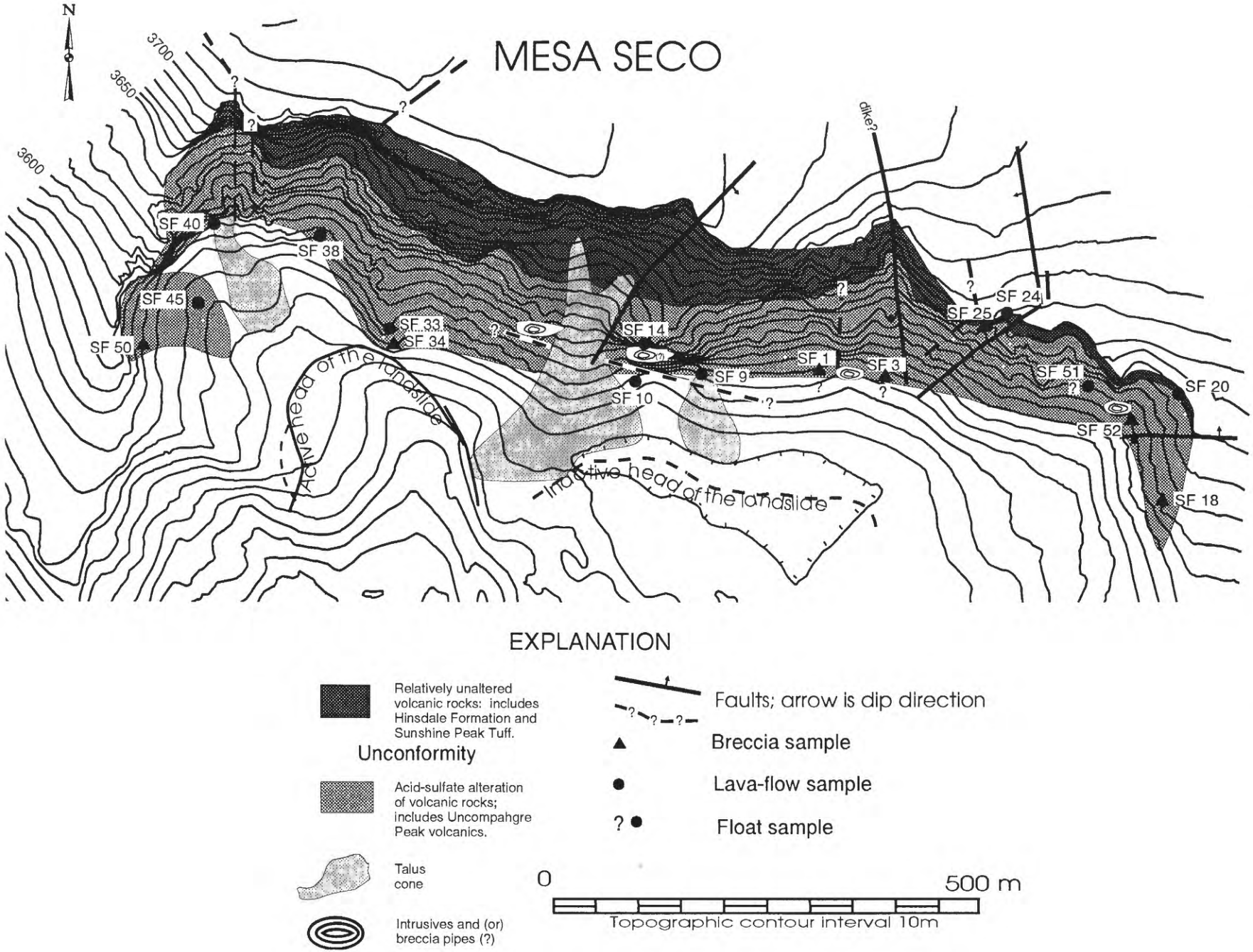

Figure 1. Preliminary geologic map of the main scarp of the Slumgullion landslide.

Table 1. Description of selected samples from the main scarp of Slumgullion landslide.

[Data compiled from hand samples, thin sections, powder X-ray diffraction, and SEM/EDX. Blank boxes under "Primary minerals" column imply that alteration has completely obscured the original mineralogy of the sample. Sample locations identified on figure 1]

Sample number	Type of deposit	Mineralogy			Structural/textural associations
		Primary minerals	Alteration minerals	Sulfides/sulfates	
SF 1	Breccia		Alunite breccia fragments, jarosite cement		Slickensides
SF 3	Breccia		Alunite, silica, iron oxides		Abundant void space
SF 9	Lava flow	Plagioclase, biotite, opaques	Kaolinite(?)		
SF 10	Lava flow	Plagioclase, biotite, altered mafics, opaques	Alunite		Microfractures filled with clay
SF 14	Porphyry intrusive(?)	Sanidine, plagioclase, quartz, biotite		Pyrite, barite (occurs with rare-earth phosphates)	
SF 18	Breccia		Jarosite, iron oxides		Only outlines of original phenocrysts remain
SF 20	Lava flow	Plagioclase, biotite, olivine, opaques			
SF 24	Lava flow	Plagioclase, biotite, clinopyroxene, opaques			Iron oxide- and clay-lined microfractures
SF 25	Breccia		Alunite, silica, chlorite(?)		
SF 33	Lava flow	Plagioclase, biotite, hornblende, opaques			Iron oxide-lined microfractures
SF 34	Breccia		Jarosite, chalcedonic quartz, gypsum, potassium feldspar, sericite, chlorite (?)		Geopetal textures in voids; mineral-filled fractures
SF 38	Lava flow	Plagioclase, biotite, clinopyroxene, quartz			
SF 40	Lava flow		Alunite		
SF 45	Breccia (?)		Jarosite, smectite, chlorite(?), gypsum		
SF 50	Breccia (?)		Jarosite, silica, gypsum		
SF 51	Lava flow	Plagioclase, biotite, clinopyroxene, hornblende, opaques		Pyrite	Pyrite-filled microfractures
SF 52	Breccia	Remnant plagioclase outlines	Alunite, silica, sericite		Silica-filled fractures

INTRUSIVES

Steep, dangerous topography prevented close examination of many of the intrusives recognized on aerial photographs. The porphyry intrusives and associated breccia pipes occur in rough alignment along the trend of the main scarp and along fault traces (fig. 1).

A domal intrusive sampled at the intersection of two major faults in the main scarp (fig. 1) is a medium-gray porphyry composed of 30–35 percent phenocrysts of feldspar, quartz, and biotite, and is mineralized with pyrite, barite, and rare-earth minerals. The feldspar phenocrysts are altered to clay minerals, and pyrite cubes are highly etched.

BRECCIAS

Breccias are abundant and are important because their porous and permeable texture allowed the influx and passage of mineralizing solutions (fig. 2). The stratigraphy exposed in the main scarp is complicated by the presence of flow

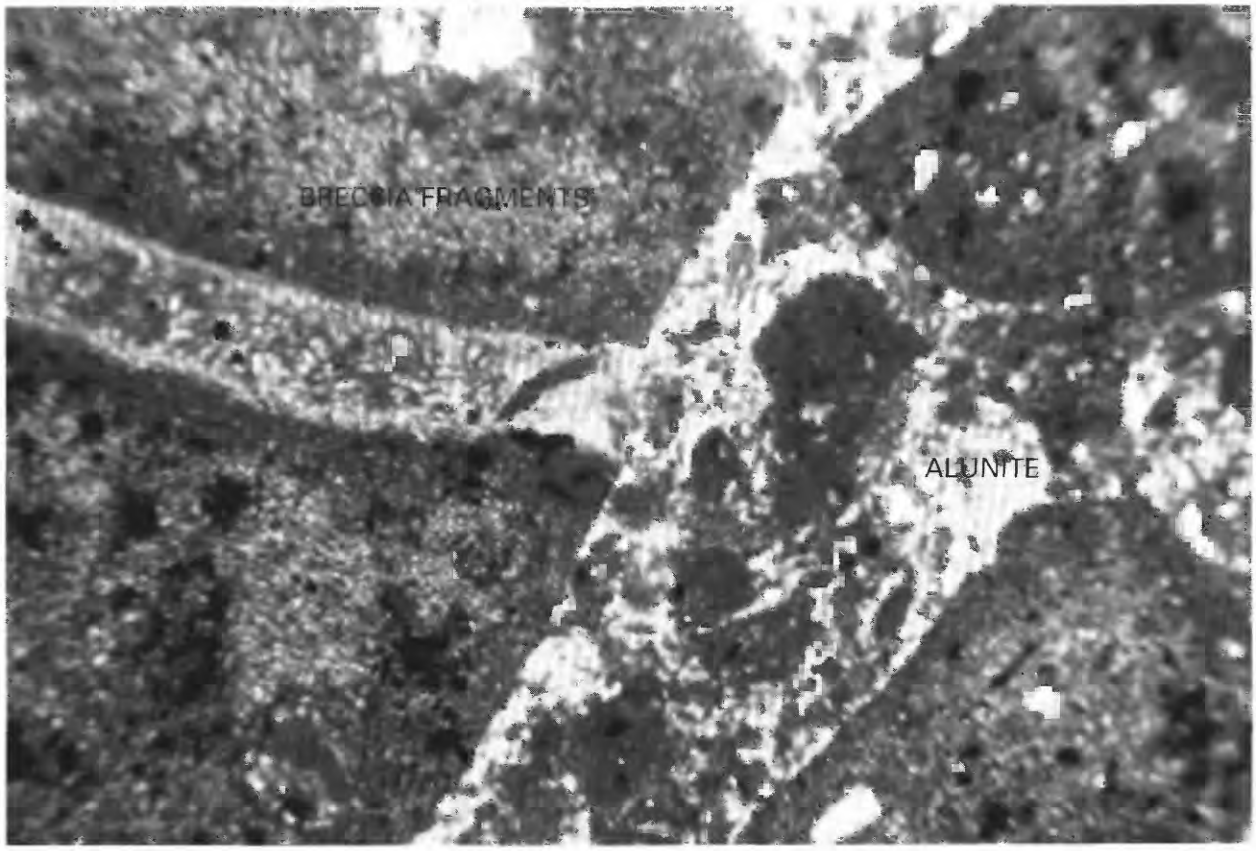

Figure 2. Photomicrograph of sample SF 25 (see fig. 1). Very angular breccia fragments cemented by silica and alunite. Horizontal field of view is approximately 2.5 mm.

breccias, fault breccias, and breccia pipes, which are difficult to differentiate from one another. Their distribution is associated with faults and intrusives (fig. 1). Furthermore, there are surfaces of ferricrete that resemble breccias. Breccia fragments are very angular (fig. 2) and are composed of alunite-altered, as well as fresh, volcanic rock fragments. Breccias are commonly cemented by (1) silica and alunite (fig. 3), (2) silica and jarosite, and (3) iron oxides.

Alteration zones surround the breccia pipes. The alteration zones consist of vuggy silica, quartz-alunite veins, and argillite. The alteration mineralogy follows the classic hydrothermal alteration zonation (fig. 4) typified at Summitville, Colorado, and geothermal systems in general (Hayba and others, 1985, p. 153; Silberman and Berger, 1985). Rare xenoliths of pink granite occur in quartz-alunite cemented breccia.

The earliest period of brecciation and mineralization is assumed to be 23.1 Ma. This date for hydrothermal activity is based on dates for similar mineral and breccia deposits in the alunite deposit at Red Mountain, located about 8 km west of the Slumgullion landslide within the Lake City caldera (Bove and Hon, 1990).

STRUCTURE

FAULTS

The volcanic rock is weakened by the intersection of numerous, discontinuous, curvilinear faults (fig. 1), which are evident on aerial photographs. Faults are confirmed by breccias, alteration minerals, and slickensides. Breccias composed of breccia fragments of alunite with jarosite cement, and alunite-silica altered rock, are commonly associated with faults (table 1; fig. 1). Samples of these rocks commonly have slickensides that show several periods of movement. Faults were important as conduits for hydrothermal fluids in the region (Lee, 1986) and may have been a focus for hydrothermal fluid flow in the main-scarp area. A network of silica-filled veins occur at the extreme eastern and western portions of the main scarp (for example, samples SF 18 and SF 52), and these veins are associated with breccia pipes and fault traces shown on figure 1.

Active rock-avalanche chutes are located along fault traces and at fault intersections (figs. 1 and 5). These chutes funnel debris from the main scarp onto talus cones at its base (fig. 5). The talus cones are composed of unsorted, angular

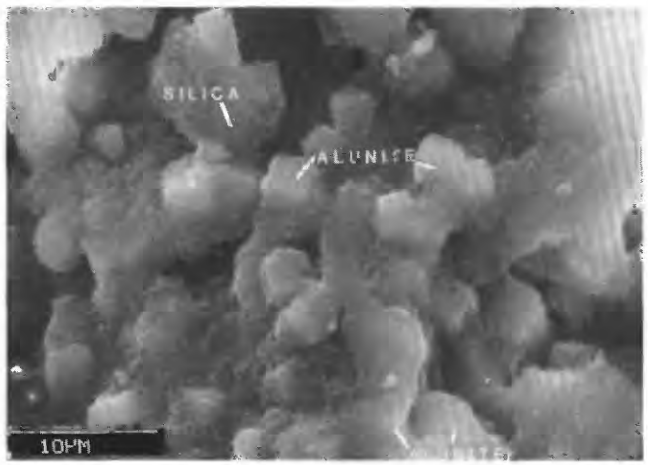

Figure 3. Scanning electron photomicrograph of sample SF 3 (see fig. 1) showing alunite crystals coated with silica.

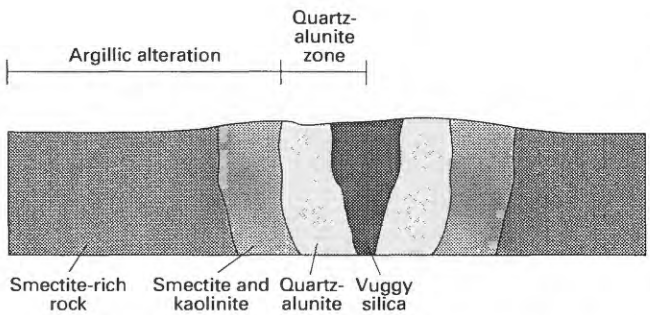

Figure 4. Sketch showing typical hydrothermal alteration zones in breccia pipes along the main scarp. Modified from Steven and Ratté (1960).

cobble- to boulder-size blocks of volcanic rock. The boulders are derived from failure of the main scarp due to vertical, through-going joints in the Hinsdale Formation.

HYDROTHERMAL MINERALIZATION

Hydrothermal explosion brecciation is suggested by the presence of siliceous veins and sulfide and rare-earth mineralization. The sulfide minerals have interacted with potassium-rich hydrothermal fluids and are sources for acid sulfate solutions. Pyrite occupies a microfracture network and is disseminated through portions of the volcanic sequence. Other diagenetic products of hydrothermal activity, identified by X-ray diffraction and scanning electron microscope, are chalcedonic quartz, potassium feldspar, sericite, smectite, kaolinite, jarosite, and alunite-group minerals. These assemblages of minerals are similar to the hydrothermal deposits at nearby Red Mountain (Bove and others, 1990). Chalcedonic quartz, sericite, and pyrite are early main alteration products in the lava flows. These minerals line void spaces and fill fractures. Chalcedonic quartz also acts as a cement in some breccia deposits.

Of interest is the distribution of the alunite and jarosite minerals, which are later alteration products (fig. 3). The presence of these potassium sulfate minerals suggests that hydrothermal fluids associated with the intrusives were potassium rich. Alunite occurs with silica (opal?) around the intrusives in breccia zones and along the fault system. Jarosite, the more iron-rich potassium sulfate mineral, is peripheral to the alunite and forms a cement between breccia fragments. Smectitic clay is found in the main scarp but is more common near and in the active head of the landslide (fig. 1).

Plagioclase phenocrysts are commonly altered to kaolinite in the main-scarp volcanic rocks. This alteration process releases calcium ions into solution. In addition, pyrite has oxidized to release sulfur into solution. The calcium and sulfur ions combine in an oxidizing environment to form gypsum—a soluble salt. The formation of these surficial alteration minerals suggests that the ground water contains a high concentration of total dissolved salts.

The effect of soluble salts on clay minerals, especially in the yellow, sulfate-rich landslide material, and on their material properties is a problem that is addressed by Chleborad and others (this volume). Flocculation of clay platelets is one problem that may be caused by the low pH environment and (or) the abundance of total dissolved salts in the ground water.

DISCUSSION

Because altered rock is interbedded with unaltered flows within the Uncompahgre Peak volcanics, acidic solutions probably flowed laterally along horizontal platy jointing or flow lines in the andesitic and rhyolitic volcanic rocks. Perhaps because they are more porous and of rhyolitic composition, flow breccias of the Uncompahgre Peak volcanics were especially susceptible to acid sulfate alteration.

Alteration products in the volcanic rocks at the Slumgullion landslide are similar to those in the nearby Red Mountain alunite deposits near Lake City, Colo. Both are hydrothermal deposits in which an abundance of sulfur and water were introduced into the rock (Bove and Hon, 1990).

There appear to be several generations of brecciation and hydrothermal alteration as evidenced by (1) alunite-silica-altered rock fragments that occur with unaltered rock fragments in breccia deposits, (2) mineral-filled, in situ fractures in alunite-cemented breccia deposits, and (3) alunite-coated slickensides in breccia deposits.

The weathering of sulfides, which produces acid-sulfate solutions, is responsible for the precipitation of surficial alteration products such as limonite and gypsum. Jarosite

Figure 5. Portion of the main scarp showing Hinsdale Formation overlying Uncompahgre Peak volcanics and the major talus cone.

may be a cold-water alteration product as well as a hydrothermal mineral. The precipitation of jarosite requires a low pH and a high-sulfate environment. These alteration minerals, as well as clay minerals, that are common in the main scarp also compose the bulk of the landslide material.

CONCLUSIONS

The instability of the main scarp is attributed to steep topography, intersection of faults, and to the high degree of alteration of the volcanic rocks. The main-scarp area of the Slumgullion landslide has been subjected to several generations of hydrothermal brecciation and alteration. The high degree of alteration in conjunction with the structural fabric is considered to be a prime factor in the original failure of the rock that formed the landslide. Failure of the main scarp has occurred in wide argillitic alteration zones surrounding the breccia pipes.

Fractures and void spaces in the altered volcanic rocks were flushed by meteoric waters resulting in infilling with smectitic clays, jarosite, and gypsum. Surficial cold-water alteration processes are important in the production of soluble salts, such as gypsum, in the landslide material.

ACKNOWLEDGMENTS

Discussions with Dana Bove, Miles Silberman, and Karen Wenrich, U.S. Geological Survey, were very helpful in establishing the identity of the alteration mineralogy. Philip Powers assisted with the computer graphics.

REFERENCES CITED

Bove, D.J., and Hon, Ken, 1990, Compositional changes induced by hydrothermal alteration at the Red Mountain alunite deposit, Lake City, Colorado: U.S. Geological Survey Bulletin 1936, 21 p.

———1992, Geologic and alteration map and drill-core logs of the Red Mountain area near Lake City, Hinsdale County, Colorado: U.S. Geological Survey Miscellaneous Investigations Series Map I–2286, scale 1:12,000.

Bove, D.J., Rye, R.O., and Hon, Ken, 1990, Evolution of the Red Mountain alunite deposit, Lake City, Colorado: U.S. Geological Survey Open-File Report 90-0235, 30 p.

Cross, Whitman, 1909, The Slumgullion mud flow: Science, New Series, v. 30, no. 760, p. 126–127.

Hayba, D.O., Bethke, P.M., Heald, Pamela, and Foley, N.K., 1985, Geologic, mineralogic, and geochemical characteristics of volcanic-hosted epithermal precious-metal deposits, *in* Berger,

B.R., and Bethke, P.M., eds., Geology and Geochemistry of Epithermal Systems: Reviews in Economic Geology, v. 2, chap. 7, p. 129–167.

Howe, Ernest, 1909, Landslides in the San Juan Mountains, Colorado: U.S. Geological Survey Professional Paper 67, 58 p.

Larsen, E.E., 1913, Alunite in the San Cristobal quadrangle, Colorado: U.S. Geological Survey Bulletin 530–F, p. 179–183.

Lee, Keenan, 1986, Map showing areas of limonitic hydrothermal alteration in the Lake City caldera area, western San Juan Mountains, Colorado: U.S. Geological Survey Miscellaneous Field Studies Map MF–1868, scale 1:48,000.

Lipman, P.W., 1976, Geologic map of the Lake City caldera area, western San Juan Mountains, southwestern Colorado: U.S. Geological Survey Miscellaneous Investigations Series Map I–962, scale 1:48,000.

Sharp, W.N., Martin, R.A., and Lane, M.E., 1983, Mineral resource potential and geologic map of the Powderhorn Wilderness Study Area and Cannibal Plateau Roadless Area, Gunnison and Hinsdale Counties, Colorado: U.S. Geological Survey Miscellaneous Field Studies Map MF–1483–A, scale 1:50,000.

Silberman, M.L., and Berger, B.R., 1985, Relationship of trace-element patterns to alteration and morphology in epithermal precious-metal deposits, *in* Berger, B.R., and Bethke, P.M., eds., Geology and Geochemistry of Epithermal Systems: Reviews in Economic Geology, v. 2, chap. 9, p. 203–247.

Steven, T.A., and Ratté, J.C., 1960, Geology and ore deposits of the Summitville district, San Juan Mountains, Colorado: U.S. Geological Survey Professional Paper 343, 70 p.

CHAPTER 4

RETREAT OF THE SLUMGULLION MAIN SCARP

By Robert L. Schuster *and* William K. Smith

INTRODUCTION

The nearly vertical main scarp (fig. 1) of the Slumgullion earth flow is approximately 1,000 m long and 230 m high. This magnificent scarp, which formed in hydrothermally altered Tertiary volcanics, is slowly retreating in response to freeze-thaw activity, sapping, and erosion. The volcanic rock has been weakened by jointing and by numerous faults that add to the instability of the main scarp (Diehl and Schuster, this volume).

Active rock-avalanche chutes are located along main-scarp faults and fault intersections. These chutes funnel rock debris from the main scarp to the talus apron at its base (fig. 2). The talus deposits are made up of angular cobble- to boulder-sized blocks of volcanic rock. The large boulders, some as large as automobiles (fig. 3), are derived from failure of the main scarp along vertical joints in the resistant Hinsdale Formation at the top of the scarp (Diehl and Schuster, this volume). The talus deposits load part of the head of the landslide and potentially serve as a long-term driving force applied to the mass. However, we have little idea of the rate of accumulation of this rock-fall/rock-avalanche material, and it seems to have little effect on the currently active part of the landslide.

USE OF ARCHIVAL PHOTOGRAPHS TO ESTIMATE MAIN-SCARP RETREAT

Chandler and Cooper (1988) have reviewed methods of using archival aerial or terrestrial photographs to determine morphologic changes of hillside slopes. These methods can be used to compare digital terrain models (DTM's) from stereographic photographs (stereopairs) taken at time intervals in order to quantify a "DTM of difference," i.e., one digital terrain model is "subtracted" from another. The comparison can be used to quantitatively measure landslide movement or slope retreat. Vertical aerial photography, oblique aerial photography, or terrestrial photography can be used, but the photos must give stereo coverage.

High-quality individual terrestrial (i.e., ground-based) photographs of the Slumgullion main scarp taken in 1905 by Whitman Cross of the U.S. Geological Survey are available from the Photo Archives of the U.S. Geological Survey Library, Denver, Colo. Unfortunately, no archival stereopairs of the main scarp are available; thus, quantitative analysis of morphogenetic changes are not possible. Instead, these photographs were replicated by the authors in 1992 and 1993 from the exact sites at which the archival photos were taken. This was done with a modern 35-mm camera and a 35-mm to 105-mm "zoom" lens that could closely approximate the framing of the 1905 photos. By careful comparison of the new photos with the archival photos, it is possible to note local changes in main-scarp geometry, but it is not possible to determine quantitatively the amount or volume of retreat at these points. An example comparing 1905 Cross photography of the main scarp and a photograph taken by the authors in 1992 is presented in figure 4. Comparison of these photos indicates that, since 1905, major changes in surface geometry have occurred in weaker rocks (Diehl and Schuster, this volume) at mid-height on the rock face near the center of the wall (between the arrows in fig. 4*A*). Little change has taken place in the more resistant rocks at the top of the wall.

Beginning in 1982, the authors have taken their own terrestrial photographs of the more active parts of the main scarp, avalanche chutes, and talus deposits, especially in the sector of the scarp between the arrows in figure 4*A*. These photographs are being compared to current photos and will be compared to future photos taken from the same positions to obtain rough estimates of degradation of the most active parts of the scarp. An example of such a comparison over a period of 3 yr is presented in figure 5, where differences in distribution of rock-fall boulders from the main scarp can be seen at the toe of the talus apron.

Figure 1. Main scarp of the Slumgullion landslide (August 1992 photograph).

ANALYTICAL USE OF STEREOGRAPHIC PHOTOGRAPHS TO DETERMINE RATE OF MAIN-SCARP RETREAT

A quantitative approach to determining the rate of retreat of the main scarp can utilize recent developments in analytical photogrammetry that permit monitoring morphologic changes of slopes or vertical faces from stereoscopic ground photos taken with high-quality cameras and calibrated lenses (Chandler and Cooper, 1988; Chandler and Moore, 1989). In 1992, we occupied nine permanent camera stations (fig. 6) about 100 m apart on a line about 1 km in front of the main scarp. From these, a series of stereographic photo pairs (fig. 7) was taken with a calibrated Hasselblad camera. A vertical topographic map of the main scarp as it was in 1992 will be produced using these stereopairs. In future years, the camera stations can be reoccupied, the 1992 stereopairs replicated, and new vertical topographic maps produced. By "subtracting" a new DTM from the 1992 version, the amount of retreat and the volume of failed main scarp can be determined. Because the rate of retreat is very slow, it may be decades before substantial changes will be noted. Thus, our photos will be placed in USGS archives for future use and comparisons.

Figure 2. Talus cones forming an apron of volcanic rock-fall material (foreground and left center) beneath the main scarp of the Slumgullion landslide (August 1992 photograph). Approximate camera position is depicted as a circled "2" on map in figure 6.

CONCLUSIONS

Rock material that falls, rolls, bounces, or slides from the main scarp has a long-term effect in loading the head of the Slumgullion landslide and, thus, could be a factor in future landslide activity. Probably the most efficient means of determining the amount of material that moves from the main scarp to the head of the landslide is by means of photogrammetric study of the main scarp from terrestrial photographs taken over time spans measured in years or tens of years. Archival terrestrial photos taken by Cross in 1905 can be used to qualitatively determine morphogenic changes in the main scarp, avalanche chutes, and talus deposits. Stereoscopic photography from predetermined ground stations can be used with future replicated stereographic photographs and an analytic plotter or computer analysis to obtain quantitative measures of spatial retreat of the main scarp and deposition of failed rock material onto the head of the landslide.

REFERENCES CITED

Chandler, Jim, and Cooper, Mike, 1988, Monitoring the development of landslides using archival photography and analytical photogrammetry: Land and Minerals Surveying, Royal Institution of Chartered Surveyors, v. 6, p. 576–584.

Chandler, J.H., and Moore, R., 1989. Analytical photogrammetry: A method for monitoring slope instability: Quarterly Journal of Engineering Geology, v. 22, p. 97–110.

Figure 3. Large boulders at toe of talus apron (July 1993 photograph). Approximate camera position is depicted as circled "3" on map in figure 6.

Figure 4 (facing page). Comparison of 1905 main-scarp photograph (*A*) by Whitman Cross to September 1992 photograph (*B*) from same position by the authors. The two photographs indicate that, during this 87-yr period, considerable material was removed from midheight of the main scarp in the area between the two arrows of the 1905 photograph. The approximate camera position is depicted as a circled "4" on figure 6.


A


B


A

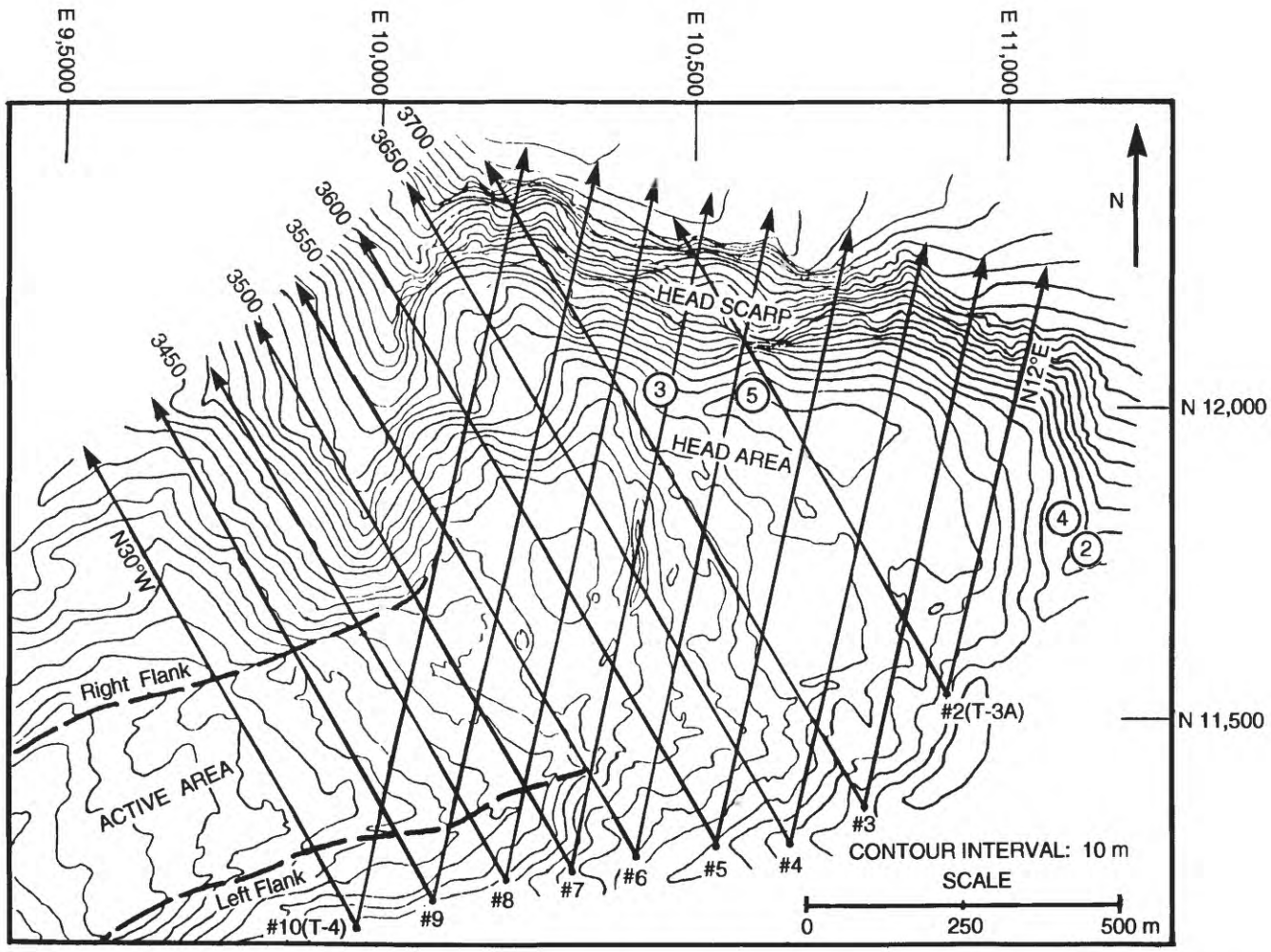

Figure 6. Map showing locations of nine permanent camera stations from which stereopairs (fig. 7) were taken at bearings of N. 12° E. and N. 30° W. in September 1992. Approximate camera positions for photographs in figures 2, 3, 4, and 5 are indicated by circled numbers. Grid ticks on map borders represent local coordinate system in meters.

Figure 5 (facing page). Comparison of fallen rocks at toe of talus apron beneath the main-scarp area shown between the arrows in figure 4*A*. Photograph *A* was taken by A. E. Farkas (Geocon, Inc., San Diego, Calif.) in October 1989. Photograph *B* was taken by the authors in September 1992. A few large boulders that fell during this 3-yr period are indicated by arrows in photograph *B*. The approximate camera position is depicted as a circled "5" in figure 6.

Figure 7. Stereographic photographs of portion of main scarp taken with Hasselblad camera from permanent photographic stations no. 8 (photograph *A*) and no. 7 (photograph *B*), September 26, 1992. Positions of photographic stations are indicated in figure 6. This stereopair and pairs taken from other stations can be used to produce a "vertical" topographic map of the main scarp.

CHAPTER 5

RADIOCARBON AGE OF A NEWLY IDENTIFIED SLUMGULLION LANDSLIDE DEPOSIT

By Alan F. Chleborad

INTRODUCTION

A newly identified landslide deposit covering an area of more than 100,000 m^2 immediately adjacent to an upper part of the Slumgullion landslide (fig. 1) was studied to determine its origin, age, and relationship to the Slumgullion landslide. The deposit was mapped, surface features and materials were examined and described, stratigraphic relationships were noted, and samples of wood buried in the deposit were collected for radiocarbon dating (Chleborad, 1993). The surface of the newly identified landslide deposit is composed of fine-grained, altered volcanic debris and scattered and locally concentrated fragments and blocks of volcanic rock. The overall appearance of the deposit is similar to other parts of the Slumgullion landslide that have been characterized as older and inactive. Figure 2 shows the location of the newly identified deposit with respect to previously recognized boundaries of the inactive and active parts of the Slumgullion landslide. The location, orientation, and composition of the deposit indicate that it is part of a landslide that originated in the Slumgullion landslide source area. Comparison of the location of the deposit with a published reconstruction of the pre-Slumgullion topography suggests that a large volume of landslide debris that originated near the present 250-m-high main scarp filled the upper valley below the main scarp and spilled over a 60-m-high, east-west trending ridge (divide). The spillover (newly identified landslide deposit) moved in a southwesterly direction down a ravine in the drainage basin of Slumgullion Creek. Subsequent mass movement of the valley fill within the previously recognized bounds of the Slumgullion landslide truncated the original deposit, leaving a steep scarp and exposing a basal contact with underlying colluvium (fig. 2). The apparent sensitivity of the movement of the newly identified landslide debris to the existing topography suggests that it was emplaced as a relatively slow moving landslide rather than as a catastrophic failure that overran the topography. Based on initial results of the study, it was concluded (Chleborad, 1993) that the newly identified landslide deposit was emplaced as part of a major, early episode of Slumgullion landsliding, and truncation of the original deposit was the result of one or more later episodes of Slumgullion landsliding. All this predates the occurrence of the currently active part of the Slumgullion landslide (fig. 2). Results of a subsequent examination of the degree of pedologic soil development relative to other parts of the Slumgullion landslide (Madole, this volume) further supports this conclusion. Accurate age dating of the newly identified deposit is crucial to an understanding of the early history and chronology of Slumgullion landsliding.

RADIOCARBON AGE OF THE NEWLY IDENTIFIED DEPOSIT

Wood found buried in clay-rich landslide debris at the distal and truncated ends of the deposit (locations AC-2, AC-4, AC-5, and AC-6 in fig. 2) yielded conventional radiocarbon ages ranging from 1,130 to 1,630 yr B.P. (table 1). At locations AC-2 and AC-6, near the distal end, samples were taken from each of two partly buried logs (partly exposed by erosion) located several meters above the base of the deposit (fig. 3). Wood samples AC-2 and AC-6 were identified as Abies (fir) and Pinus (pine), respectively (Paleo Research Laboratories, unpub. report, 1994). The logs were not extensively decayed allowing sampling and dating of the outer 10 to 20 rings. Partial excavation revealed tree bark and branches on outer parts of the logs indicating that few, if any, of the external rings were missing as a result of decay or erosion. At locations AC-4 and AC-5, at the truncated end of the deposit, wood fragments (maximum dimension approximately 0.2 m) concentrated in a zone at the basal contact with the pre-slide surface were also sampled for dating. Calibrated $\pm 2\sigma$ ranges for the radiocarbon ages of the samples (table 1) were obtained by applying the tree-ring calibration curves of Stuiver and Reimer (1993).

Figure 1. Panoramic view (looking north) of the area of the newly identified landslide deposit (middle foreground). Arrows point to the exposed lower (distal) part of the deposit and the tree-covered, hummocky upper part. The 250-m-high main scarp of the Slumgullion landslide is in background. Photograph taken from Windy Point Overlook, located approximately 0.8 km south of the deposit.

CONCLUSIONS

The close agreement in age of the sampled logs from the distal end of the deposit suggests that a single event (the landsliding) may have caused the death of the trees. The radiocarbon ages indicate that the landsliding probably occurred between 880 and 1,330 yr ago (relative to A.D. 1994), assuming that an insignificant amount of time elapsed between the death of the trees and burial. The indicated maximum age for wood collected at the truncated end of the deposit (1,630±50 ^{14}C yr B.P.) corresponds to a calibrated age of 1,395 to 1,740 yr (relative to A.D. 1994), which is interpreted as the probable maximum age for the deposit at that location. The time of occurrence of the now inactive part of the Slumgullion landslide has been reported as about 700 yr ago (Crandell and Varnes, 1960, 1961). Based on initial results of the study (Chleborad, 1993) and the radiocarbon ages shown in table 1, I conclude that Slumgullion landsliding involving a significant volume of landslide debris probably occurred as much as several hundred years prior to that time.

REFERENCES CITED

Chleborad, A.F., 1993, Description, origin, and implications of a newly identified Slumgullion landslide deposit, San Juan Mountains, southwestern Colorado: U.S. Geological Survey Open-File Report 93-548, 17 p.

Crandell, D.R., and Varnes, D.J., 1960, Slumgullion earthflow and earth slide near Lake City, Colorado [abs.]: Geological Society of America Bulletin, v. 71, no. 12, pt. 2, p. 1846.

———1961, Movement of the Slumgullion earthflow near Lake City, Colorado, *in* Short Papers in the Geologic and Hydrologic Sciences: U.S. Geological Survey Professional Paper 424–B, p. B136–B139.

Parise, M., and Guzzi, R., 1992, Volume and shape of the active and inactive parts of the Slumgullion landslide, Hinsdale County, Colorado: U.S. Geological Survey Open-File Report 92-216, 29 p.

Stuiver, M., and Reimer, P.J., 1993, Extended ^{14}C data base and revised calib 3.0 ^{14}C age calibration program: Radiocarbon, v. 35, p. 215–230.

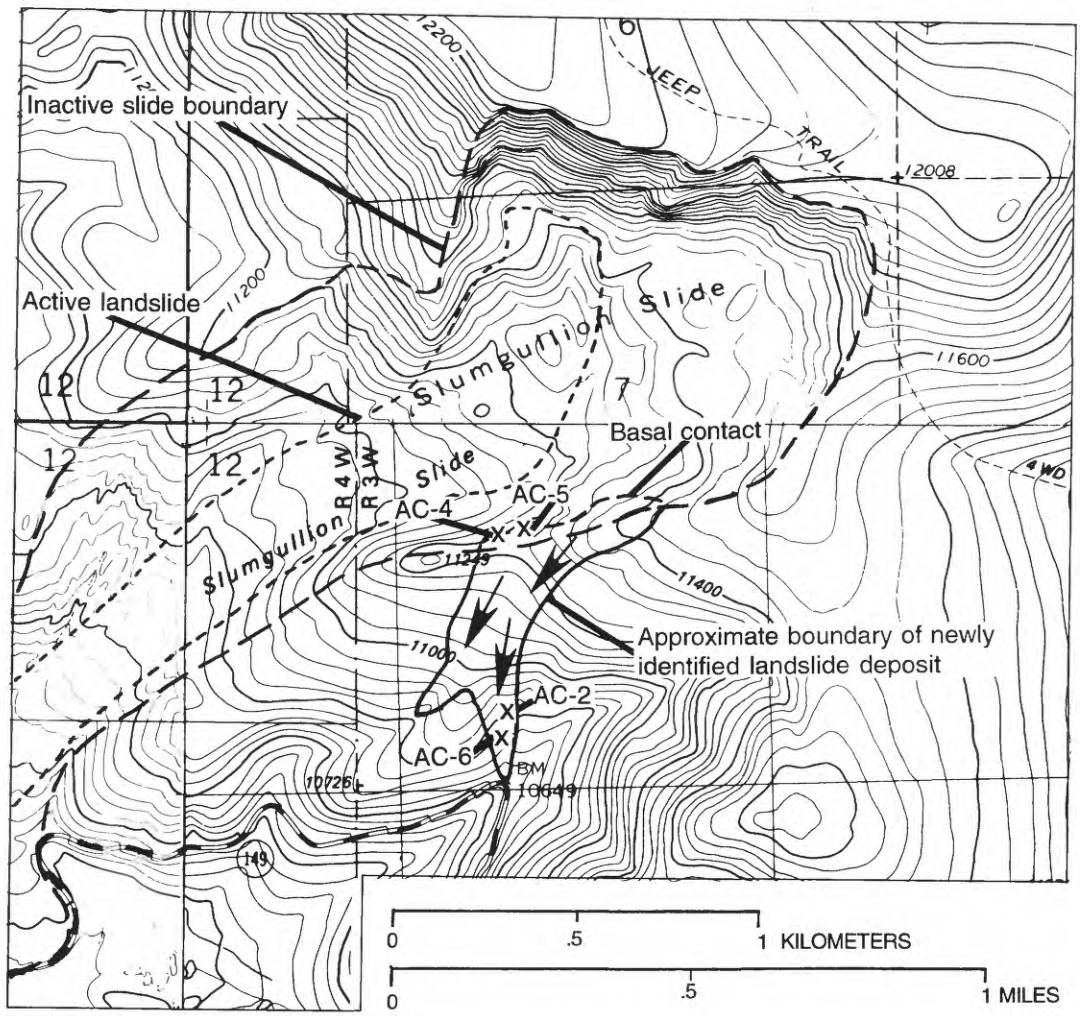

Figure 2. Topographic map of the upper area of the Slumgullion landslide showing the location of the newly identified landslide deposit. The previously recognized active and inactive landslide boundaries are from Parise and Guzzi (1992). The X's mark the locations of radiocarbon sample sites AC-2, AC-4, AC-5, and AC-6. Arrows indicate the apparent direction of movement of landslide debris at the time of deposition. Contour interval 40 feet. Base from U.S. Geological Survey 1:24,000 Cannibal Plateau, 1963 (photorevised 1982); 1:24,000 Lake San Cristobal, 1964; 1:24,000 Lake City, 1963 (photorevised 1982); 1:24,000 Slumgullion Pass, 1986.

Figure 3. Photograph of partly buried log located at an elevation of about 3,290 m on the distal end of the newly identified landslide deposit (AC-2 on fig. 2). Wood from the outer 10–20 rings of the log yielded a conventional radiocarbon age of 1,130±60 yr B.P. (table 1). Bark is present on buried part of log.

Table 1. Radiocarbon ages and corresponding calibrated ages in years before present of wood from newly identified Slumgullion landslide deposit.

[B.P., before present; frags, fragments]

Site	Material sampled	Laboratory sample no.	Conventional[1] radiocarbon age ± 1 σ (^{14}C yr B.P.)	δ^{13}C ( )	Calibrated[2] age at ± 2 σ (yr B.P.)
Distal end of deposit (AC-2)	Log (outer 10–20 rings)	Beta-63502	1,130±60	–21.9	1,270–835
Distal end of deposit (AC-6)	Log (outer 10–20 rings)	Beta-67265	1,180±70	–20.6	1,290–920
Truncated end of deposit (AC-5)	Wood frags (relation to bark layer unknown)	Beta-67264	1,490±60	–22.5	1,495–1,295
Truncated end of deposit (AC-4)	Wood frags (relation to bark layer unknown)	Beta-65145	1,630±50	–22.5	1,700–1,350

[1]Age calculations made with half-life of radiocarbon taken as 5,568 years; ± 1 σ represents the error from counting of the modern standard, background, and the sample being analyzed. All samples were corrected for isotopic fractionation (δ^{13}C values).

[2]Radiocarbon ages were converted to calendar years using the tree-ring-based calibration program CALIB 3.0 (Stuiver and Reimer, 1993). Calibration used bidecadal data set, and a laboratory error multiplier of 1.5 was used to account for analytical uncertainties not accounted for in the conventional radiocarbon ages.

CHAPTER 6

SLUMGULLION LANDSLIDE DAM AND ITS EFFECTS ON THE LAKE FORK

By Robert L. Schuster

INTRODUCTION

The Slumgullion earth flow (fig. 1) dammed the Lake Fork of the Gunnison River approximately 700 yr ago, impounding Lake San Cristobal, Colorado's second largest natural lake (fig. 2). The original impoundment was 4.3 km long and had a surface area of 1.8 km^2. During the past 700 yr, sediment entering the lake from the headwaters of the Lake Fork of the Gunnison River and from Slumgullion Creek have formed large deltas (figs. 3 and 4) in the lake; the Lake Fork delta at the head of the lake has reduced the length of the lake to 3.3 km and the two deltas together have reduced lake surface area to 1.34 km^2 . The maximum depth of the lake is 27 m and its estimated volume is 14 million m^3.

Landslide dams are common natural phenomena (Schuster and Costa, 1986; Costa and Schuster, 1988). However, unlike the Slumgullion blockage, most landslide dams fail fairly soon after formation by overtopping and surface erosion or by piping (internal erosion). Some landslide dams become long-lasting geologic features (Schuster and Costa, 1986; Costa and Schuster, 1988). However, a few landslide dams have failed after many years of stability. For example, in 1966 the rock- and debris-fall dam that formed Lake Yashinkul on the Tegermach River in the Kirghiz Republic, U.S.S.R., failed by piping after having been stable for 131 yr (Pushkarenko and Nikitin, 1988). This poses the question: Even though the Slumgullion landslide dam is at least 700 yr old, is there a possibility of it failing?

GEOMETRY OF THE DAM AND ITS NATURAL SPILLWAY

In damming the Lake Fork of the Gunnison River, the landslide buried the original channel of the Lake Fork for a straight-line length of about 2.8 km (fig. 5), of which about 1.8 km (line AB) currently is buried under the subaerial part of the landslide and about 1.0 km (line BC) lies under the part of the landslide that has been submerged by Lake San Cristobal. The average gradient of this pre-landslide stretch of the Lake Fork was 0.9 percent (based on a straight-line projection of the stream as shown by line ABC in fig. 6). Today's natural lake outlet channel around the toe of the landslide (fig. 5) has a "straight-line" length of about 1.6 km and a true length (including bends and curves) of 1.9 km. Because of the height of the dam, the straight-line and true gradients for this stream channel are much steeper than the original stream gradient; the gradient for the straight-line projection is about 3.5 percent; for the actual stream length, it is 2.7 percent. Both are on the order of three times as steep as the pre-landslide stream gradient. If it is assumed that the original stream had roughly the same deviation from a straight line as today's outlet channel has, its buried length can be estimated at 3.3 km, of which 2.1 km is under the exposed part of the landslide and 1.2 km lies buried beneath the submerged part of the slide. The original average gradient for this stretch was then about 0.8 percent, which compares closely with today's average gradient between Lake City and the upper end of Lake San Cristobal of 1.06 percent.

As shown in figure 6, the crest of the dam is about 70 m high directly above the inferred location of the old stream bed. At this point, the original stream bed lay about 200 m east of today's outlet from Lake San Cristobal (fig. 5). However, this was not the low point of the crest of the dam, which lay against the west valley wall near the location of today's Lake Fork. By extending the present-day topography near the dam crest downslope (i.e., westward) from the section in figure 6 to the toe of the slide, I find that the minimum elevation of the crest of the dam was about 2,750 m and; thus, the height of the dam at that point before spillway erosion occurred was about 50 m above the original stream elevation.

Figure 1. Oblique aerial view of the Slumgullion earth flow. The toe of this landslide formed the natural blockage of the Lake Fork of the Gunnison River that impounds Lake San Cristobal. Path of natural lake outlet channel across the dam at the toe of the landslide is indicated by arrows.

CHANGES IN GEOMETRY OF THE DAM

In referring to the toe of the landslide, Rickard (1903) noted that, "It is said, by those living on the lake shore, to be still in motion and to be extending further across the valley." With the exception of this vague statement, there has been no evidence of historic movement of the toe of the landslide. The main change in geometry of the dam since it was formed has been deepening of the lake outlet channel caused by stream erosion. Most of this erosion has been in the toe of the landslide or in colluvium or rock-fall material from the west valley wall. Four surface projections made at right angles to line AB have shown that the average amount of downward erosion in the outlet channel since overtopping has been about 10 m and that the total amount of landslide material removed by channel erosion has been about 1 million m^3. At Argenta Falls (fig. 7) the stream has eroded through the landslide material and colluvium into more resistant Tertiary volcanic bedrock (Lipman, 1976), forming a falls that is approximately 25 m high.

Another change in the dam portion of the landslide is the large delta on the southeastern edge of the dam. This delta, which is continuing to grow into Lake San Cristobal at the mouth of Slumgullion Creek (figs. 4 and 5), is a fan composed of material eroded from the surface of the landslide and washed into the lake by Slumgullion Creek. Most of the delta probably formed soon after the landslide occurred and before vegetation obtained a hold on the landslide. Comparison of the 1992 delta in figure 4 with a similar photo taken by Larsen in 1910 shows little difference in size or character of the delta during that 82-yr period. However, considerable small-scale deposition did occur on the delta surface in 1985 both onshore and in the lake as a result of debris flows, triggered by meltwater from an unusually heavy snowpack that flowed down Slumgullion Creek. This delta-building activity will probably continue spasmodically during periods of extraordinarily heavy precipitation, causing unwanted deposition both in the lake and on the shore; however, it will have no detrimental effect on the stability of the dam.

Figure 2. Lake San Cristobal, looking upstream toward the headwaters of the Lake Fork of the Gunnison River.

STABILITY OF THE BLOCKAGE

The dam has a soil matrix (mainly clay) derived from hydrothermally altered volcanic rocks. This material has low porosity; thus, it forms a relatively water-tight dam, and, apparently, there never has been much chance of a piping failure. However, most such landslide dams have failed by surface erosion after overtopping. This one did not because the low point of the crest formed at the contact between the toe of the earth flow and the opposite bedrock and coarse-colluvium valley wall. When the rising lake overtopped the crest at its low point, it incised an average of about 10 m into the toe of the slide and the underlying colluvium/bedrock, forming an erosion-resistant stream channel across the crest about 200 m west of and 28 m higher than the pre-landslide stream. Where volcanic bedrock (Lipman, 1976) is exposed at Argenta Falls (fig. 7), the stream channel is essentially secure against erosion. The remainder of the channel has become armored by rock fragments from the colluvium that remained after removal of finer particles from the landslide material and colluvium by erosion. This spillway channel and the remaining dam have survived for 700 yr; thus, they should remain stable as the lake continues to fill with sediment from the Lake Fork and Slumgullion Creek. Lake level also will remain stable at its present elevation of 2,742 m, which is maintained by a concrete lip at the head of the spillway.

CONCLUSIONS

About 700 yrs ago, the Slumgullion earth flow dammed the Lake Fork of the Gunnison River impounding Lake San Cristobal, which today is 3.3 km long, 27 m deep, and has a volume of about 14 million m^3. Except for an average of 10 m of erosional downcutting of the natural outlet channel across the dam, little change has occurred in the geometry or character of the dam since it was formed. Because the channel now appears to be stable in regard to erosion, there is no reason to expect failure of this broad, fairly flat dam.

Figure 3. Post-landslide delta (arrows) at the head of Lake San Cristobal. This delta, which began to be deposited as the lake filled 700 yr ago, occupies about one quarter of the original lake basin.

The Slumgullion landslide dam has been considered as a possible location for construction of an embankment dam across the valley near the outlet from Lake San Cristobal (Crandell, 1958). However, such a dam does not appear to be practical because of the hazard posed by the active toe of the earth flow 1.5 km upslope and possible reactivation of the toe of the main landslide due to increase in pore pressures resulting from a higher lake level behind a man-made dam.

The two large deltas that enter Lake San Cristobal from the Lake Fork and Slumgullion Creek will not affect the stability of the natural dam. However, the Slumgullion Creek delta will continue to hinder development along the shore of the landslide dam at the northeast corner of the lake, and the two deltas will continue to slowly fill the lake basin. If rates of sedimentation from the two streams continue at the same average rate as for the past 700 yr, it can be postulated that the lake will be filled with sediment in about another 2,500 yr.

REFERENCES CITED

Costa, J.E., and Schuster, R.L., 1988, The formation and failure of natural dams: Geological Society of America Bulletin, v. 100, p. 1054–1068.

Crandell, D.R., 1958, The Slumgullion mudflow and its suitability as a dam site: U.S. Geological Survey Administrative Report, October, 8 p.

Lipman, P.W., 1976, Geologic map of the Lake City caldera area, western San Juan Mountains, southwestern Colorado: U.S. Geological Survey Miscellaneous Investigations Series Map I–962, scale 1:48,000.

Pushkarenko, V.P., and Nikitin, A.M., 1988, Experience in the regional investigation of the state of mountain lake dams in central Asia and the character of breach mudflow formation, *in* Kozlovskii, E.A., ed., Landslides and Mudflows: Moscow, UNESCO/UNEP, v. 2, p. 1359–1362.

Rickard, T.A., 1903, Across the San Juan Mountains: Engineering and Mining Journal, v. 76, p. 346.

Schuster, R.L., and Costa, J.E., 1986, A perspective on landslide dams, *in* Schuster, R.L., ed., Landslide Dams: Processes, Risk, and Mitigation: American Society of Civil Engineers Geotechnical Special Publication No. 3, p. 1–20.

Figure 4. Looking east across the downstream end of Lake San Cristobal at the delta of Slumgullion Creek (arrows; see fig. 5 for location). This delta is a fan that has formed by erosion of material on the surface of the Slumgullion earth flow and deposition of this material in Lake San Cristobal by Slumgullion Creek. Deposition probably began to occur soon after the original earth flow occurred about 700 yr ago and is continuing at present.

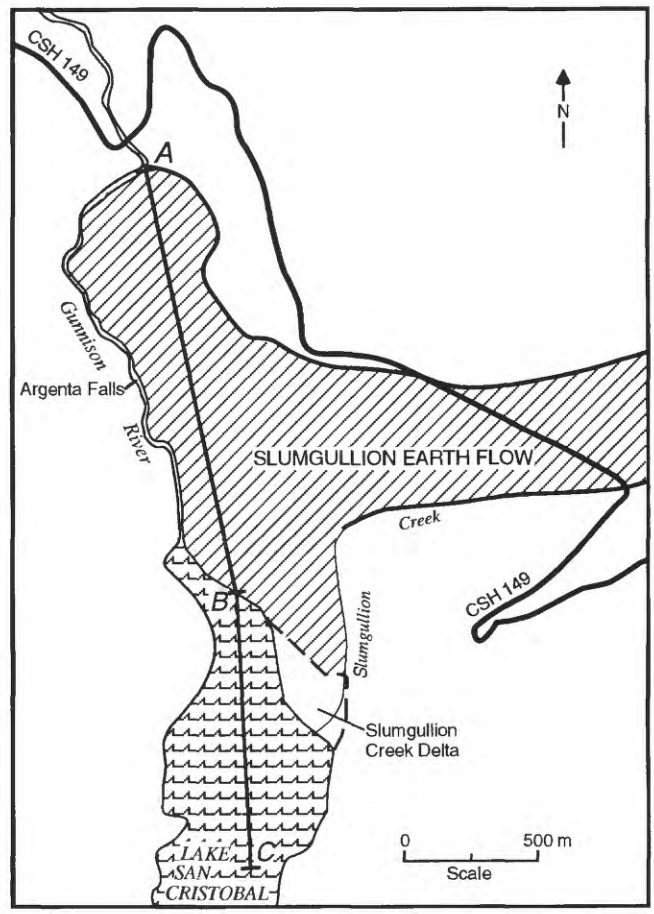

Figure 5. Outline map of the lower end of the Slumgullion earth flow and the blockage of the Lake Fork of the Gunnison River. Line ABC indicates the approximate location of the pre-landslide Lake Fork of the Gunnison River. CSH, Colorado State Highway.

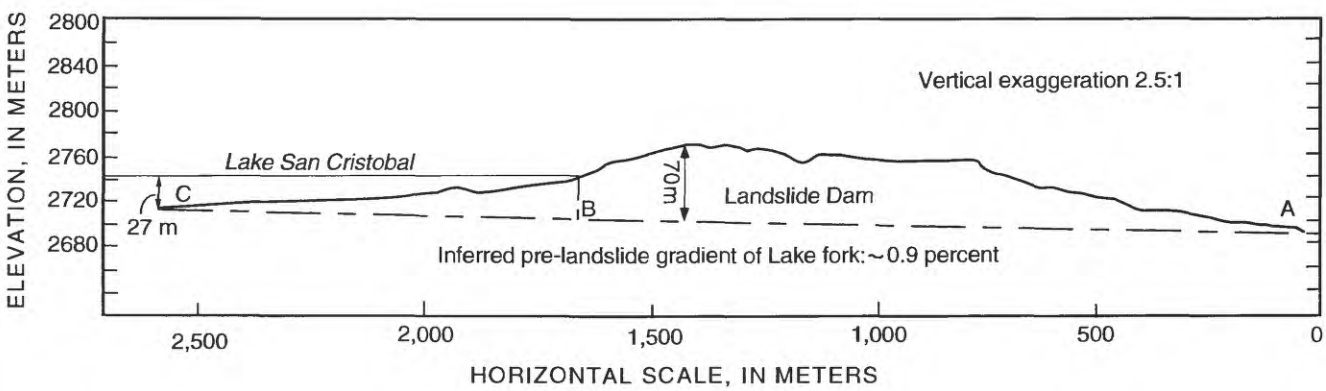

Figure 6. Surface profile across the Slumgullion landslide dam along line ABC, the estimated pre-slide position of the Lake Fork (fig. 5). The lower line shows the estimated straight-line gradient of the pre-slide Lake Fork.

Figure 7. Argenta Falls on the Lake Fork outlet channel. This 25-m-high falls has been incised in volcanic bedrock since overtopping of the landslide dam about 700 yr ago.

CHAPTER 7

DEFORMATION AND CONTROL SURVEYS, SLUMGULLION LANDSLIDE

By David J. Varnes, William K. Smith, William Z. Savage, *and* Philip S. Powers

INTRODUCTION

In 1985, the Colorado Geological Survey planned aerial photography of the Slumgullion landslide at a scale of 1:12,000 as part of its growing program on landslide hazards and offered the USGS an opportunity to share in the results. Prior to the photography, R.L. Schuster and others set out plastic strips as targets on a number of photo-control points on stable ground. Visibility between points was not a consideration and their horizontal and vertical positions were not determined at that time. In 1990, the USGS contracted for new aerial photography at scales of 1:14,000 and 1:6,000, so the 1985 points were retargeted and other control points were incorporated into a 5-km-long triangulation-trilateration control net that initially connected 17 points on stable ground. This control net, which will be briefly described below, allowed for the photogrammetric compilation of large-scale (1:1,000) topographic maps of the Slumgullion landslide from the aerial photographs taken in 1985 and 1990.

The first detailed measurements of movements of the active part of the Slumgullion landslide were begun in 1958 by D.R. Crandell and D.J. Varnes (Crandell and Varnes, 1961), who established lines of markers on the upper, active part. Movements on the body of the active slide and advance of the toe were measured occasionally for more than a decade. At the narrowest part, where the landslide is only about 160 m wide, the velocity was found to be about 6 m per year near the center and slightly less at strike-slip faults along the margins, as shown in figure 1. Movements during the period 1958–68 of a station near the center of the slide (and, for a shorter period, of a point at the base of the southern part of the toe) are shown in figure 2. Measurements were continued at a few places and at irregular intervals through 1973. In 1991, we began to investigate possible movements on the inactive part of the landslide below the active toe to determine the effects of loading by the active toe. These investigations are described in this chapter.

CONTROL SURVEYS

At the time that the triangulation net for aerial photographic control was targeted, the direction and length of the future flight line were known, but the areal coverage of individual photograph frames was not known. Because of this, the triangulation stations and targeted photo-control points turned out to be not very well distributed for photogrammetric compilation, particularly for control of the more detailed 1:6,000 photography. The distribution of the 22 triangulation points, which were in place by 1993, and some of their names are shown in figure 3. Their positions are referenced to a coordinate grid based at station WINDY (Coordinates 10,000 m north, 10,000 m east) at the Windy Point Overlook on a spur off State Highway 149. Local north was estimated from the available 1:24,000-scale topographic map. Elevations are referenced to U.S. Coast and Geodetic Survey bench mark H 169 on the old part of the landslide, near its southern border, a small distance west of the curve of State Highway 149 (fig. 4).

Although the distribution of triangulation points was sparse owing to difficulty in selecting mutually visible points among obscuring ridges and within the heavy forest around the landslide, the photogrammetrists were able to construct topographic maps at 1:1,000 and other scales. These became bases for a variety of subsequent geologic and deformation studies by geologists working on the active slide, including several from the Italian National Research Council.

DEFORMATION SURVEYS BELOW THE ACTIVE TOE

As work progressed on the active slide, we turned our attention toward the apparently inactive part to determine whether it was responding to loading from the 1 m per year advancement of the 40-m-high active toe. The quickest and

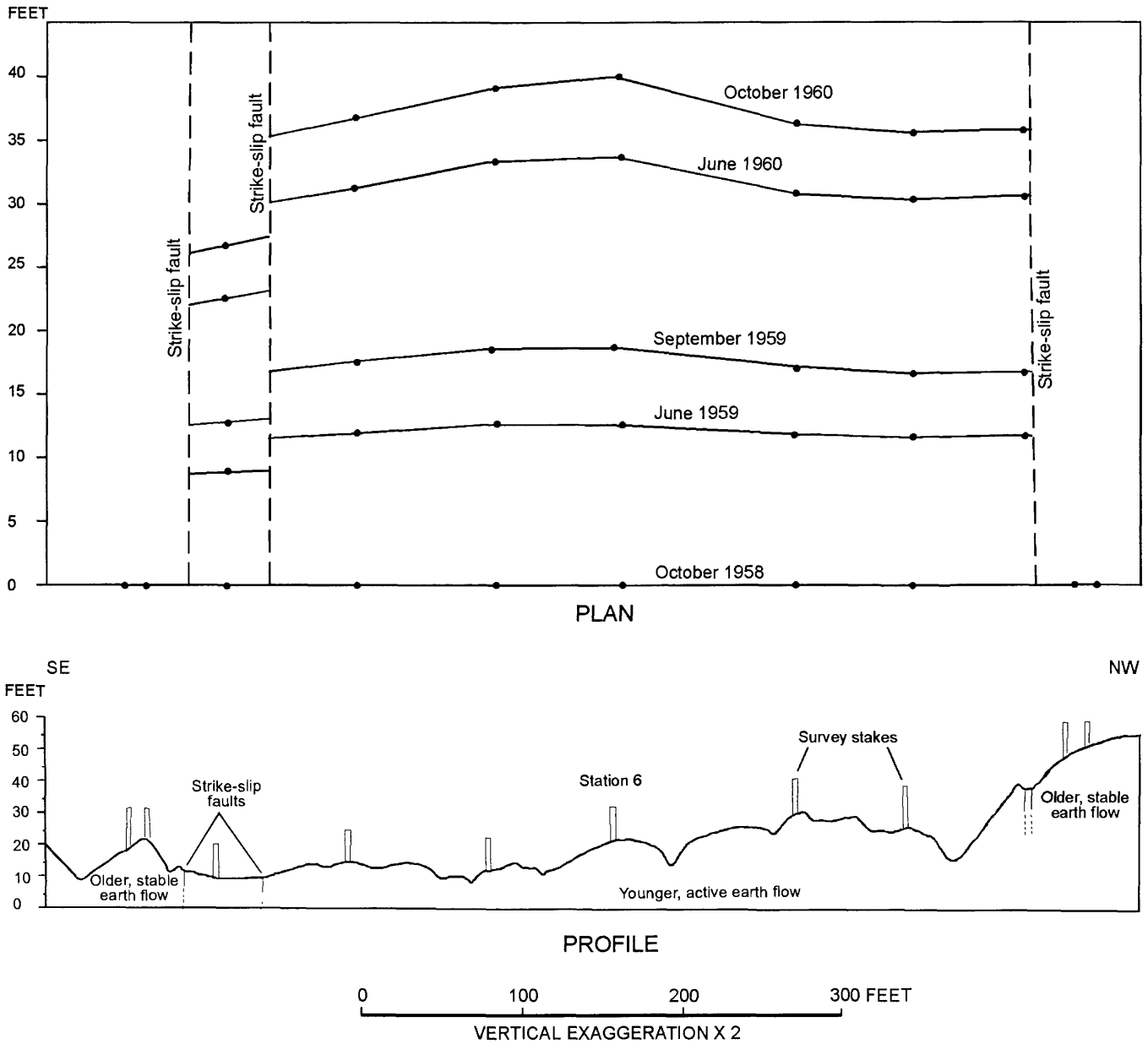

Figure 1. Plan and profile of movement at locality D (see fig. 3) in narrow part of the active Slumgullion Slide, between October 1958 and October 1960 (from Crandell and Varnes, 1961).

most accurate means to detect possible movement, although only in a vertical direction, was by leveling. The initial step was to lay out, in 1991, loops of level circuits from bench mark H 169 northeastward in front of the active toe. As bench mark H 169 is itself on the old slide, about 230 m from the active front, and may be in an unstable area next to a ravine, we also ran levels from the bench mark southwestward along State Highway 149 beyond the old slide into a supposedly stable area. The principal circuits (labeled green, blue, red, and black, respectively, from southwest to northeast) are shown in figure 4.

The first remeasurement of level lines, in 1992, showed that, during 1 yr, some points close to the active toe had moved down as much as 20 mm, while points 50 to 100 m from the front had subsided smaller but still observeable amounts. These findings made it necessary to determine whether horizontal displacements and deformations also were occurring. In 1992, to detect these horizontal movements, we laid out quadrilaterals and triangles with sides of 20 to 90 m using electronic distance measurement (EDM) in three areas in front of the active toe and located stations in a closed traverse about 1 km long around the

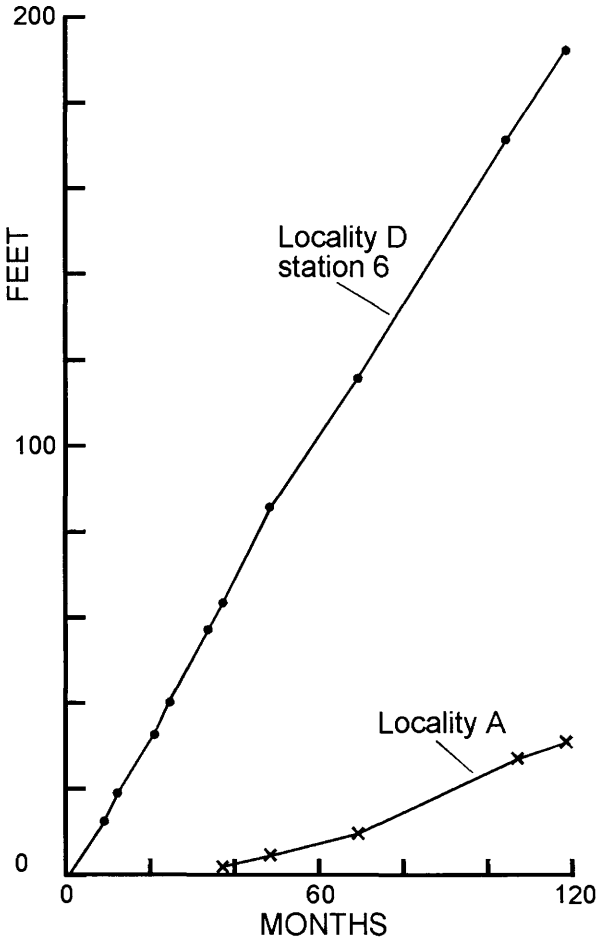

Figure 2. Displacements for the period 1958–68 of station 6, locality D, near the center of the slide, and at locality A, at the toe of the active front (see fig. 3).

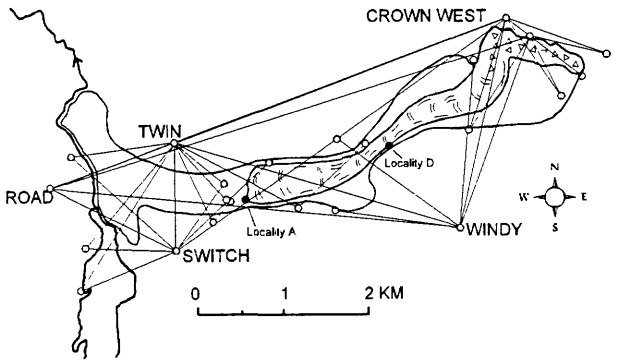

Figure 3. Triangulation-trilateration network at the Slumgullion Slide, showing a few of the station names. The active part is patterned within the borders of the older, inactive landslide.

principal (blue) level circuit. A dense triangulation-trilateration net perhaps would yield more closely spaced data concerning deformation, but that was impractical in this forested area. The quadrilaterals and triangles were remeasured 2 months later. All results of these surveys as of the end of the 1992 field season, were summarized and subsequently published in U. S. Geological Survey Open-File Report 93-577 (Varnes and others, 1993).

The principal level lines, quadrilaterals, and triangles were again remeasured in the spring of 1993. Total changes, generally for about a 2-yr period during 1991 to 1993, are shown in figures 5, 6, 7, and 8. Continued vertical movements near the active front resulted in the accumulated changes shown in figure 5. All movements were down except at three places very close to the active toe—two on prominent rising rolls at the northwest border of the toe near station T13 and at TP7 near the southeast border on wet unstable ground—and at TP77 along the highway (see figs. 5 and 6). The use of points in the broad hillside shoulder and ditch along the highway has become questionable. Point TP79, showing the large 29.2 mm depression during a period of 1 yr, may have been run over by road equipment; TP77, showing a 4.5-mm rise in 1991–92 was later torn out of the ground. Otherwise, the subsidence along the active front noted in 1992 continued into 1993, with some indications that depression is more rapid near the northern part of the front than at the southern part.

The braced quadrilateral shown in figure 6 near the curve in State Highway 149 was laid out in 1992. Unrecognized problems during the resurveying in 1993 apparently involved the westernmost station, TP200. All three triangles that include that point do not close within acceptable errors, even though the horizontal angles observed at TP200 added up satisfactorily to 360°. Farther north, in the quadrilateral and triangle at POND (figs. 6 and 7), four of the eight lines had changes in horizontal distance of more than 4 mm in 1 yr. All of these lines involve station TP204, which is on marshy ground and may be unstable.

The four triangles in the red level circuit on the bench northeast of POND (see fig. 8) show many changes in distances and angles during 1 yr that are larger than the probable errors of adjusted observations. The probable errors are not yet established, but, in small triangles such as these, they are believed to be about 2–4 mm in distance and about 5 seconds in angle. The measurements made so far suggest that stations TP30 and TP202 are both moving away from station TP31A, which is close to the active front. Triangle TP32–TP202–TP32B appears to be contracting slightly and uniformly.

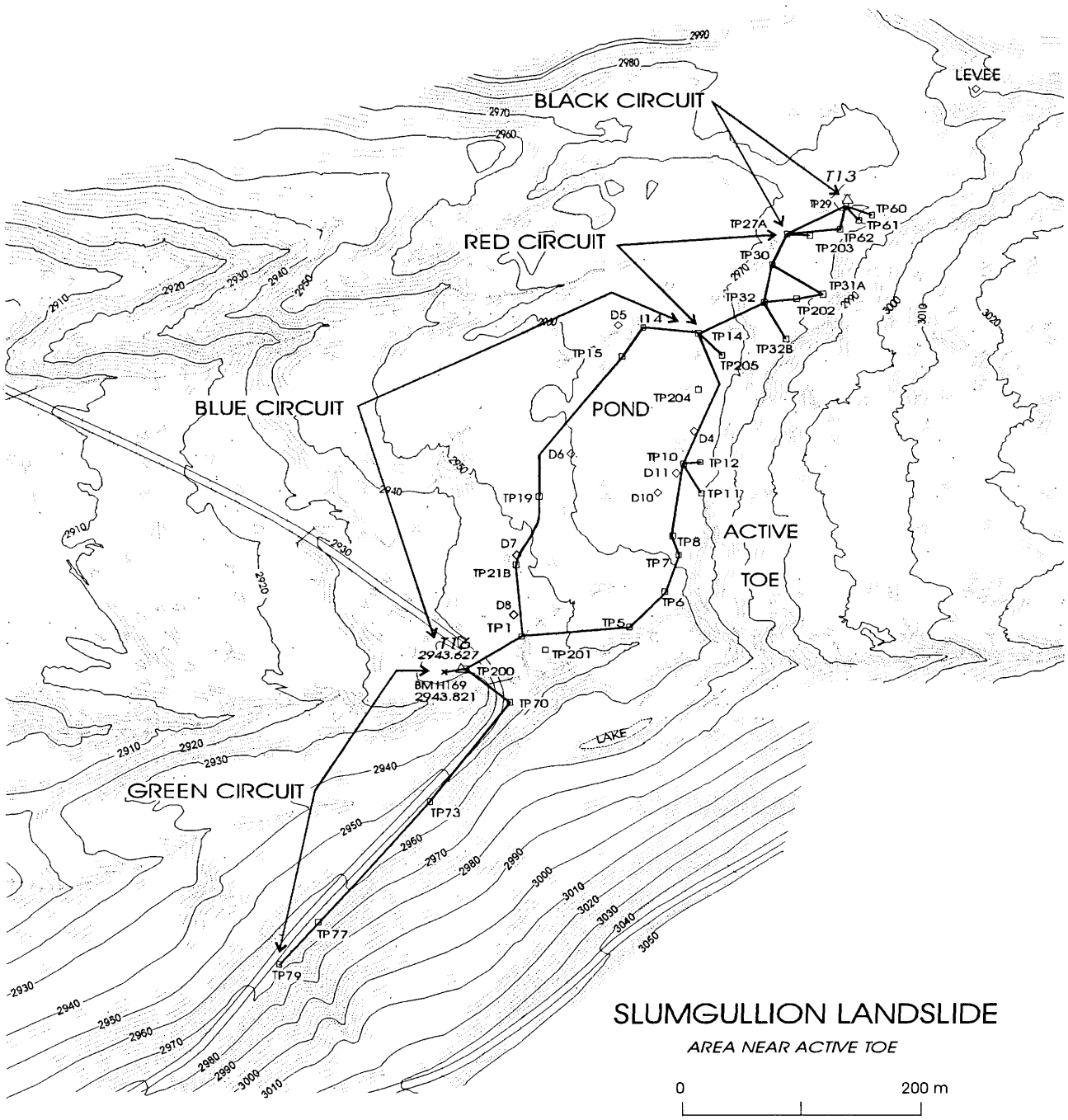

Figure 4. Map of the area near the active toe of the Slumgullion Slide, showing circuits of leveled lines.

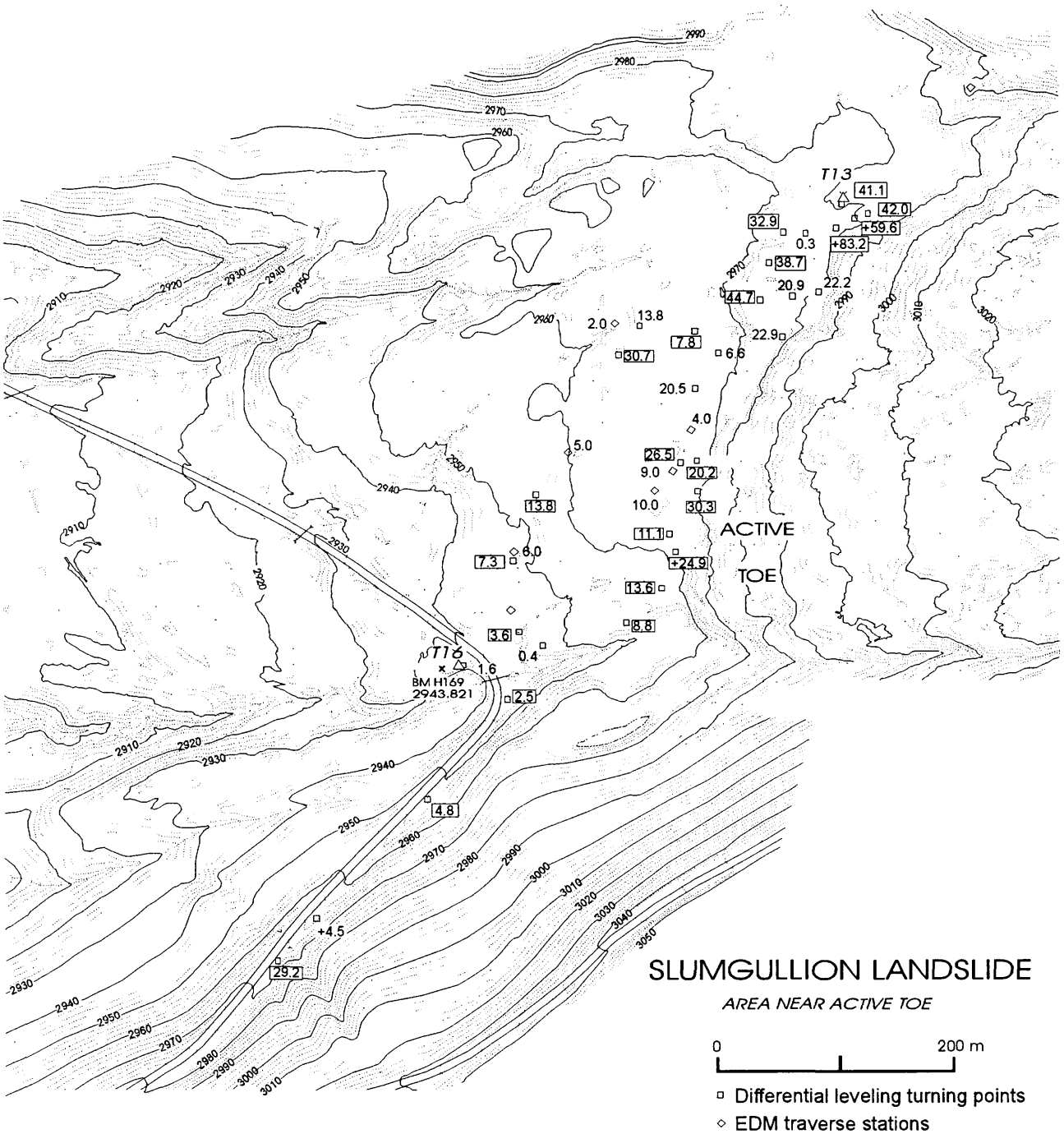

Figure 5. Vertical movements, in millimeters, near the active toe, 1991–93. All movements are downward unless marked "+." Boxed values are for 2 yr, unboxed values are for 1 yr only. EDM, electronic distance measurement.

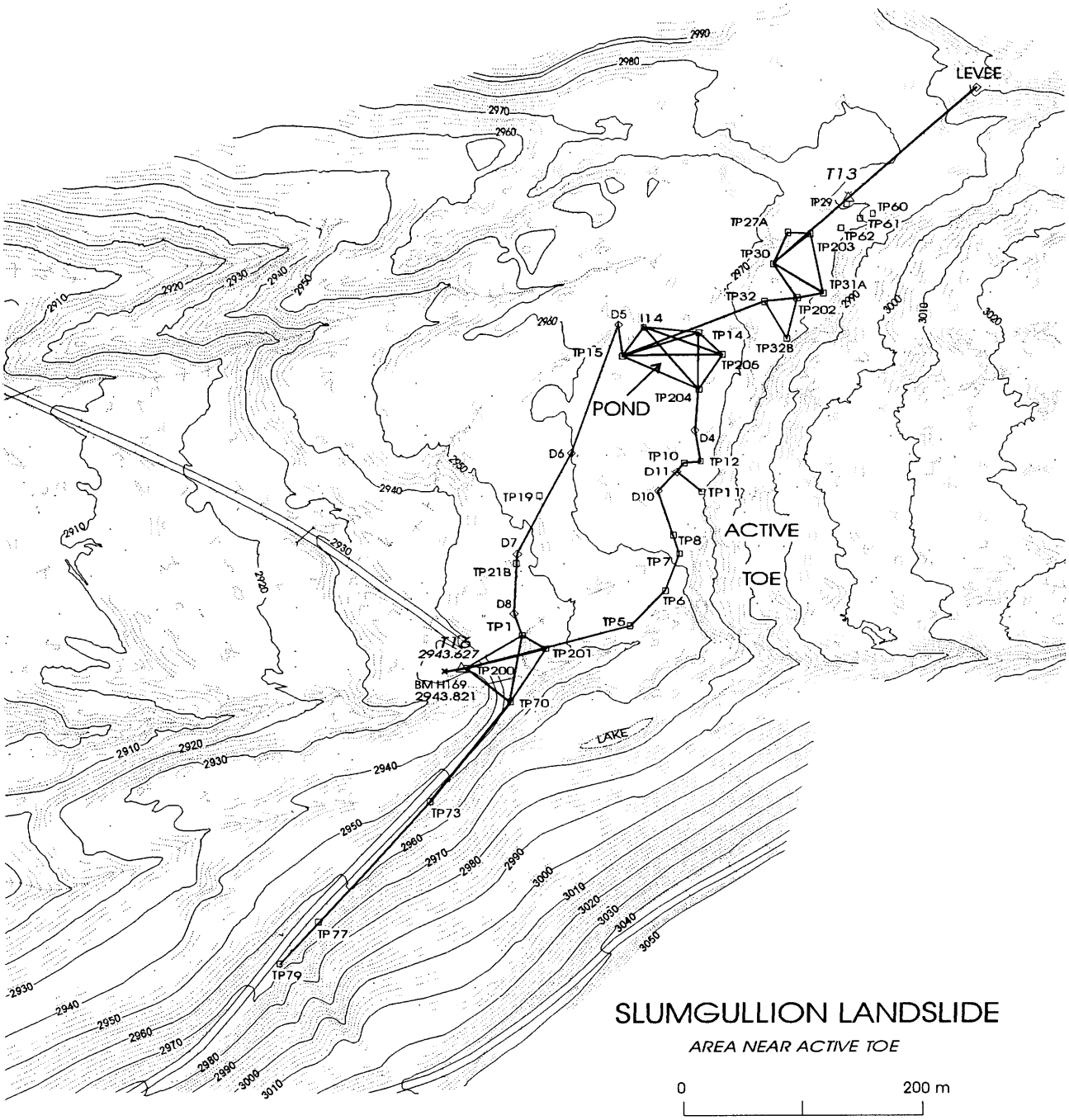

Figure 6. Map of the area near the active toe of the Slumgullion Slide, showing electronic distance measurement (EDM) traverses, quadrilaterals, and triangles.

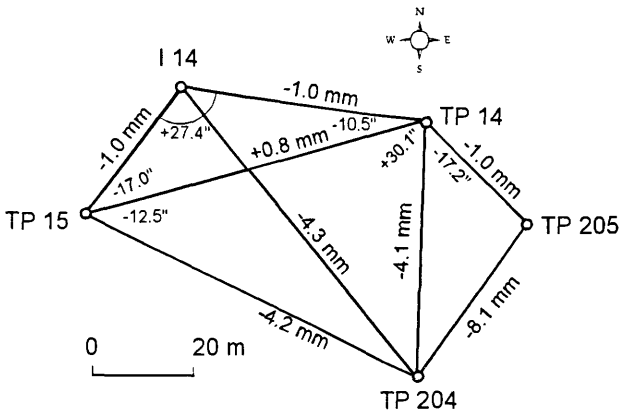

Figure 7. Sketch of pentagon at POND showing changes in length (mm) and angle changes (seconds of arc) from May 1992 to June 1993.

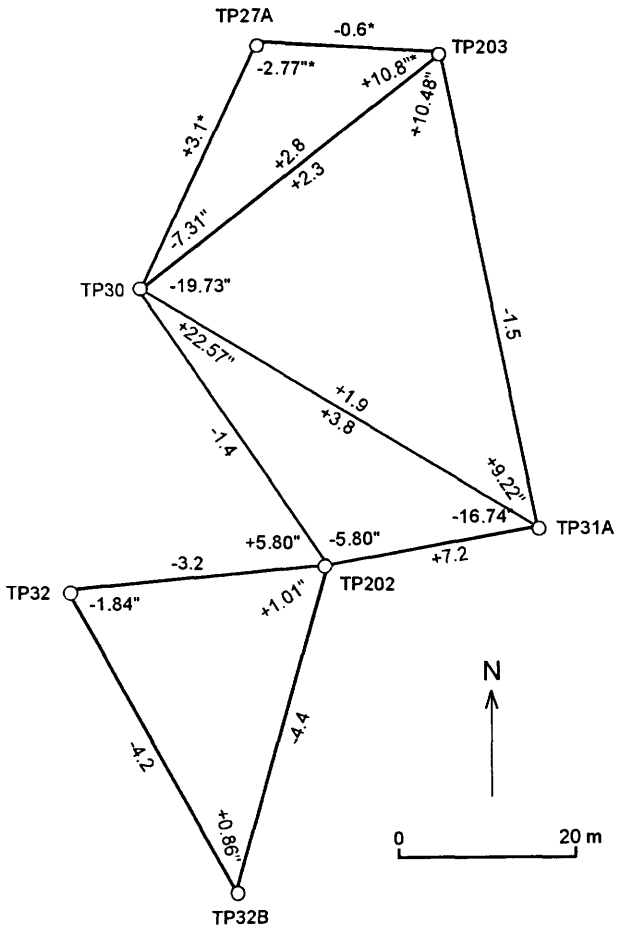

Figure 8. Sketch of triangles near TP30, showing length (mm), and angle changes (seconds of arc) from May 1992 to June 1993.

CONCLUSIONS

Surveys to date indicate that the inactive part of the Slumgullion landslide is responding to changing loads caused by the advancing toe and is not as stable as previously assumed. In general, ground is depressed in front of the advancing toe, the amount decreasing with distance from the toe. However, three points very close to the toe have risen significant amounts (20–80 mm) in 2 yr. We are continuing to monitor these movements and expect a clearer deformation pattern to emerge.

ACKNOWLEDGMENTS

We thank our colleagues who assisted at various times in the leveling and deformation surveys, including M. Arattano, S. Cannon, M. Chiarle, S. Diehl, D. Eversoll, R. Fleming, M. Giardino, R. Guzzi, M. Paresi, J. Savage, and K. Varnes.

REFERENCES CITED

Crandell, D.R., and Varnes, D.J., 1961, Movement of the Slumgullion earthflow near Lake City, Colorado, *in* Geological Survey Research 1961: U.S. Geological Survey Professional Paper 424–B, p. 136–139.

Varnes, D.J., Smith, W.K., Savage, W.Z., and Varnes, K.L., 1993, Control and deformation surveys at the Slumgullion Slide, Hinsdale County, Colorado—A progress report: U.S. Geological Survey Open-File Report 93-577, 15 p., 1 pl.

CHAPTER 8

A DIGITAL PHOTOGRAMMETRIC METHOD TO MEASURE HORIZONTAL SURFICIAL MOVEMENTS ON THE SLUMGULLION LANDSLIDE, HINSDALE COUNTY, COLORADO

By Philip S. Powers *and* Marta Chiarle

INTRODUCTION

The traditional approach to making aerial photographic measurements uses analog or analytic photogrammetric equipment. This method usually yields accurate results (accurate to 0.5 m at 1:12,000 scale) but requires expensive instruments, takes considerable time, and requires a trained operator to set the models and acquire the results. We have developed an alternative digital method for making measurements from aerial photographs by using Geographic Information Systems (GIS) software and mostly DOS based PC computers. This method was applied to determining the movements of visually identifiable objects, such as trees and large rocks, on the surface of the active portion of the Slumgullion landslide. The technique is based on the concept that a direct visual comparison can be made between images derived from two sets of aerial photographs taken at different times. Horizontal displacement vectors on the active slide have been measured directly from ortho-images that were produced by digital photogrammetric techniques using 1985 (1:12,000 scale) and 1990 (1:6,000 scale) aerial photographs.

For the concept to work, there must be enough movement during the period between times of the aerial photography to make measurements with accceptable accuracy. Excessive movement between aerial photographs can also be a problem, as it may be difficult to relate the two images directly. In the 5-yr period between our aerial photographs, the fastest moving portion of the landslide should have moved about 25 to 30 m (Crandell and Varnes, 1961). We estimated that over most of the active slide, 15 to 20 m of displacement should occur in a 5-yr period. A 2-m measurement error (approximately 10 percent) for a direct comparison method was our minimum standard.

METHODOLOGY

Before accurate measurements can be made between two sets of aerial photographs, tilt and distortion must be removed. In our study, this could only be done by processing the photographs and transforming the images into relief-corrected ortho-images, which became the most difficult part of the work.

The process of producing tilt-free, differentially rectified, digital ortho-photos (ortho-images) from aerial photographs taken in mountainous terrain requires excellent ground control information and sophisticated software. Desktop Mapping System (DMS) with Softcopy Photo Mapper (DMS/SPM) 3.1(c), by R-Wel, Inc. 1992, was used at the GIS laboratory, USGS National Mapping Division, Rocky Mountain Mapping Center, to produce the ortho-images. DMS/SPM runs on a DOS-based 386/486 PC computer and uses the same rigorous photogrammetric techniques as those used in standard photogrammetry.

Part of the ground control necessary to produce an ortho-image with DMS/SPM is an accurate digital elevation model (DEM) of the area. Photogrammetric work had been completed by 1992 on both sets of aerial photographs, and accurate digital elevation models had been created from the digital contour data (Powers and others, 1992).

THE PROCESS OF MAKING AN ORTHO-IMAGE

Photographic color transparencies (diapositives) of the landslide aerial photographs were scanned at 400 dpi (dots per inch) with a Howtek scanner attached to a Macintosh computer running Adobe Photoshop. An image

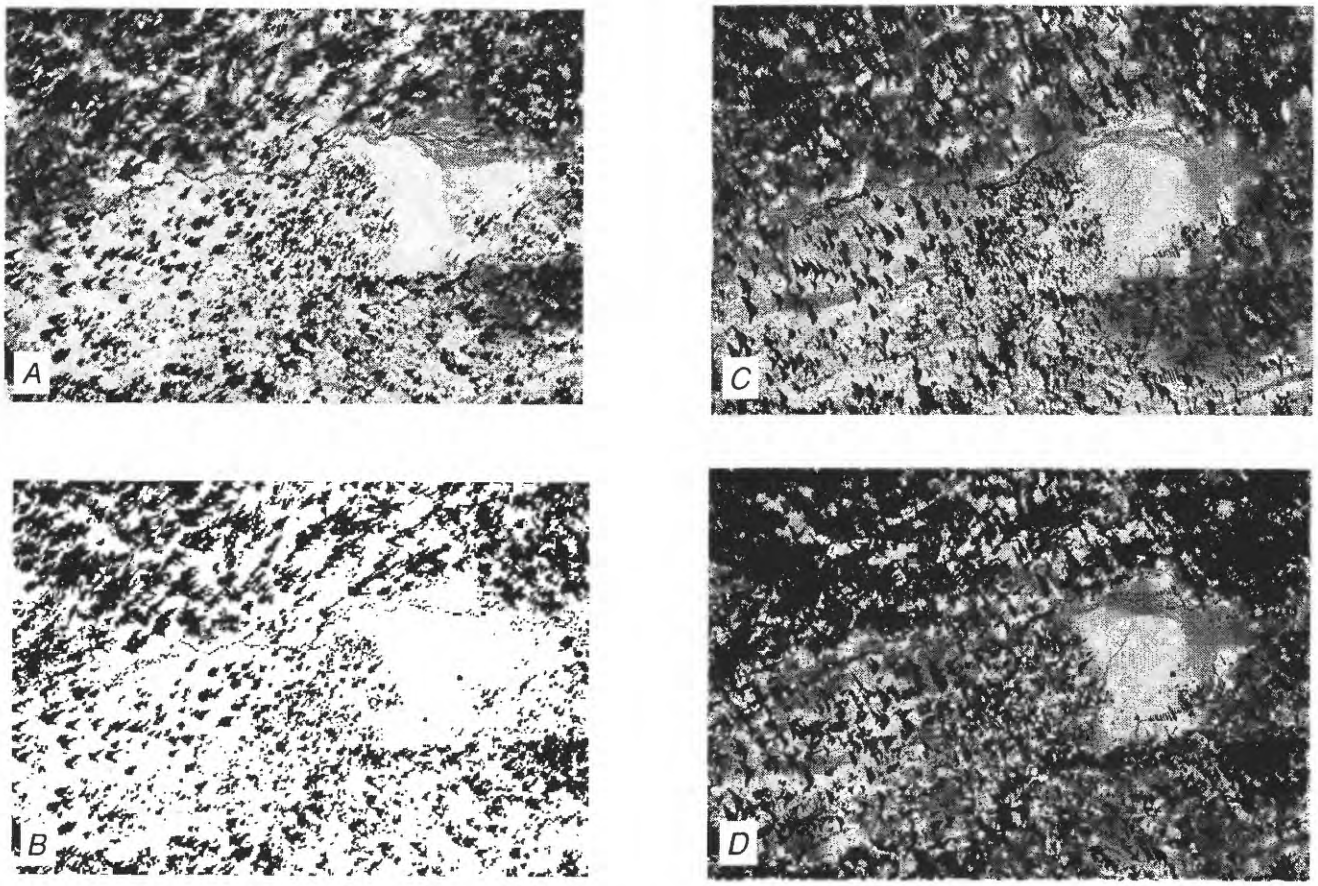

Figure 1. *A*, Gray-scale ortho-image above active toe (1985); *B*, Monochrome ortho-image above the active toe (1985); *C*, Gray-scale ortho-image above active toe (1990); *D*, Gray-scale 1990 image visible though monochrome 1985 image.

produced from a scanned diapositive contains more visual detail than a photographic print. The complete color diapositive was scanned, including the fiducal marks, and then converted to 256 shades of gray. Each image required approximately 14 MB of disk space. The scanned images were then transferred over a network to the DOS-based PC that runs DMS software.

Using established survey ground control coordinates (Varnes and others, 1993), we then established the relationship between the image and the survey coordinate system. The survey ground control coordinates were entered in a file, where the *x, y, z* values for each control point were identified by a unique identification number. The identification numbers were then related to the displayed image by clicking on their screen location with the digitizing device (mouse). This process was done for each image of a stereo pair: the two images do not need the same ground control points.

The orientation was then computed for each image, and the effect each ground control point had on the solution was analyzed. It was at this stage that a ground control point could be removed, or additional points could be added later if desired. At least five points for each image are required by the DMS/SPM program to compute the orientation.

Working with the stereo model as an anaglyph display of red and blue images on the computer screen, and using red-and-blue-lens spectacles, we measured the coordinates for survey and photogrammetric control points. This was done by positioning the floating mark (dot) on the ground surface at the point to be measured and recording the *x, y, z* coordinates. The coordinates were then checked against the ground control points for accuracy.

The coverage for the ortho-photo is then selected from either the left or right scanned aerial photos. The cubic convolution method, the DEM, and the exact photogrammetric solution derived earlier with the DMS/SPM program are then used to generate the differentially rectified ortho-image. Note that this DEM must cover the entire area that is to be ortho-rectified.

The ortho-image, which was still referenced to our local coordinate system, was then checked against the ground control and photogrammetric points. The image was then converted to a Tagged Image File Format (TIFF) image, transferred to a different PC, imported into a raster editing program for processing, and then imported to CorelDraw for direct comparison with a second image.

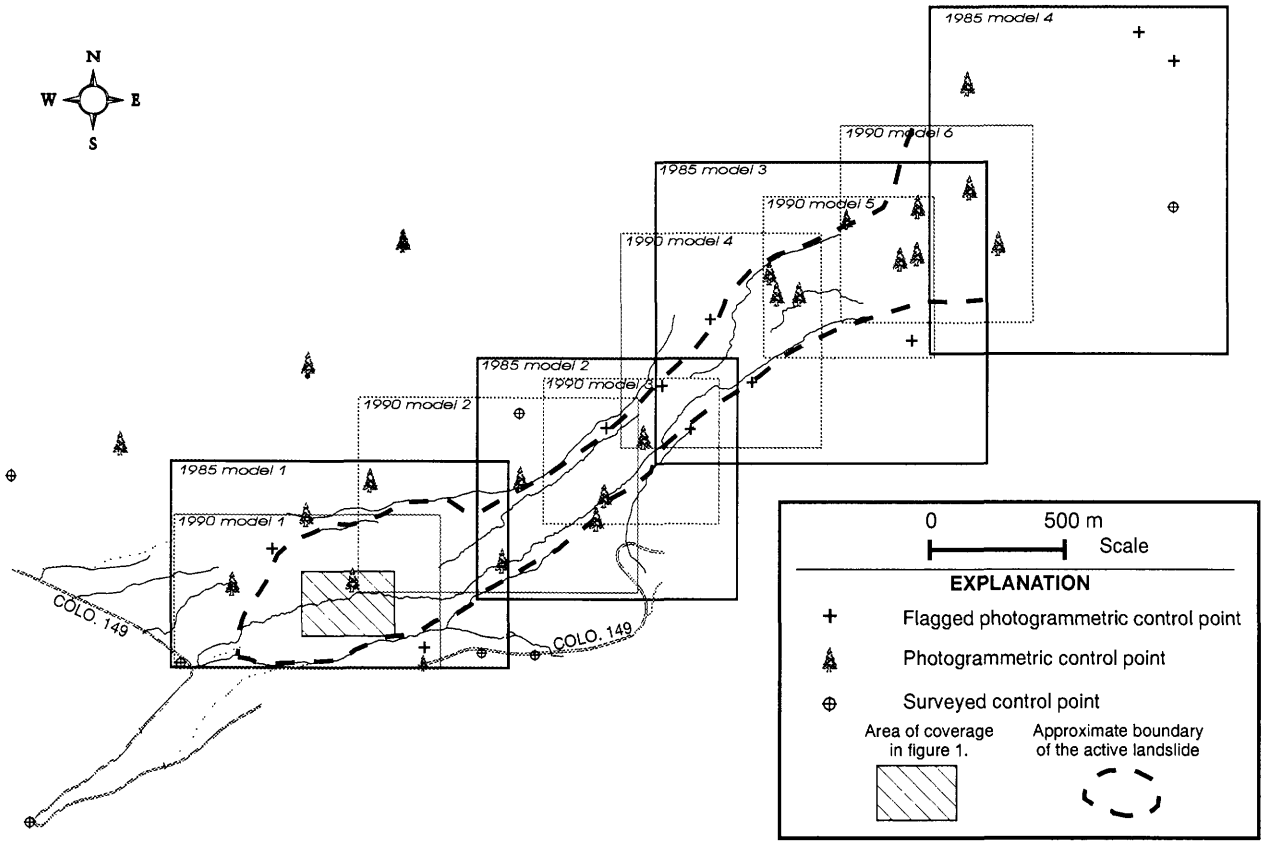

Figure 2. Distribution of ground control points and positions of stereo models with relation to the active landslide.

MAKING THE DIRECT COMPARISON

We were able to directly compare two ortho-photos by registering each to ground control and mapping the junction of trees and their shadows in the open areas of the active slide. This was done by converting a 1985 gray-scale image to a monochrome image with a passive white (transparent) and a black color, and mapping from the 1985 monochrome image to the 1990 gray-scale image through the transparent zones of the 1985 image (fig. 1). This process was continued until the stereo pairs for both 1985 and 1990 (fig. 2) were combined in one 32.5-MB file and all the displacement vectors representing movements of points on the landslide were drawn (fig. 3).

PROCESSING THE DISPLACEMENT DATA

The first step in processing the displacement data was to separate the vectors from the remainder of the CorelDraw file. Because the vectors were in units used in the plotting program, ARCINFO and a spreadsheet program were used to convert the vectors to proper units of magnitude and direction (meters and degrees). The processed spreadsheet file was then used as an input into Golden Software's SURFER program, and the magnitudes were contoured using a minimum-curvature algorithm. This contour file was then imported into CorelDraw and combined with the vectors to produce a final plot.

ACCURACY

The photogrammetric work done by Smith (1993) provided numerous ground control check points to verify the accuracy of our results. Smith's photogrammetric work was reported to have a standard deviation of 0.44 m in horizontal position.

Accuracies were measured at three different stages. The first stage was during viewing of the DMS stereo model. The next series of accuracies were recorded while viewing the geocoded ortho-image. The last and final set of accuracies was recorded in CorelDraw prior to drawing the displacement vectors. Table 1 is a summary of the simple averaged differences.

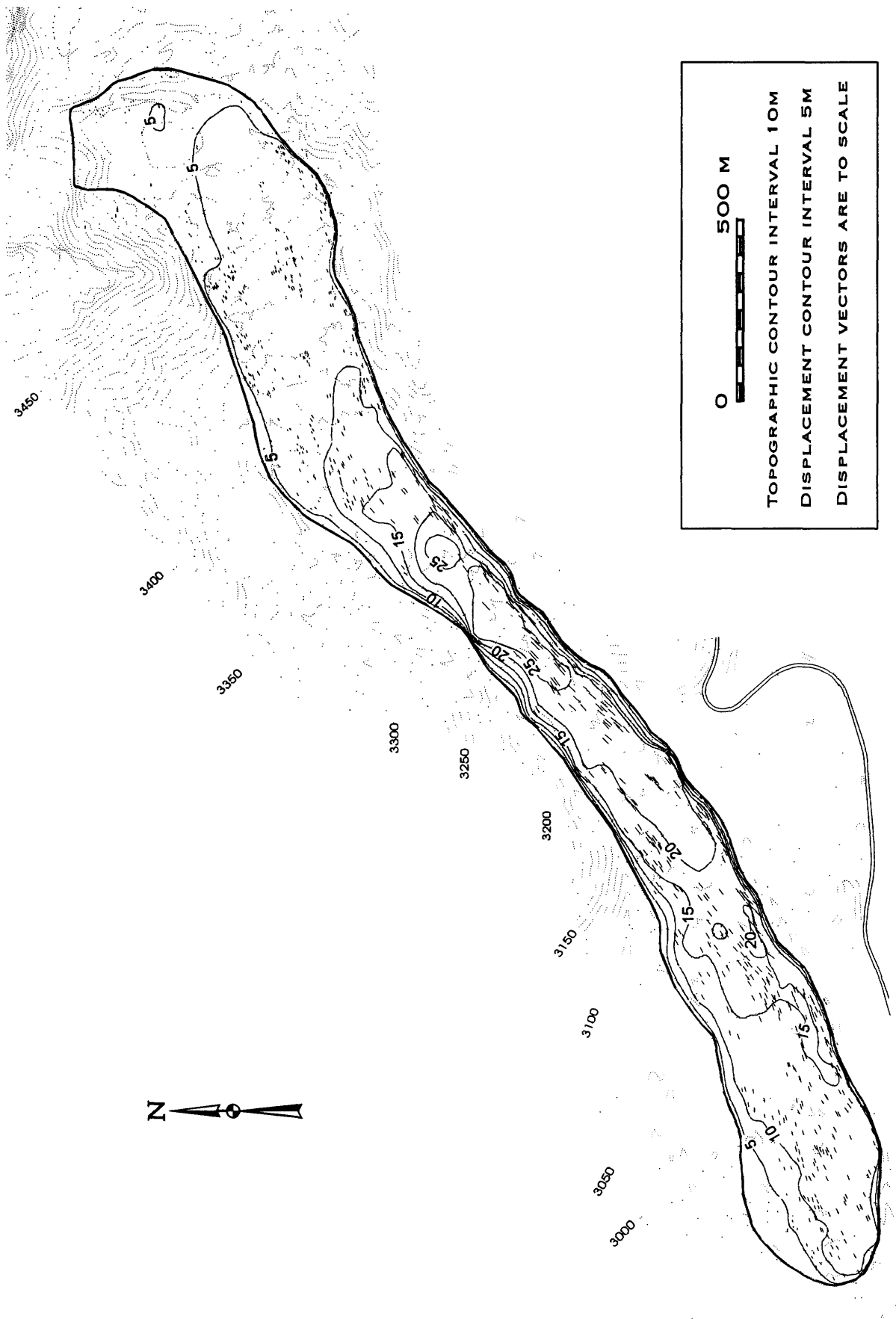

Figure 3. Slumgullion landslide horizontal displacement vectors and contours, 1985–90.

Table 1. Summary of accuracies.

[*x*, east-west; *y*, north-south; *z*, vertical; Avg err, average errors. Leaders (--) indicate no data]

	Avg err in *x* (m)	Avg err in *y* (m)	Avg err in *xy* (m)	Avg err in *z* (m)
Stereo models 1990	0.9	1.4	1.7	3.3
Stereo models 1985	1.3	2.0	2.4	5.2
Ortho-images 1990	1.2	1.1	1.6	--
Ortho-images 1985	1.6	1.3	2.1	--
CorelDraw 1990	1.1	1.1	1.6	--
CorelDraw 1985	1.7	1.0	2.0	--

The average errors of the ortho-images and the CorelDraw images are almost the same. This suggests that there is no loss of accuracy during the conversion. The stereo model errors are slightly larger, probably due to the difficulty of viewing portions of the image in three dimensions: good three-dimensional perspective is necessary to make accurate measurements. The slightly higher average errors in the table for the 1985 data are caused by the difference in scale between the original aerial photographs (1:12,000 for 1985, and 1:6,000 for 1990).

CONCLUSIONS

Direct visual comparisons can be made between ortho-images produced from two sequences of aerial photographs taken at different scales. Horizontal motion vectors can be measured accurately between ortho-images by direct comparison. This approach provides a method to measure motion over more of the slide surface in a shorter period of time than the standard photogrammetric approach.

More than 800 motion vectors have been drawn on the active slide surface, and a horizontal vector displacement map with displacement contours has been produced showing the 5-yr movement between 1985 and 1990 (fig. 3). The map is in AutoCad DXF format and is available for additional studies.

We learned from this study that distribution of ground control is most important and must be taken into account prior to the taking of any aerial photographs. Ground control must be evenly distributed along both sides of the area of interest, with several points within the area of interest. We found that the accuracy of the ortho-images greatly improved after adding additional control points. These points, from the photogrammetric work of Smith (1993), were added along the sides and within the slide (fig. 2).

The newly developed digital technique proved to be a viable tool for the analysis of the Slumgullion aerial photographs, especially when comparing two different sets of aerial photographs. It has been applied to the measurement of surficial movements on an active slide, but could be useful in the study of aerial photographs of any kind of feature that changes position with time. The method is not a definitive one: the choice among topographic survey, analog (or analytic) photogrammetry, and digital photogrammetry must take in account the economic, human, and time resources available and the requirements of accuracy.

ACKNOWLEDGMENTS

The authors wish to thank Robert Desawal and Michael Crane of the USGS National Mapping Division, Rocky Mountain Mapping Center.

REFERENCES CITED

Crandell, D.R., and Varnes, D.J., 1961, Movement of the Slumgullion earthflow near Lake City, Colorado, *in* Geological Survey Research, 1961: U.S. Geological Survey Professional Paper 424–B, art. 57, p. 136–139.

Powers, P.S., Varnes, D.J., and Savage, W.Z., 1992, Digital elevation models for Slumgullion landslide, Hinsdale County, Colorado based on 1985 and 1990 aerial photography: U.S. Geological Survey Open-File Report 92-535, 5 p.

Smith, W.K., 1993, Photogrammetric determination of movement on the Slumgullion Slide, Hinsdale County, Colorado, 1985–1990: U.S. Geological Survey Open-File Report 93-597, 17 p.

Varnes, D.J., Smith, W.K., Savage, W.Z., and Varnes, K.L., 1993, Control and deformation surveys at the Slumgullion Slide, Hinsdale County, Colorado—A progress report: U.S. Geological Survey Open-File Report 93-577, 15 p., 1 pl.

CHAPTER 9

PHOTOGRAMMETRIC DETERMINATION OF SLOPE MOVEMENTS ON THE SLUMGULLION LANDSLIDE

By William K. Smith

INTRODUCTION

As part of the multidisciplinary study of the Slumgullion landslide, aerial photographs taken August 12, 1985, and August 25, 1990, were compared using photo-identifiable natural features to determine the displacements of different parts of the active slide between the two dates.

There is scant literature describing the use of photogrammetry to determine displacements of natural features on active landslides. At the La Frasse landslide, Switzerland, aerial photographs at scales of 1:25,000 and 1:40,000 were used to calculate displacements of natural points over four time periods between 1957 and 1982 (Bonnard, 1984). Baum and Fleming (1991) used aerial photogrammetry to determine the displacement of about 150 points on the Twin Lake landslide, Utah, and integrated these measurements with detailed field mapping to identify different elements of the slide. Baum and Reid (1992) determined the displacements of about two dozen ground points and about 100 points on roofs of houses on an active slide in Hawaii.

Theoretically, the use of natural photo-identifiable targets gives the interpreter an almost unlimited supply of potential data points, without the need for placing large arrays of artificial targets in the field. Furthermore, the photographs themselves provide a permanent record of the conditions existing at the time of exposure, which allows one to go back and get more data points or to remeasure questionable ones. One may also be able to make kinematic interpretations of the measurements with respect to physical features (such as faults or cracks) visible on the photographs. Another advantage is that photographs record positions of all points at an instant; significant movements may take place during an extensive conventional survey. Once corresponding points are identified, it is faster to locate them photogrammetrically than by conventional field surveying, although at the cost of some loss of accuracy. The principal advantage of the method, however, is that one can measure displacements on older photographs, provided that suitable targets on the moving slide can be identified, and that a sufficient number of photogrammetric control points on stable ground can be identified.

METHODOLOGY

A local Cartesian coordinate system was developed in 1990 by a survey to establish photogrammetric control for both the 1985 and 1990 photography and to provide a consistent reference system for other studies of the Slumgullion landslide. Measurements on both sets of photographs were based on this local system. Varnes and others (1993, this volume) provide more detailed descriptions of the coordinate system and the survey network.

The method for determining displacements at individual points consists of finding the same photo-identifiable points on both the 1985 and 1990 photographs, then measuring the coordinates of the points with a stereoplotting instrument with an attached microcomputer. Instruments used were a Kern DSR-11 analytical plotter and a computer-assisted Kern PG-2 mechanical plotter. In both instruments, a computer calculates and displays the coordinates and elevation of the measuring mark (floating dot) based on the input coordinates of photo control points and photogrammetric parameters. The photo-identifiable points, other than targeted control points, consisted entirely of the bases of trees and bushes.

The accuracy and reproducibility of coordinate measurements from photographs depend on a variety of factors. Based on remeasurement of 28 points on several models of the 1985 photography, the standard deviation of a horizontal position measurement, $[((\Delta x)^2+(\Delta y)^2)^{1/2}]$, in this study is about 0.44 m, resulting in a standard deviation of a calculated vector displacement of 0.63 m (Smith, 1993). The reproducibility of the elevation measurements is not as good as that of horizontal position. Of the 28 remeasured points, 17 had elevation discrepancies greater than 0.5 m. These discrepancies occur because it is often difficult to place the floating dot accurately on the ground at the base of the tree as the surrounding ground detail is obscured by the tree's shadow on one side and the image of the tree on another. The difficulty increases with larger trees and steeper ground.

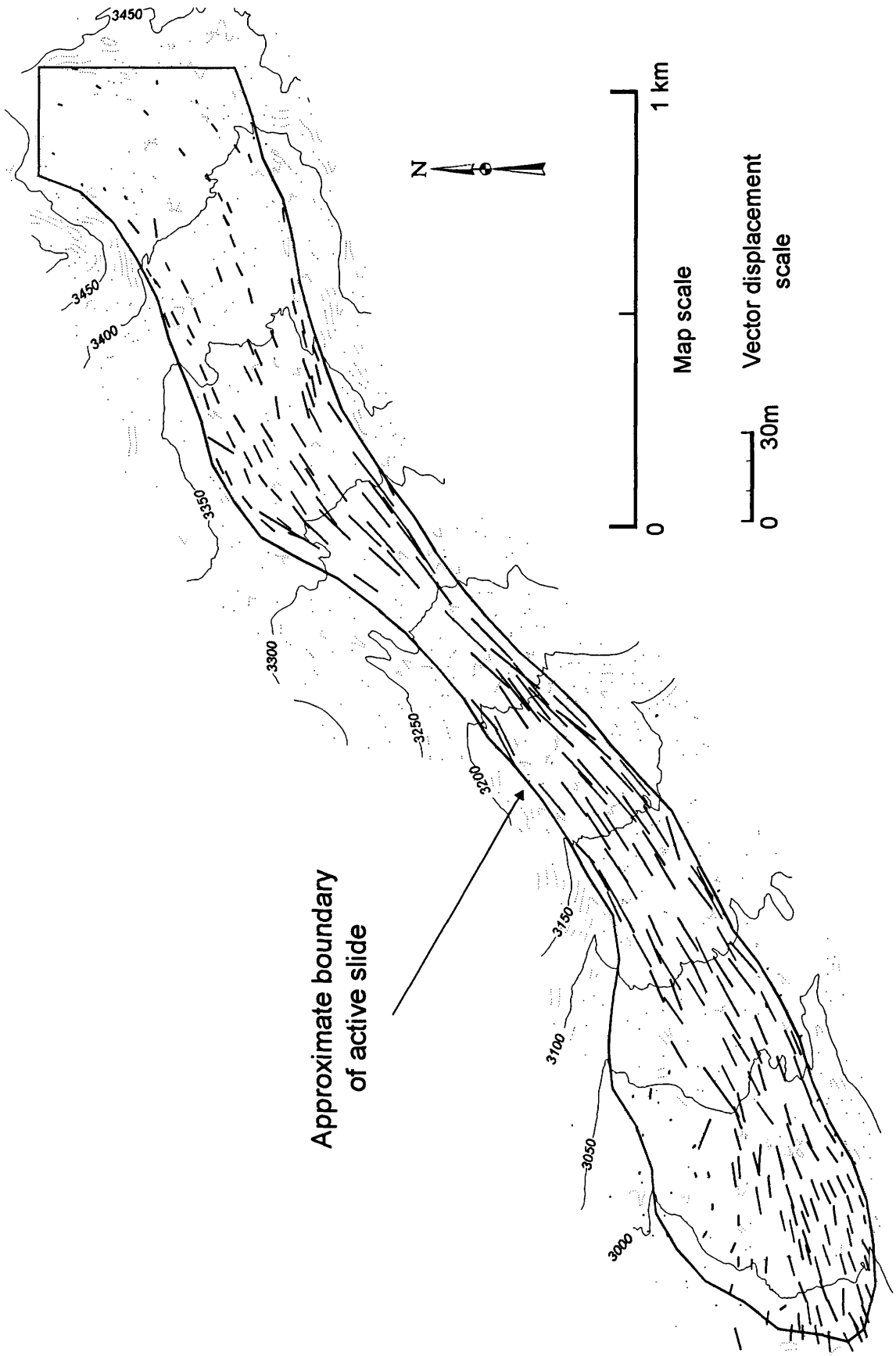

Figure 1. Map of active part of the Slumgullion landslide showing vectors of horizontal displacement between 1985 and 1990. Topographic contour interval is 10 m. All vectors are directed downslope, from upper right to lower left.

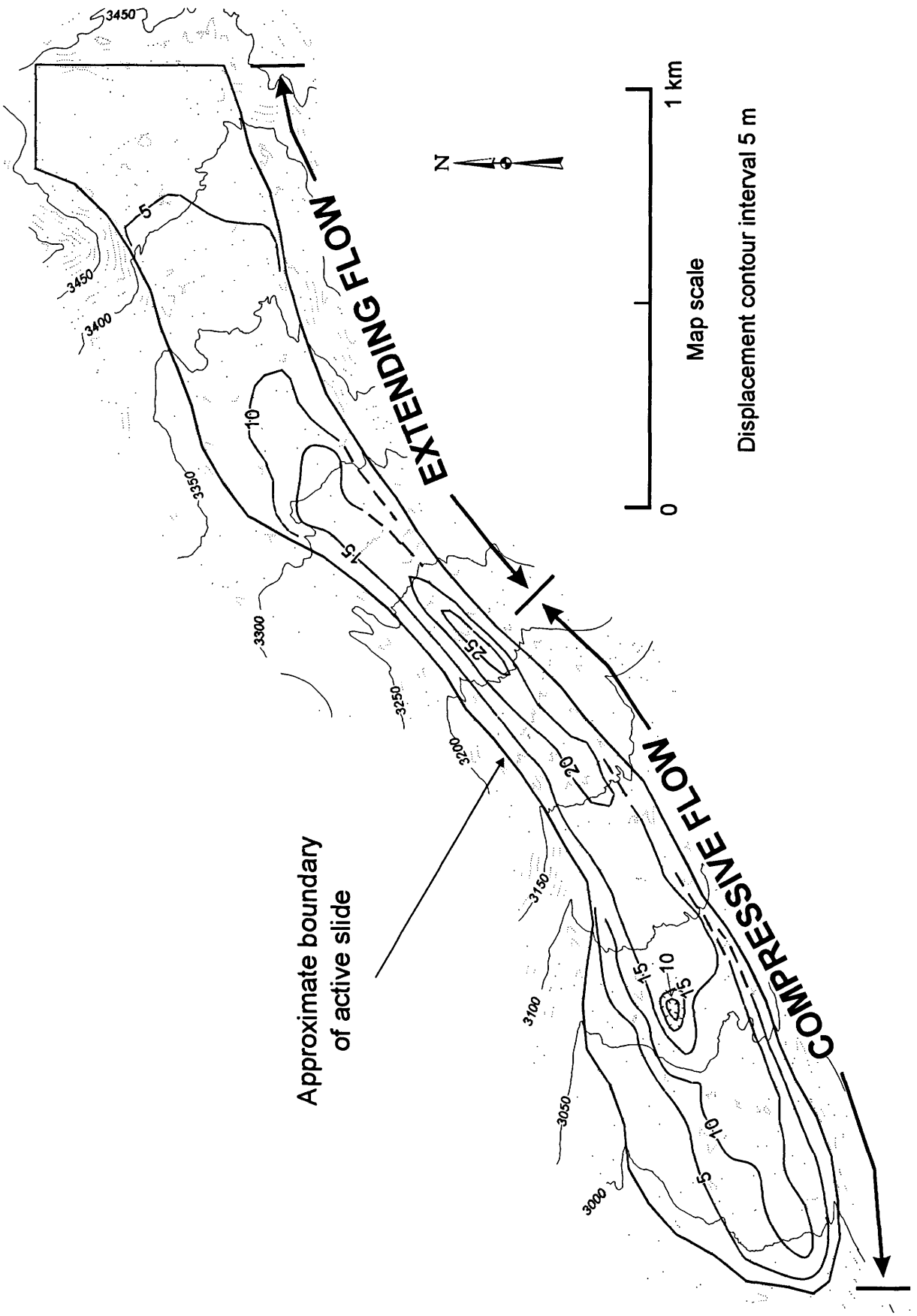

Figure 2. Map of active part of the Slumgullion landslide showing contours of horizontal displacement between 1985 and 1990. Contours were drawn by hand from magnitudes of vectors shown in figure 1.

RESULTS

A total of 310 natural points (trees and bushes) were identified and measured on the two sets of photographs. Details of the measurements are given by Smith (1993). Figure 1 is a map of the active portion of the slide showing the horizontal displacement vectors, and figure 2 shows the contours of net horizontal displacement over the 5-yr period. Displacements from 1985 to 1990 ranged from less than 0.25 m to more than 25 m. The pattern of the overall movement on the landslide surface shows the largest displacements in the central, narrow part of the slide. The upper part of the slide is undergoing extending (active) flow while the lower part is undergoing compressive (passive) flow. Points just above the active toe are advancing at the rate of about 1 m per year, whereas material in the narrow, central portion of the slide is advancing at about 5.7 m per year. These displacements are similar to those measured at several points by Crandell and Varnes (1961): 2.5 ft per year at the toe and 20.0 ft per year in the central part. They also concluded that the rate of movement is fairly constant from year to year and season to season. Similar values were found at the toe and in the narrow part from the fault creep studies of Savage and Fleming (this volume).

Analysis of the displacement contours (fig. 2) indicates a zone of extending flow from the basin below the main scarp to the upper part of the narrow section and a zone of compressive flow from the narrow part to the active toe. It is possible to apply formulas from the theory of plasticity to the displacement measurements to calculate various components of the velocity and strain fields. Velocities, rather than the total displacements, are used to calculate normal- and shear-strain rates, principal-strain rates and their direction, and maximum shear-strain rates. Details and results of this analysis are given in a forthcoming article (Smith, in press).

CONCLUSIONS

Photogrammetry is an effective tool for monitoring actively moving landslides and for analyzing the velocity or strain-rate fields. Photogrammetric methods allow one to use archival photographs to determine displacements over long periods of time, provided that a sufficient number of identifiable points on stable ground are visible on each set of photographs to control the stereo models, and also provided that corresponding objects on the active slide can be positively identified on both sets of photographs. With the equipment used in this study (computer-assisted PG-2), horizontal positions of suitable trees and bushes can be measured with a standard deviation less than 0.5 m. Field surveys are generally more precise than photogrammetric measurements, but they involve more personnel and require recoverable points that will not be disturbed between surveys. Also, one cannot obtain additional points to fill in detail in areas of particular interest.

Measured displacements can be analyzed using two-dimensional plastic-flow theory to obtain principal- and shear-strain rates and principal-strain-rate trajectories. Finally, the data indicate, that for future experimental or theoretical studies, this landslide might be suitably modeled as a purely cohesive material extruding by its own weight through a constriction on a sloping surface.

REFERENCES CITED

Baum. R.L., and Fleming, R.W., 1991, Use of longitudinal strain in identifying driving and resisting elements of landslides: Geological Society of America Bulletin, v. 103, no. 8, p. 1121–1132.

Baum, R.L., and Reid, M.E., 1992, Geology, hydrology and mechanics of the Alani-Paty landslide, Manoa Valley, Oahu, Hawaii: U.S. Geological Survey Open-File Report 92-501, 87 p.

Bonnard, Christophe, 1984, Determination of slow landslide activity by multidisciplinary measurement techniques, *in* Kovari, K., ed., Field Measurements in Geomechanics: Rotterdam, Balkema, Proceedings of the International Symposium, Zurich, September 5–8, 1983, v. 1, p. 619–638.

Crandell, D.R., and Varnes, D.J., 1961, Movement of the Slumgullion earthflow near Lake City, Colorado, *in* Geological Survey Research 1961: U.S. Geological Survey Professional Paper 424–B, p. 136–139.

Smith, W.K., 1993, Photogrammetric determination of movement on the Slumgullion Slide, Hinsdale County, Colorado, 1985–1990: U.S. Geological Survey Open-File Report 93-597, 17 p., 2 pl.

———in press, Measurement of landslide displacements by aerial photogrammetry, Slumgullion Slide, Colorado: Association of Engineering Geologists Bulletin.

Varnes, D.J., Smith, W.K., Savage, W.Z., and Varnes, K.L., 1993, Control and deformation surveys at the Slumgullion Slide, Hinsdale County, Colorado—A progress report: U.S. Geological Survey Open-File Report 93-577, 15 p., 1 pl.

CHAPTER 10

MODELING DEFORMATION AT THE ACTIVE TOE OF THE SLUMGULLION LANDSLIDE

By William Z. Savage, David J. Varnes, William K. Smith, *and* Philip S. Powers

INTRODUCTION

Precise leveling in front of the active toe of the Slumgullion landslide has been carried out annually since 1991 (Varnes and others, 1993). The leveling observation points near the active toe are shown in figure 1*A*. These leveling surveys establish a general pattern of downward displacement of older slide material in response to the advance of the younger, overriding active toe. Because we do not know how far ahead of the advancing active front the effects of the surcharge may eventually be felt, or at what rate deformation over large areas, if any, is occurring, a theoretical model to supplement intermittent field measurements and to predict this deformation was developed. This model is described in this chapter.

THE DEFORMATION MODEL

The measured downward deflections are consistent with the predicted response of an elastic half-space to surface loading applied as shown in figure 2. The load, which consists of a thick strip with beveled edges, extends infinitely in the direction normal to the *x*-*y* plane, and is symmetric about the *y*-axis. Because of this symmetry, only the right half of the load is shown in the figure. The details of the elastic solution, which is based on Muskhelishvili's (1953) complex variable method, will not be presented, because of their complexity.

The vertical loading for the elastic solution is given by

$$P(x) = \rho g h \quad 0 \le x \le b \tag{1}$$

and

$$P(x) = \rho g h \left[\frac{x-a}{b-a}\right] \quad b \le x \le a \tag{2}$$

where

ρ is density,

g is gravitational acceleration,

h is height of the toe,

x is a distance from an origin on the slide, and

a and b are parameters controlling the geometry of the loading.

The right-half of the load, shown in figure 2, has a shape roughly comparable to shapes of the toe cross sections A-A′ and B-B′ shown in figure 1*B*, particularly for $b \le x \le a$. Vertical deflections for $y=0$ and for $0 \le x < \infty$ caused by this loading can be shown to be given by

$$\begin{aligned} V(x) = \frac{\rho g h (1-\nu^2)}{\pi E (a-b)} \Big\{ & (x-a)\,(|x+a|)\,\ln\left[\frac{|x+a|}{|x-a|}\right] \\ & - (x-b)\,(|x+b|)\,\ln\left[\frac{|x+b|}{|x-b|}\right] \\ & + 2a\,(x+a)\,\ln\left[\frac{|x+a|}{|a|}\right] - 2a\,(x-a)\,\ln\left[\frac{|x-a|}{|a|}\right] \\ & + 2b\,(x-b)\,\ln\left[\frac{|x-b|}{|a|}\right] - 2b\,(x+b)\,\ln\left[\frac{|x+b|}{|a|}\right] \\ & + 4b^2 \ln\left(\frac{b}{a}\right)\Big\} - \frac{4\rho g h (1-\nu^2)}{\pi E} \end{aligned} \tag{3}$$

where

E is Young's modulus, and

ν is Poisson's ratio.

Figure 3*C* shows predicted nondimensional deflections given by the two normalized loadings before and after the advance of an idealized landslide (fig. 3*A* and fig. 3*B*). The displacements are normalized by dividing both sides of equation 3 by $4\rho g h(1-\nu^2)/E$. The change in normal loading and the consequent change in deflections shown in figures 3*C* and 3*D* are taken to be analogous to the deformational response caused by the forward advance of the toe of an actual landslide. Note in figure 3*D* that the greatest change in the predicted deflections occurs in the vicinity of $x/a=1$, that is, near the active toe.

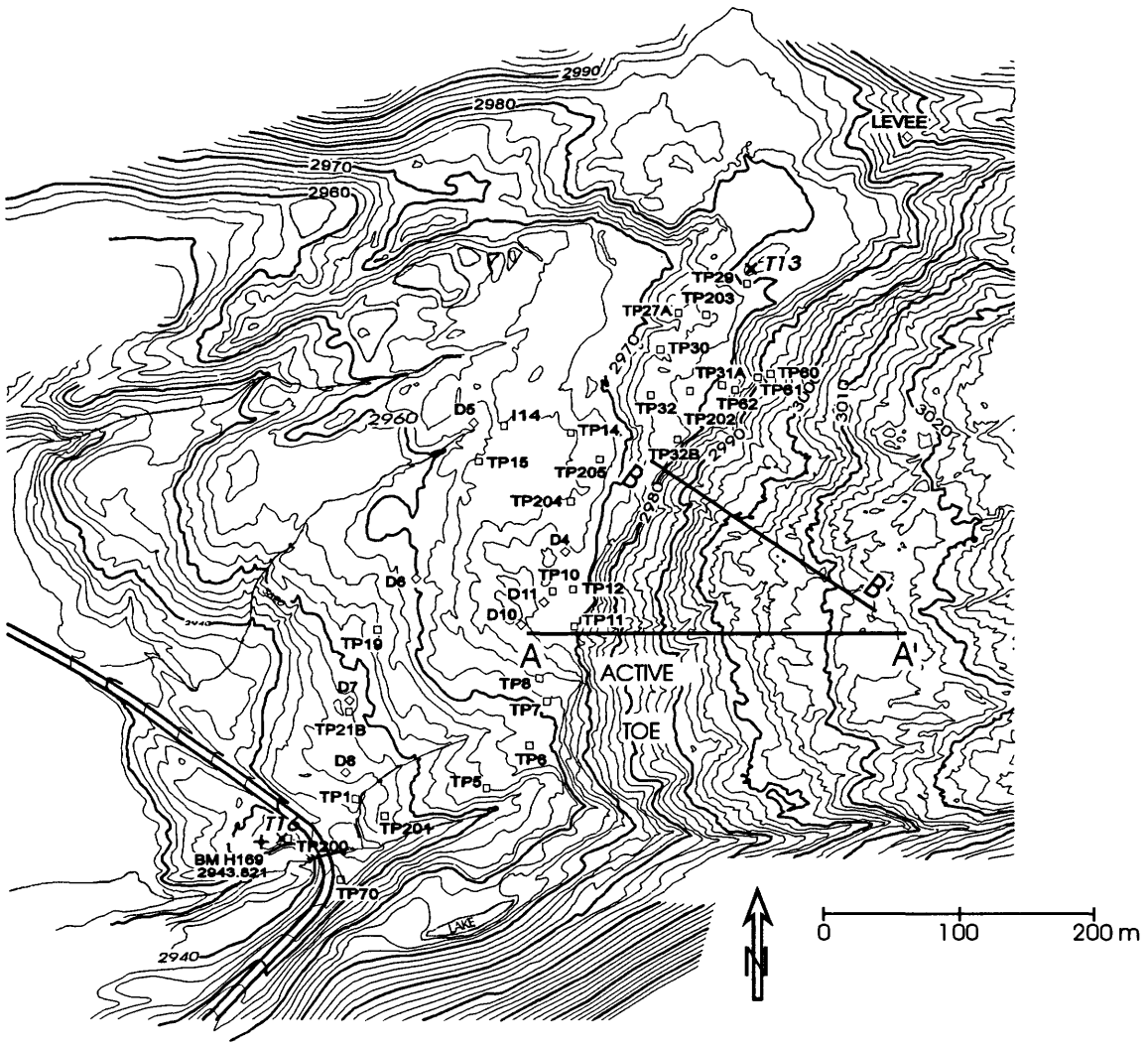
2990
2980
2970
2960
2950
2940
LEVEE
T13
TP29
TP203
TP27A
TP30
TP31A
TP60
TP61
TP62
TP32
TP202
TP32B
TP14
TP15
TP205
TP204
D5
I14
D4
D6
TP10
TP12
D11
D10
TP11
TP19
D7
TP21B
D8
TP1
TP5
TP8
TP7
TP9
TP201
T16
TP200
BM H169
2943.821
TP70
LAKE
A
A'
B
B'
ACTIVE
TOE
N
0
100
200 m

A

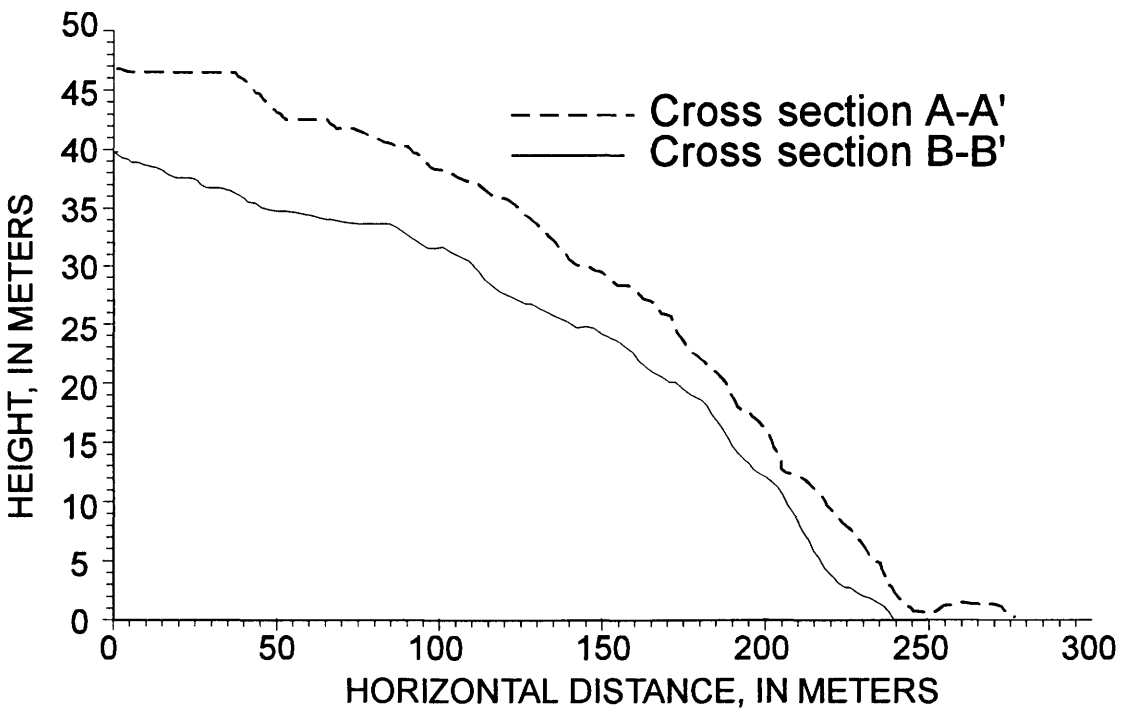
Cross section A-A'
Cross section B-B'
HEIGHT, IN METERS
HORIZONTAL DISTANCE, IN METERS
0
5
10
15
20
25
30
35
40
45
50
0
50
100
150
200
250
300

B

Measured and predicted deflections for an annual advance of the toe of 1 m are shown in figure 4. The measured and predicted deflections show that greatest displacements are near the active toe with diminishing deformation away from the toe.

Annual deflections measured during the period 1991–93 are summarized in table 1. The distance from the toe given in table 1 is the shortest distance from a leveling station to the edge of the active toe. Note that all leveling-station elevations, and hence their changes, are measured relative to BM H169, which itself is on the old slide (fig. 1*A*). With the exception of deflections measured at TP7 and TP14 for 1991–92, all annual deflections shown in table 1 are downward. Linear regression of $\ln\Delta V$ against distance yields the exponential expression ΔV=–0.015exp(–0.011d), where d is the distance in front of the edge of the active toe for the measured downward annual deflections shown on figure 4. This exponential expression is fit to the measured data because it gives a reasonable approximation to the theoretical curve and provides a simpler form for least-squares analysis. The correlation coefficient, r, for this exponential fit is 0.53. This correlation coefficient is significant at the 99.9 percent confidence level (Volk, 1958, p. 231); that is, there is only one chance in a thousand of obtaining a correlation coefficient this large if there is no correlation between downward displacement and distance from the front of the landslide toe.

The parameters used for the predicted deflection for the advance of the Slumgullion landslide are a=175 m, b=0 m, a'=176 m, b'=1 m, and $4\rho gh(1-\nu^2)/E$=0.02. Here, a and b are the geometric parameters describing the initial shape of the toe of the landslide, and a' and b' are the geometric parameters describing the shape of the toe of the landslide after an advance of 1 m. The values for the geometric parameters, a, b, a', and b' give the triangular loading shown by the long dashed line in figure 5. Only the line for the geometric parameters, a and b is shown because of the short 1-m annual displacement of the toe of the landslide. Note that the loading shown in figure 5 is approximately 75 m shorter than the triangular loading that one might infer from figure 1*B*. This suggests that slide material to the left of b and perhaps the upper part of the triangular loading between b and a in figure 2 will have little or no effect on measured deflections. This inference must also be tested against further leveling measurements. If the average height of the slide, h, is taken to be 40 m, the density, ρ, to be 2,000 kg/m^3, and Poisson's ratio, ν, to be 0.5, then the Young's modulus, E, of the overridden slide material is predicted to be 2.35×10^6 N/m^2.

Figure 1 (facing page). *A*, Map of the area of the active toe of the Slumgullion landslide, Colorado, showing leveling observation points and locations of the topographic cross sections A-A′ and B-B′; *B*, Topographic cross sections A-A′ and B-B′.

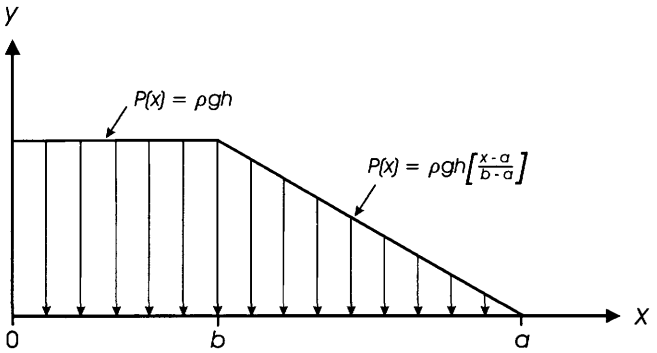

Figure 2. Normal load distribution, which approximates the shape of the landslide toe. The height of the toe is h, gravitational acceleration is g, and density of toe material is ρ. Note that the loading is symmetric about the plane x=0.

Table 1. Annual vertical displacements at leveling observation stations, 1991–93.

[chng, change; leaders (--) indicate no data]

Station	Distance from toe (m)	Elevation chng 1991-92 (m)	Elevation chng 1992-93 (m)
TP11	0	-0.0150	-0.0153
TP32B	2	--	-0.0229
TP31A	7	-0.0200	-0.0222
TP60	7	-0.0207	-0.0213
TP12	10	-0.0084	-0.0118
TP7	16	0.0307	-0.0058
TP29	21	-0.0234	-0.0178
D4	22	--	-0.004
TP6	23	-0.0056	-0.0080
TP10	24	-0.0139	-0.0126
TP203	26	--	-0.0003
TP202	27	--	-0.0209
TP8	27	-0.0095	-0.0016
D11	29	--	-0.009
TP204	31	--	-0.0205
T13	33	-0.0225	-0.0186
D10	39	--	-0.010
TP32	41	-0.0229	-0.0218
TP205	42	--	-0.0066
TP27A	43	-0.0106	-0.0223
TP30	54	-0.0202	-0.0185
TP5	57	-0.0049	-0.0039
TP14	69	0.0020	-0.0098
I14	115	--	-0.0138
TP15	115	-0.0072	-0.0235
D6	124	--	-0.005
TP201	135	--	-0.0004
D5	137	--	-0.002
TP19	147	-0.0114	-0.0024
TP1	154	-0.0032	-0.0004
D7	156	--	-0.006
TP21B	156	-0.0070	-0.0003
TP70	181	--	-0.0040
TP200	208	--	-0.0016

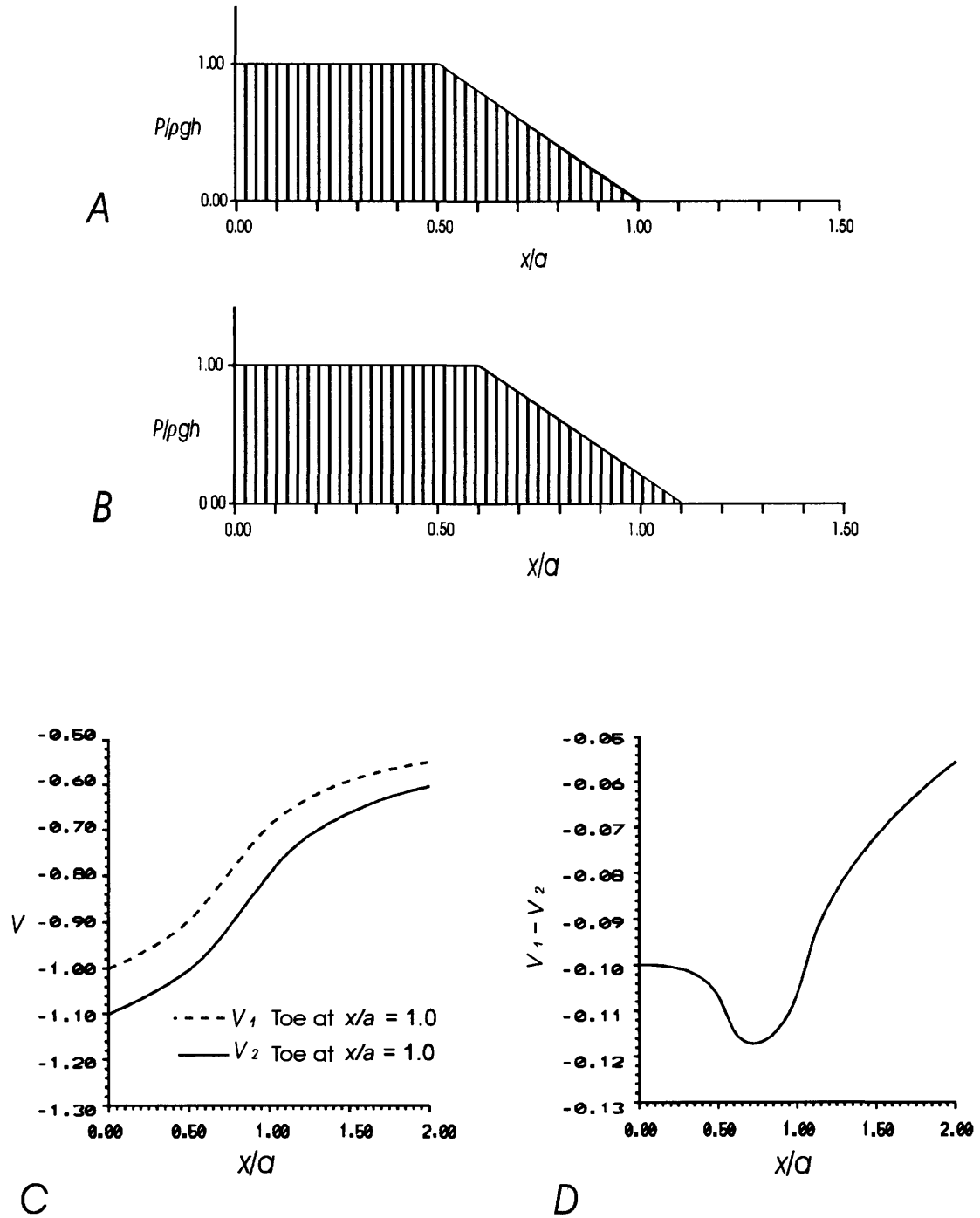

Figure 3. *A*, Normalized vertical loading for an idealized landslide with a toe initially at x/a=1.0. *B*, Normalized vertical loading after the toe of the landslide has advanced to x/a=1.1. *C*, Normalized deflection, V_1, caused by the initial loading and normalized deflection, V_2, caused by the additional loading after advance of the toe. *D*, Deflection differences caused by the advance of an idealized landslide toe from x/a=1.0 to x/a=1.1.

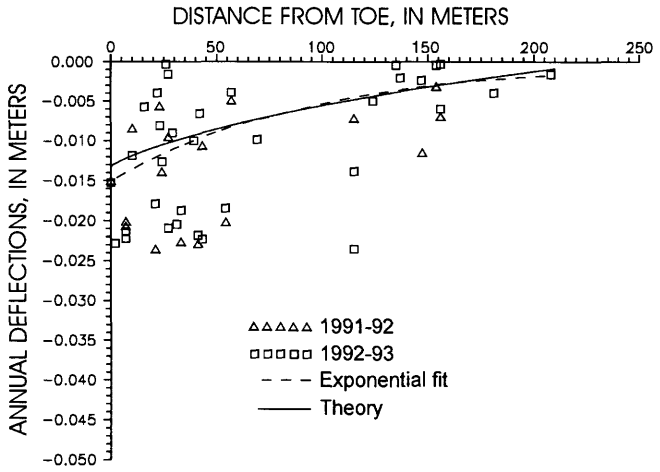

Figure 4. Predicted and measured annual downward deflections ahead of the active toe of the Slumgullion landslide 1991–93.

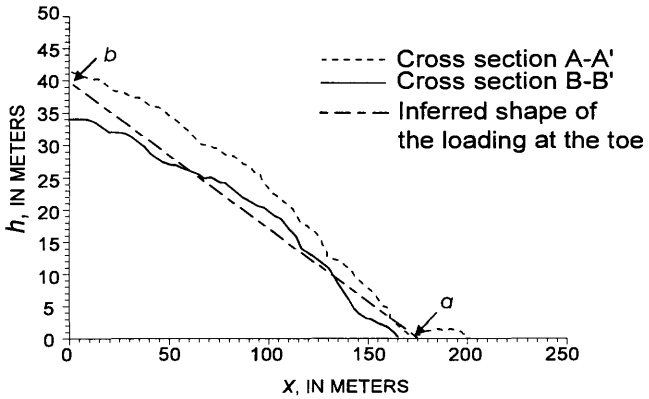

Figure 5. Comparison of the cross sections through the toe with the inferred shape of loading used in the theoretical prediction of deflections shown in figure 4.

CONCLUSIONS

Although this theoretical model can provide some basis for predicting how far ahead of the advancing front the effects of the surcharge may be felt, it has two principal shortcomings. The first is the assumed symmetry of the loading about the *y*-axis. This symmetry does not exist in the landslide. The second is the assumption of vertical loading only. Shear tractions will be produced where the active slide overrides the inactive slide. An improved model will be developed to address these problems.

REFERENCES CITED

Muskhelishvili, N.I., 1953, Some Basic Problems of the Mathematical Theory of Elasticity: Groningen, Netherlands, P. Noordhoof, 704 p.

Varnes, D.J., Smith, W.K., Savage, W.Z., and Varnes, K.L., 1993, Control and deformation surveys at the Slumgullion Slide, Hinsdale County, Colorado—A progress report: U.S. Geological Survey Open-File Report 93-877, 15 p.

Volk, W., 1958, Applied Statistics for Engineers: New York, McGraw-Hill, 354 p.

CHAPTER 11

GEOTECHNICAL PROPERTIES OF SELECTED MATERIALS FROM THE SLUMGULLION LANDSLIDE

By Alan F. Chleborad, Sharon F. Diehl, *and* Susan H. Cannon

INTRODUCTION

Two fine-grained, clay-rich materials (altered volcanic materials), which are commonly exposed on the surface of the active part of the Slumgullion landslide and easily distinguished in the field on the basis of gross color differences (one mostly various hues of yellow and the other mostly reddish brown), were block sampled to obtain material for laboratory strength and physical-property testing. The two materials appear to form much of the matrix of the landslide debris and also occur as local masses within the deposit. Consequently, we consider them important to the characterization of the geotechnical properties of the landslide deposit. "Popcorn weathering," characteristic of many soils with a high smectite content, was observed at both sampling locations (fig. 1) and at many other locations on the slide surface where similar materials were exposed. Slender, needlelike gypsum (selenite) crystals, as much as 10 cm long, are common in and on surface exposures of the yellow material (AT-1). These crystals were rarely observed in or on exposures of the reddish-brown material (AT-3).

COMPOSITION AND GEOTECHNICAL PROPERTIES

Semiquantitative, bulk compositional data for AT-1 and AT-3 were collected on a Cambridge Mark 2 scanning electron microscope (SEM) with an attached energy dispersive X-ray (EDX). The compositional analyses show that AT-1 is relatively rich in sulfur and calcium, whereas sample AT-3 has a higher iron content (fig. 2*A*). The higher sulfur content for sample AT-1 relative to AT-3 is consistent with the higher sulfate mineral (gypsum) content of the yellow material noted in the field.

Prior to X-ray analyses, the samples were crushed, dispersed in distilled water, and centrifuged to achieve a ≤2-μm clay suspension. X-ray analyses were performed on oriented clay mounts of the ≤2-μm clay fraction. The X-ray diffraction analyses indicate that smectite is the only clay present in detectable amounts in the sample of yellow material, but both discrete smectite and kaolinite are present in the reddish-brown material. A scanning electron photomicrograph of sample AT-3 (fig. 2*B*) shows a webby, highly crenulated morphology that is characteristic of smectite. The complex microstructure of the clays suggest that their engineering behavior is complex; however, no general quantitative relationship has been established between microstructure of clays and engineering properties.

Grain size curves for the two materials indicate a clay-size (<0.002 mm) fraction of 58 percent for the yellow material and 36 percent for the reddish-brown sample (fig. 3). Preliminary examination of the >200-sieve-size (silt and fine- to medium-sand sizes >0.075 mm) fraction of the reddish-brown sample using a binocular microscope revealed that fraction is composed almost entirely of angular, reddish-brown volcanic rock fragments. The >200-sieve-size fraction of the yellow material consists almost entirely of white to pale yellow, subangular to subrounded, volcanic rock fragments.

Atterberg limits were determined according to ASTM standards (ASTM, 1994). The natural moisture content of the samples was maintained prior to testing and the samples were oven-dried to equilibrium at a temperature of 60°C (4 days drying time) to reduce the degree of dehydration of gypsum that could occur at the standard 110°C drying temperature (ASTM, 1994). The samples were then dried to equilibrium an additional 24 hr at 110°C to determine the additional moisture loss and possible effect of the higher drying temperature on the limits determination. Although the effect of the higher drying temperature was greatest for the

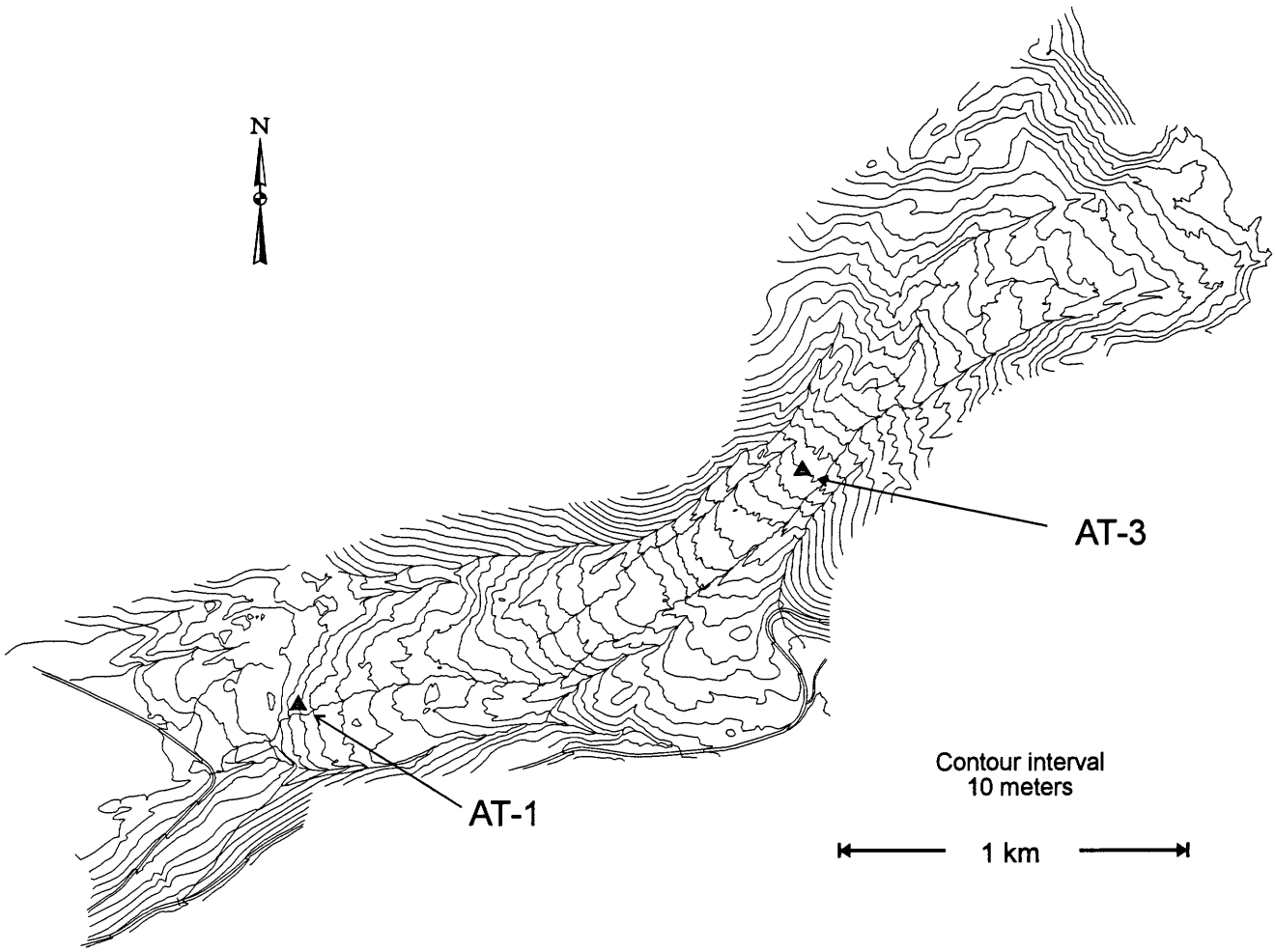

Figure 1. Map showing the locations of block sample sites AT-1 and AT-3 on the active portion of the Slumgullion landslide. Based on a local coordinate system (Cartesian north (N)-east (E)-elevation in meters) developed by Varnes and others (1993). The locations of block sample sites AT-1 and AT-3 are 10,175 N; 7,505 E; 2,980 m; and 10,785 N; 8,950 E; 3,200 m, respectively.

yellow sample (table 1), possibly reflecting a higher gypsum and clay content, both changes are minor and suggest that additional dehydration of gypsum or other hydrous compounds in the samples at the higher temperature does not significantly affect the results. Comparison of plots for the two materials on Casagrande's plasticity chart (fig. 4*A*) with those for the common clay minerals (fig. 4*B*) shows that sample AT-3 plots near the zone typical for montmorillonites (smectites), but sample AT-1 (the yellow material) exhibits apparently anomalous plasticity characteristics by plotting below the "A-line." In contrast, both materials exhibit a high dry strength that is characteristic of clays with high plasticity. It has been reported that the composition and concentration of soluble salts in a soil can affect liquid and plastic limits. For example, a reduction in the liquid limit of sodium montmorillonite may result from increased salt concentration due to a corresponding decrease in interparticle repulsion (Warkentin, 1961). Compositional analyses and field observations indicate that sulfates are the most abundant soluble salts in samples AT-1 and AT-3; however, the effect of the sulfates on salt concentration and the limits is undetermined.

Likewise, the data are insufficient to account for the apparent discrepancy in the activities of the samples. It has been shown that a good correlation exists between the activity of a clay (defined as the ratio of plasticity index to percent by weight of the clay fraction) and clay type (Holtz and Kovacs, 1981). As shown on figure 5*A*, neither of the materials displays high activities characteristic of montmorillonites.

The swelling potentials of the two materials were estimated by plotting the activity versus clay fraction on the swelling potential classification chart developed by Seed and others (1962) (fig. 5*B*). As shown on figure 5*B*, swelling potential of both materials falls in the high category. The indicated swelling potentials suggest that variations in

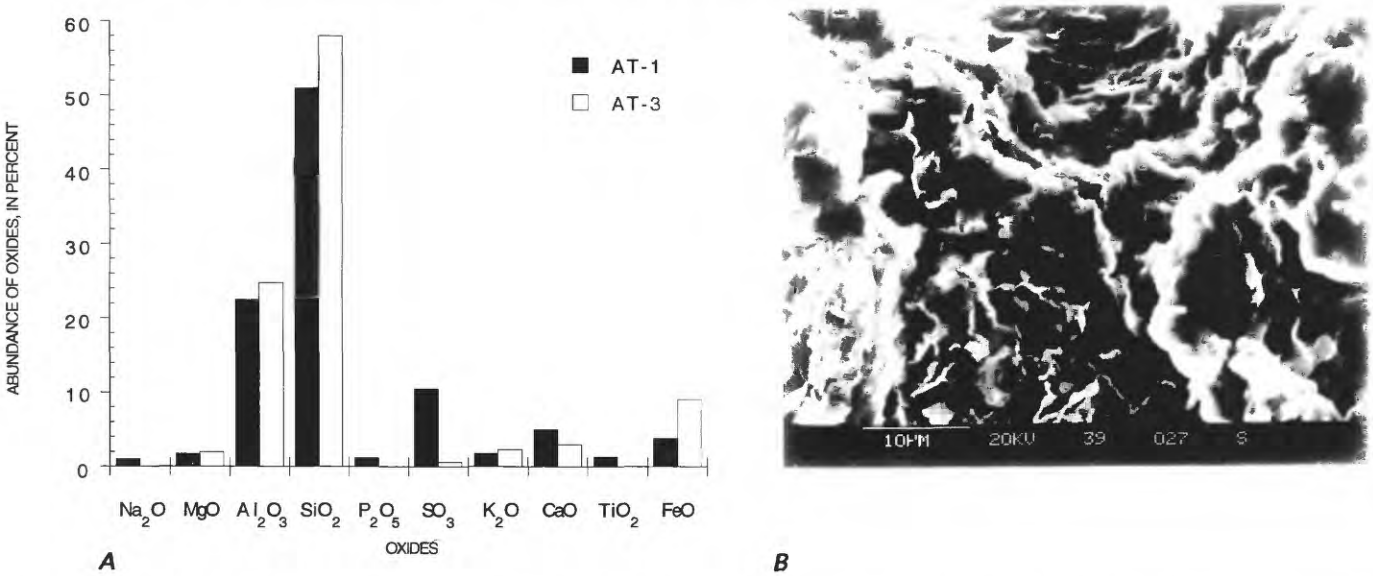

Figure 2. *A*, Bulk composition data for samples AT-1 and AT-3. Results are the averages of three analyses of AT-1 and two analyses of AT-3. *B*, Scanning electron photomicrograph of smectite from Slumgullion landslide sample AT-3.

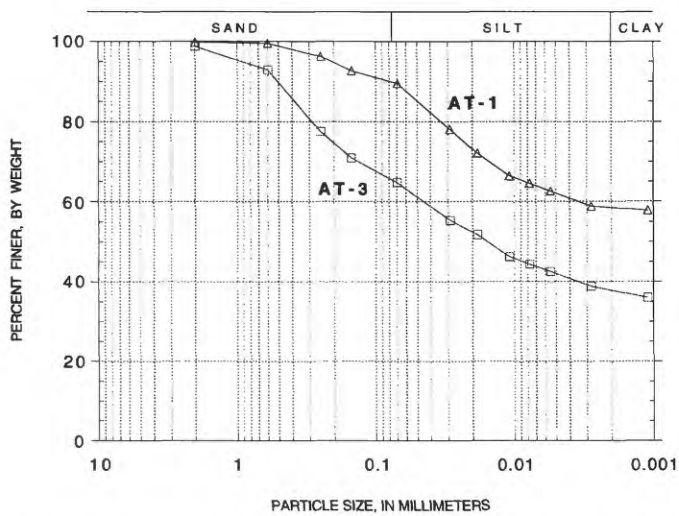

Figure 3. Particle size distribution curves for samples AT-1 and AT-3 from the active part of the Slumgullion landslide.

moisture content of the materials in the field may result in measurable seasonal movement of the ground surface. Such movements may be significant in deformation studies to detect movement of the ground surface associated with landsliding. Mielenz and King (1955) report that gypsum in sodium bentonite (1) will effect partial cation exchange upon wetting of the material and (2) impedes swelling.

Undrained shear strength of the two materials was estimated in the field using an in-situ hand vane tester. The instrument consists of a torque head, including a direct-reading scale, which is turned by hand. Subsequent to excavation of a 3-ft-deep pit, a 0.75-inch-diameter vane was inserted into the soil to an additional depth of 6 inches. The vane was rotated at a constant shearing rate of 1 revolution per minute. to obtain estimates of both maximum and minimum shear strength. A set of ten tests on both materials yielded average maximum undrained shear strength values of 575 lb/ft^2 (28 kPa) for the yellow soil (AT-1) and 785 lb/ft^2 (38 kPa) for the reddish-brown soil (AT-3). Average minimum shear strength values of 90 lb/ft^2 (4 kPa) for the yellow material and 110 lb/ft^2 (5 kPa) for the reddish-brown material were obtained by the continued rotation of the vane after maximum strength was reached. Subsequent to testing, the sheared material was examined for evidence of rock fragments or other hard materials that might have affected the results of the test. In the few instances where this was found to be the case, the data were discarded and a new test location in an undisturbed area of the pit was selected. Natural moisture contents of 56 percent for the yellow material and 38 percent for the reddish-brown material (table 1) were determined in the laboratory subsequent to field testing. Consolidated-undrained triaxial testing of the two materials to determine strength and stress-strain relationships is in progress.

SUMMARY

Preliminary testing and examination of two fine-grained materials (highly altered volcanic material), commonly exposed on the surface of the active part of the Slumgullion landslide, indicate that both are low-strength, clay-rich materials with medium to high plasticity and high swelling potential. Anomalously low activities of the smectite-bearing materials cannot be explained with the available data.

Table 1. Atterberg limits and natural moisture contents of selected materials from the active part of the Slumgullion landslide.

[LL, liquid limit; PL, plastic limit; PI, plasticity index]

Sample no.	Atterberg limits						Natural mositure content (%)
	Drying temp = 60°C			Drying temp = 110°C			
	LL	PL	PI	LL	PL	PI	
AT-1 (yellow)	92	49	43	95	45	50	56
AT-3 (reddish-brown)	62	23	39	65	26	39	38

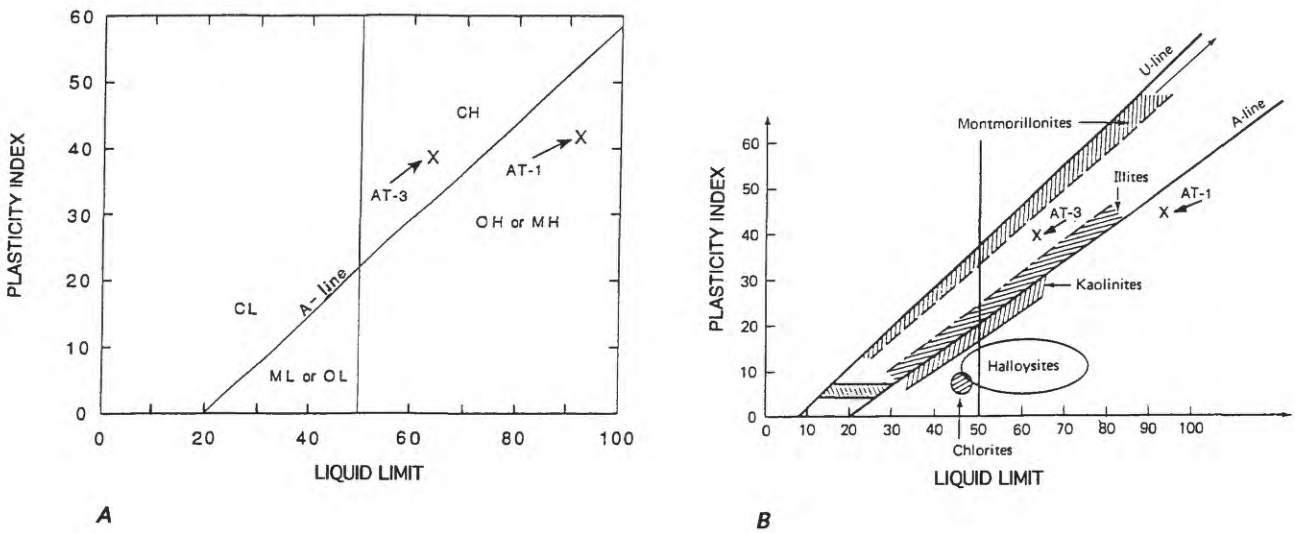

Figure 4. *A*, Plasticity chart showing the plotted locations of samples AT-1 and AT-3 from the active portion of the Slumgullion landslide. Symbols identify types of materials that typically plot in the respective areas of the graph as follows: CL, inorganic clays of low to medium plasticity; ML or OL, inorganic silts and very fine sands with very low plasticity and organic silts and silt-clay mixtures of low plasticity; CH, inorganic clays of high plasticity; and OH or MH, organic silts and clays of medium to high plasticity and inorganic silts. Soils with a high content of active clay minerals, such as montmorillonite, typically plot well above the A-line (see fig. 4*B*). *B*, Location of common clay minerals and Slumgullion landslide samples AT-1 and AT-3 on Casagrande's plasticity chart (adapted from Holtz and Kovacs, 1981).

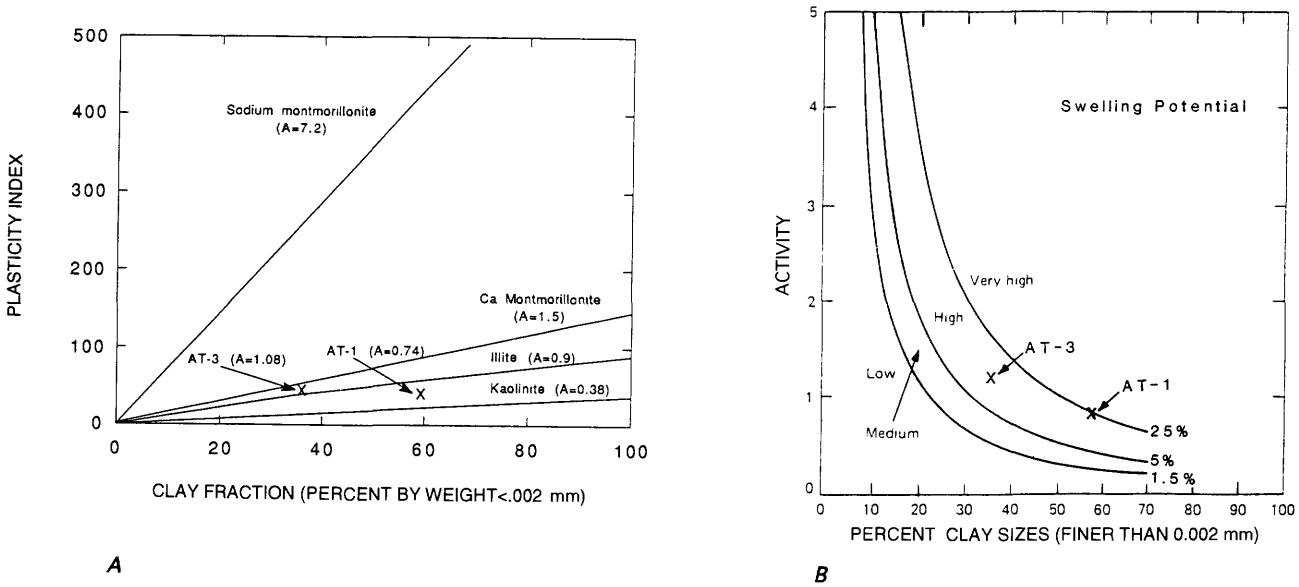

Figure 5. *A*, Graph showing relationship between plasticity index and clay fraction for common clay types (from Skempton, 1953). Soil samples AT-1 and AT-3 from the active part of the Slumgullion landslide are plotted on the graph for comparison. Typical activities (A) of the clay minerals and for samples AT-1 and AT-3 are in parentheses. Note that samples AT-1 and AT-3 have activities that are lower than might be expected for smectite-rich (montmorillonite-rich) materials, indicating that the clay size fractions of the materials do not contain significant amounts of highly active clay. *B*, Classification chart for swelling potential (after Seed and others, 1962). As shown, plotted values for samples AT-1 and AT-3 indicate swelling potentials of approximately 25 percent and 15 percent, respectively.

Further testing of materials from the active and inactive parts of the Slumgullion landslide is needed to characterize the geotechnical properties of the landslide materials. To address unanswered questions regarding the type and relative abundance of various minerals and the effect of soluble salts on material properties, additional chemical and semiquantitative analyses are needed. Planned physical-property testing of surface samples that have been collected at regular intervals on traverses across the lower, middle, and upper parts of the active part of the landslide will further characterize the geotechnical properties of the slide material.

REFERENCES CITED

American Society for Testing Materials [ASTM], 1994, Soil and Rock: 1994 Annual Book of ASTM standards, sec. 4, v. 04.08, 975 p.

Holtz, R.D., and Kovacs, W.D., 1981, An Introduction to Geotechnical Engineering: Englewood Cliffs, N.J., Prentice-Hall, 733 p.

Mielenz, R.C., and King, M.E., 1955, Physical-chemical properties and engineering performance of clays, *in* Pask, J.A., and Turner, M.D., eds., Clays and Clay Technology: California Division of Mines Bulletin 169, p. 196–254.

Seed B.H., Woodward R.J., and Lundgren R., 1962, Prediction of swelling potential for compacted clays: Journal of the Soil Mechanics and Foundation Division of American Society of Civil Engineers, v. 88, no. SM-3, p. 53–87.

Skempton, A.W., 1953, The colloidal activity of clays: Proceedings of the 3rd International Conference on Soil Mechanics and Foundation Engineering, v. 1, p. 57.

Varnes, D.J., Smith, W.K., Savage, W.Z., and Varnes, K.L., 1993, Control and deformation surveys at the Slumgullion Slide, Hinsdale County, Colorado—A progress report: U.S. Geological Survey Open-File Report 93-577, 15 p.

Warkentin, B.P., 1961, Interpretation of the upper plastic limit of clays: Nature, v. 190, p. 287–288.

CHAPTER 12

SLUMGULLION LANDSLIDE FAULT CREEP STUDIES

By William Z. Savage *and* Robert W. Fleming

INTRODUCTION

The active part of the Slumgullion landslide has been observed to be moving for nearly 100 yr, and indirect evidence suggests that it may have been active for the last 300 yr (Crandell and Varnes, 1961). Direct observations of the movement carried out during the summer months in the 1950's showed the sliding rate to be roughly constant. This remarkable behavior contrasts with that of most large translational landslides where movement rates increase or decrease dramatically in response to variations in seasonal precipitation and other factors that influence subsurface hydrology. Prior to this investigation, there were no long-term measurements of velocity of the Slumgullion landslide capable of detecting small seasonal variations.

The virtual certainty of nearly constant movement, continued year after year, makes the Slumgullion landslide an excellent field laboratory for various rate and process studies. In this study, small variations in the rate of movement across faults on the landslide were measured with four creepmeters installed during 1993. Three of the instruments are tide gages adapted to sample fault displacements at 15-minute intervals. The creepmeters were located at the toe, on a strike-slip fault above the toe and within the slide, and on a major, bounding, strike-slip fault on the left flank in the narrow part of the landslide (fig. 1). This last location is known, for historical reasons, as the Camera Station. The fourth creepmeter, a specialized high-precision instrument, was installed downslope from the Camera Station and across the same bounding left-flank strike-slip fault. This instrument was placed as part of a geophysical study, and the results obtained with it are discussed elsewhere (see Gomberg and others, this volume).

RESULTS OF THE FAULT CREEP MEASUREMENTS

The toe creepmeter was emplaced on April 9, 1993, and removed on November 9, 1993. Figure 2*A* is a sketch of the toe creepmeter installation, and figure 2*B* shows the recorded displacements. The dashed line with triangles indicates displacements between the center of the wheel on the creepmeter and the post as determined manually with a measuring tape, and the solid line in figure 2*B* indicates displacements recorded by the creepmeter. The early creepmeter record between April and mid-May was compromised by a loose pulley wheel, but movement during that interval (manually established dashed line in fig. 2*B*) was faster than the summer and fall rates. From April 9 to May 18, the manually determined apparent displacement rate at the toe was 5.2 m/yr, and from May 18 to November 9, a displacement rate of approximately 1.0 m/yr was manually obtained for this part of the landslide. The high rate from April 9 to May 18 may have been caused, in part, by observed local failure on the toe near the post. Because of instrumental problems and consequent gaps, a good creepmeter record was obtained only for about 13 of the 21 weeks that the instrument was in place. From the record that started on July 13 and ended before September 15, the creepmeter-determined displacement rate was 1.40 m/yr, and for the period from September 15 to November 9, the creepmeter-determined rate was 1.46 m/yr. The creepmeter installed on July 13, 1993, across a strike-slip fault above the toe (the location labelled Elk Trail in fig. 1) also suffered from instrumental problems and was removed on January 3, 1994. A sketch of this type of creepmeter installation, and the trigonometric relations used to obtain displacements parallel to a strike-slip fault are shown in figures 3*A* and 3*B*. Figure 4 shows the rather discontinuous record of displacements recorded at this internal strike-slip fault. Again, the dashed line with triangles indicates displacements between the center of the wheel and the post determined with a measuring tape, and the solid line indicates displacements recorded by the creepmeter. Manually determined displacement rates averaged 0.76 m/yr from July 13 to January 3, with rates of 0.74 m/yr from July 13 to September 15, 1.00 m/yr from September 15 to November 9, and 0.41 m/yr from November 9 to January 3. The 16-day creepmeter record starting on July 13 showed a displacement rate of 0.93 m/yr, and the more complete creepmeter record starting on September 15 showed a displacement rate of 1.04 m/yr.

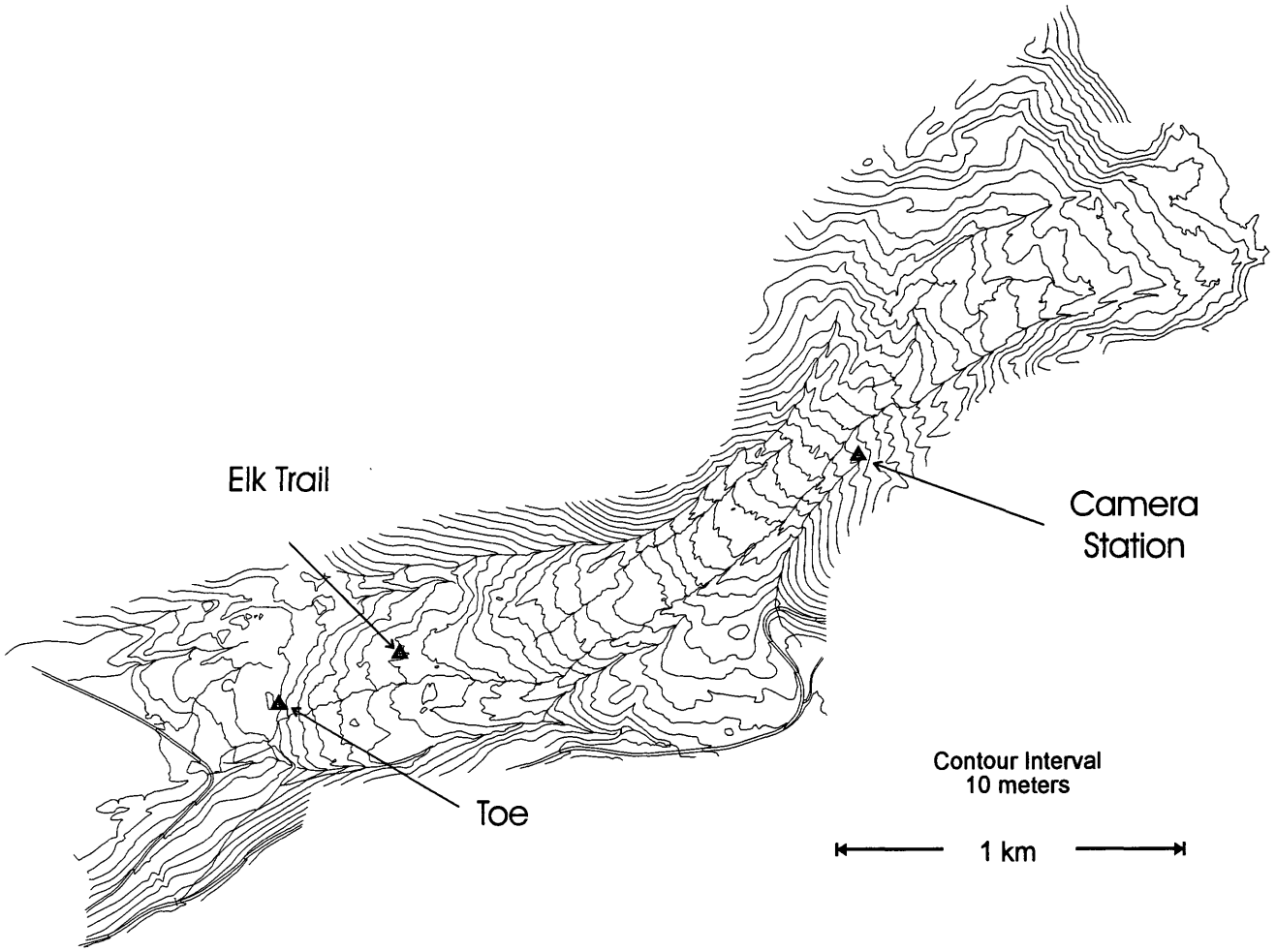

Figure 1. Creepmeter locations on the active portion of the Slumgullion landslide.

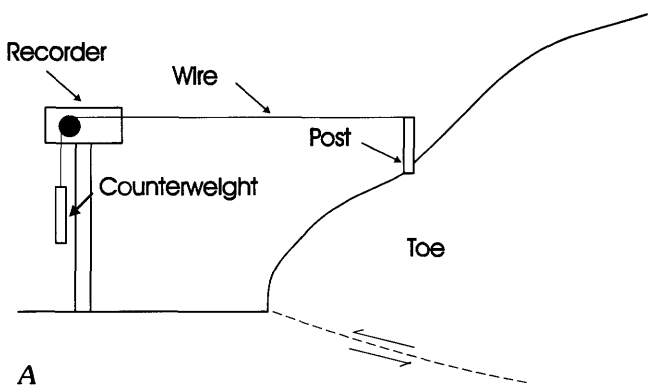

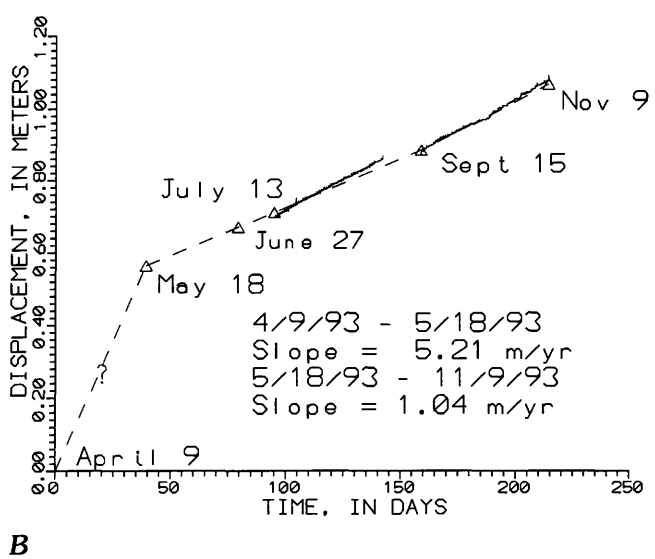

Figure 2. *A*, Sketch of the toe creepmeter installation. *B*, Displacements recorded at the toe from April 9, 1993, to November 9, 1993. Dashed lines with triangles represent manually determined displacements. Solid lines are creepmeter records.

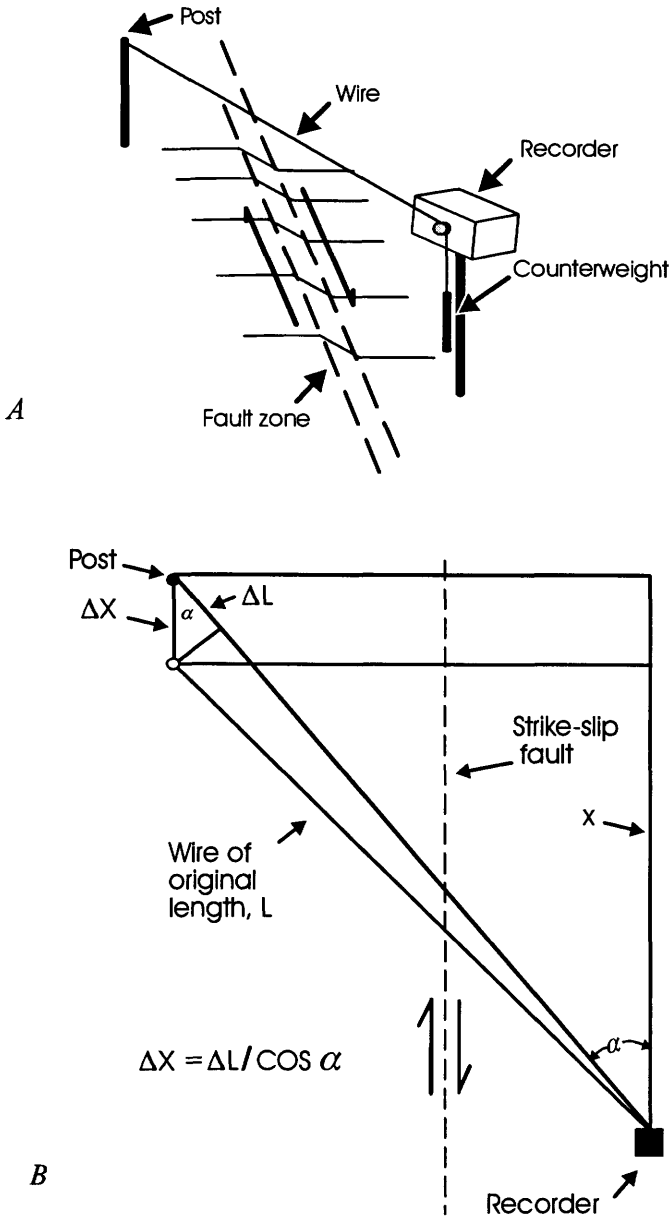

Figure 3. *A*, Sketch of creepmeter installation across a strike-slip fault, and *B*, trigonometric relations for calculating displacements parallel to the fault.

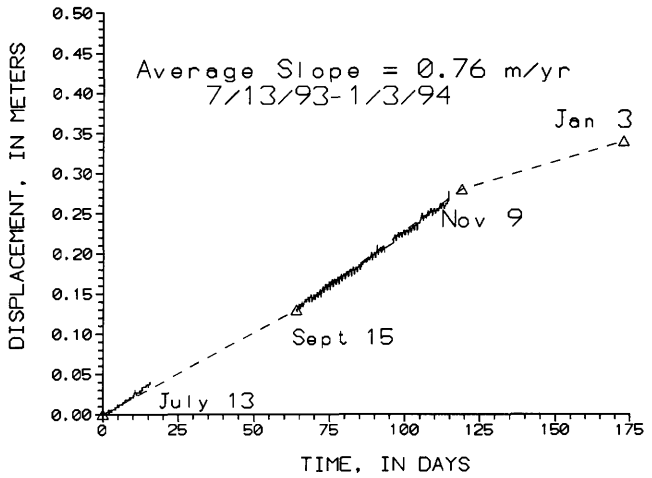

Figure 4. Displacements recorded at the Elk Trail creepmeter installation from July 13, 1993, to January 3, 1994. Dashed lines with triangles represent manually determined displacements. Solid lines are creepmeter records.

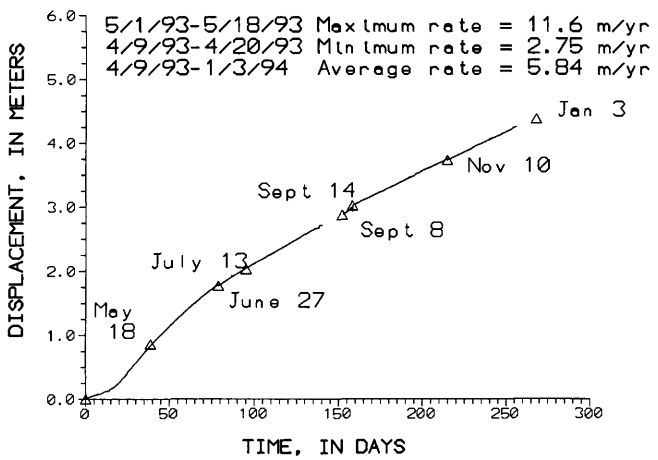

Figure 5. Displacements recorded at the Camera Station creepmeter installation from July 13, 1993, to January 3, 1994. Triangles represent manually determined displacements. Solid lines are creepmeter records.

The record obtained at the Camera Station is the most complete. The installation at this location and the trigonometric relations used to obtain displacements parallel to the strike slip fault are as shown in figures 3*A* and 3*B*. Figure 5 shows the record of displacements. Again, triangles indicate manually obtained values. Shortly after installation on April 9, 1993, velocities underwent an acceleration, presumably caused by spring snowmelt and thawing of the landslide surface. Velocities have been slowly decreasing here since midsummer. Minimum velocities of 2.75 m/yr were recorded from April 9 to approximately April 20. Maximum velocities of 11.6 m/yr were recorded from approximately May 1 to May 18. Average velocities from April 9, 1993, to January 3, 1994, are 5.84 m/yr at this location. This value of nearly 6 m/yr is believed to be the largest average velocity at any location around the perimeter of the landslide. Crandell and Varnes (1961) reported a similar velocity (5.8 m/yr) for a marker near the Camera Station but about in the middle of the slide.

CONCLUDING DISCUSSION

Long-term movement data (Crandell and Varnes, 1961; Smith, this volume) showing rates of about 0.75 to 1 m/yr in the vicinity of the toe and the lower right flank and 6 m/yr near the Camera Station appear to be an average of our measured seasonally varying rates. Variation in velocity over the course of the year suggests that there are hydrologic controls on the movement rate. However, because the movement rate appears constant over long periods, the landslide must contain various internal mechanisms that operate to regulate the rate of sliding in the face of competing factors that increase and decrease the sliding rate. For example, subsurface water pressures might be equilibrated through a network of springs or by water flow into open cracks on the landslide. The springs would bleed off excess water causing water pressures to decrease, and the flow of surface water into open cracks could cause an increase in subsurface water pressures. Such mechanisms would nullify both the effects of frozen ground in the winter that might cause the movement to decelerate and the effects of large, intense summer thunderstorms that might cause the movement to accelerate.

REFERENCE CITED

Crandell, D.R., and Varnes, D.J., 1961, Movement of the Slumgullion earthflow near Lake City, Colorado, *in* Short Papers in the Geologic and Hydrologic Sciences: U.S. Geological Survey Professional Paper 424–B, p. B136–B139.

CHAPTER 13

DETECTION OF THE BASE OF SLUMGULLION LANDSLIDE, COLORADO, BY SEISMIC REFLECTION AND REFRACTION METHODS

By Robert A. Williams *and* Thomas L. Pratt

INTRODUCTION

Detailed studies of the surface features of the Slumgullion landslide, located in the San Juan Mountains near Lake City, Colo., have been conducted since 1991. These studies have attempted to explain many of the characteristics of the slide based on surface samples and measurements. However, because no borehole data exists, seismic reflection and refraction data can potentially provide subsurface data over a wide area of the slide. This would complement the surface studies and provide information critical to determining landslide volume, pre-slide valley morphology, internal slide stratigraphy, geotechnical properties, and potential locations for future drilling.

To test the usefulness of seismic methods, north-south-oriented P-wave refraction and reflection profiles were acquired over 400 m of the slide in June 1993. The coincident profiles were sited on an older portion of the slide, below the active toe and east of State Highway 149 (fig. 1). The profile location was selected for easy vehicle access, relatively flat surface topography, and its position within a well-known survey grid. Despite the relatively good access, locally steep topography and seismic cabling limitations prevented acquisition of seismic data on the northernmost and southernmost portions of the slide. Data quality was also degraded by poor geophone coupling at the northern 50 m of the seismic profiles where the seismic line crossed a marshy beaver pond. Generally, data quality is good over the length of the profile, and the base of the slide was easily detected in both the reflection and refraction data so that the general shape of the pre-landslide valley could be interpreted.

SEISMIC DATA AQUISITION AND PROCESSING

Conventional techniques were used to acquire and process the data (table 1). For the reflection data we used standard common-depth-point (CDP) acquisition and processing methods (Mayne, 1962; Yilmaz, 1987). A 24-channel recording system, a shotgun source, and 28-Hz geophones were used to produce the 12-fold, 1-second CDP profile. Receiver spacing was 4 m, source spacing was 8 m, with two shot records acquired at each of the receiver stations.

For refraction data acquisition, we used two receiver arrays of 24 channels spread over 230 m. For each array we fired shots in the middle, at the ends, and, where possible, at a distance off the end of the array. The first refracted arrivals were visually picked from a display of the shot records (fig. 2) and analyzed using a ray-trace modeling program. The program starts by generating an approximate depth model based on the delay-time method described by Pakiser and Black (1957), then it uses this depth model as input for iterative ray tracing. Model adjustments are then made by the computer to minimize the discrepancies between the picked travel times and those determined by ray tracing (Scott and others, 1972). Some key assumptions made in the refraction analysis are: (1) layers are continuous and extend from one end of the refraction line to the other, and (2) layer velocities increase with layer depth.

The 90-Hz dominant frequency of the shotgun reflection data, combined with stacking velocities of 1.7 km/s, permits a minimum vertical resolution of about 4–5 m at 70 m depth. These resolution limits are based on the 1/4 wavelength criteria of Widess (1973). Clear hyperbolic reflection curves like the curve labeled "slide-base reflection" in

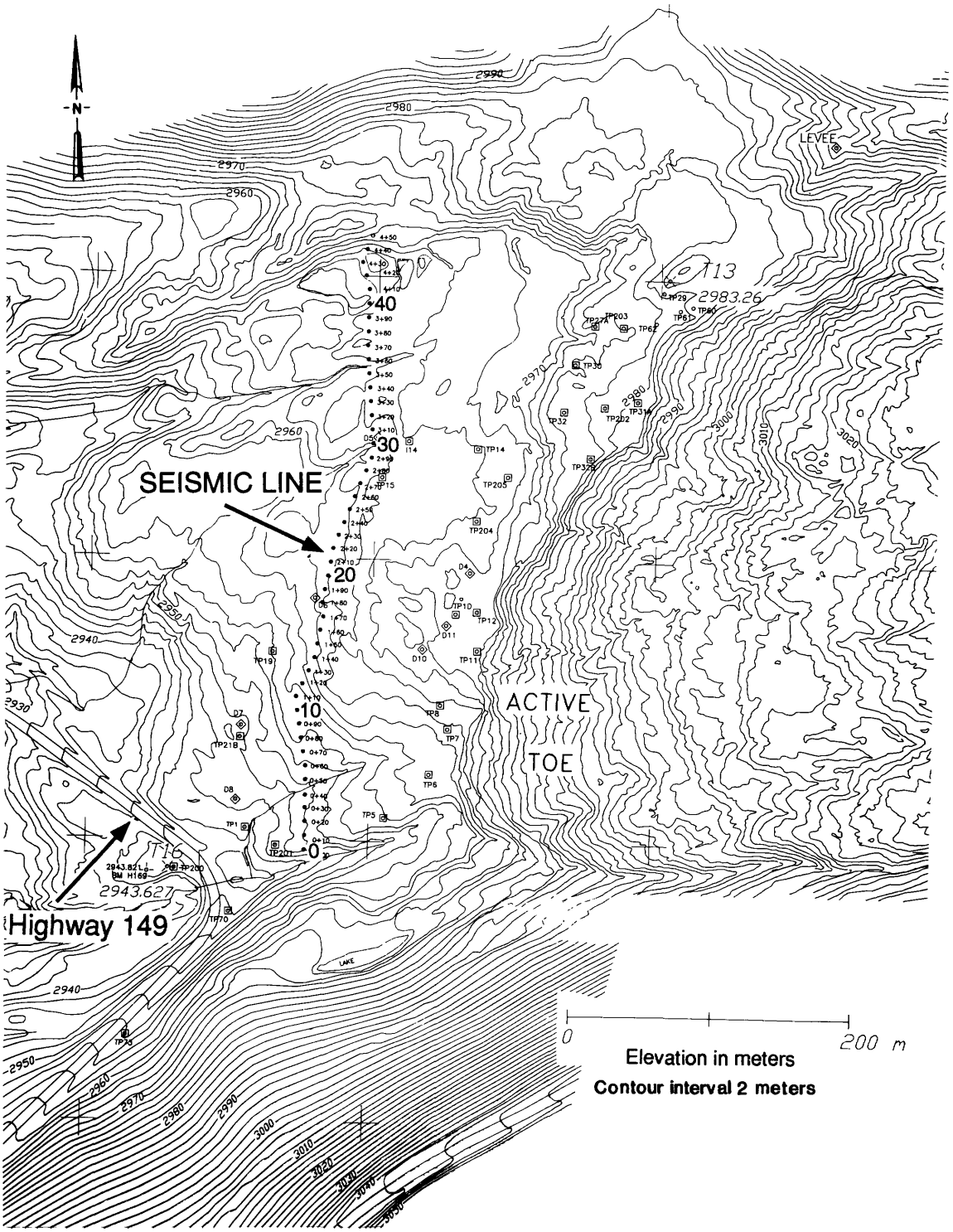

Figure 1. Location map of co-located north-south seismic refraction and reflection profiles. Seismic lines are located on the older, inactive portion of the slide, just below the active toe. Solid circles are stations for the refraction survey. Diamonds and squares are preexisting survey grid stations. Large numbers (0, 10, 20, 30, and 40) on the seismic line are reference positions, located about 100 m apart, that are used in the text to describe the data. These numbers also annotate the data at the top of figures 4 and 5. Small numbers (0+10, 0+20, etc.) annotate intermediate seismic stations. Stations beyond position 40 are in a marshy area. Elevations in meters. Contour interval 2 m.

Table 1. Data-acquisition and processing parameters.

Acquisition parameter	Refraction data	Reflection data
Source:	1/3 lb. Kinestik	12-ga. shotgun, 1-oz. slug
Shot hole depth:	1 m	0.3 m
Shots per station:	10 for total profile	Two, on alternate stations
Source point interval:	Approximately 50 m	8 m
Geophone array:	12, 28-Hz, bunched	12, 28-Hz, bunched
Geophone interval:	10 m	4 m
Recording geometry:	24 channels, reversed	24 channels., in-line, off-end
Near trace offset:	5–210 m	8–16 m
Recording pass band:	0–500 Hz	20–500 Hz
Recording system:	I/O DHR-2400	I/O DHR-2400
Sampling interval:	0.001 s	0.001 s
Record length:	1.0 s	1.0 s

Reflection data processing sequence

[Migration of shotgun reflection data degraded data quality and is not shown here]

1. Automatic gain control (amplitude scaling window 0.2 s)
2. Band-pass frequency filter (30-40-120-160 Hz)
3. Air-blast attenuation–velocity filter (0.3 km/s)
4. Elevation static corrections (datum elev./velocity: 2,958 m/1.5 km/s)
5. Surface-wave removal by frequency-wave number (FK) filter
6. Common midpoint (CMP) sort
7. Normal-moveout correction (from 1.45 km/s at S. end to 1.9 km/s at N. end at 0.08 s)
8. Band-pass frequency filter (30-40-120-160 Hz)
9. Predictive deconvolution filter (prediction distance 0.01 s, operator length 0.1 s)
10. Surface consistent maximum-power residual statics (maximum shift –0.008 s)
11. CDP stack (average 12-fold)
12. Band-pass frequency filter (30-40-120-160 Hz)
13. Time-to-depth conversion (using velocities derived from refraction interpretation)

figure 3 produce stacking velocities with an estimated uncertainty of 10 percent for the slide-base reflection. This results in depth estimates having errors of ±5.0 m for a bed at 70-m depth.

An additional depth uncertainty of as much as 12 m is introduced by the assumption that the reflection data is minimum phase. This means that one assumes that most of the energy in the seismic wavelet produced by an explosive source is concentrated in the front of the wavelet, and, hence, the front end of the seismic wavelet gives the travel time of the wavelet from the source down to the reflector and up to the receiver. This minimum-phase assumption seems accurate, however, because the slide-base refractor depths derived from the refraction data (also minimum phase) correspond to the depths derived from interpreting the onset of the reflection as the top of the reflector. If this phase assumption is not correct, then a large uncertainty exists because the top and bottom phases of the doublet reflection wavelet are as much as 12 m above and below the central negative phase. The dominant frequency of the first-arrival refraction data is about 25 Hz, so the reflection data, with shorter geophone intervals and higher frequency seismic waves, does give better resolution of the slide-base interface.

REFRACTION AND REFLECTION DATA INTERPRETATION

A large, positive acoustic contrast is interpreted to represent the base of Slumgullion slide. We infer the base of the slide from a clear deflection in refraction first-arrival phases to a high-seismic-velocity unit on all refraction shots (fig. 2) and as a prominent reflection at 0.09–0.12 s on many of the reflection shots (fig. 3). The refraction data indicate that the seismic velocity jumps from 2.3 km/s within the slide to 5.4 km/s for the material underlying the slide. This 5.4 km/s value is characteristic of hard crystalline rock, such as granite or volcanic rock (Dobrin, 1976). Layered, densely welded tuffs were mapped by Lipman (1976) adjacent to the slide near the seismic profiles, and their shallow dip (5°) suggests

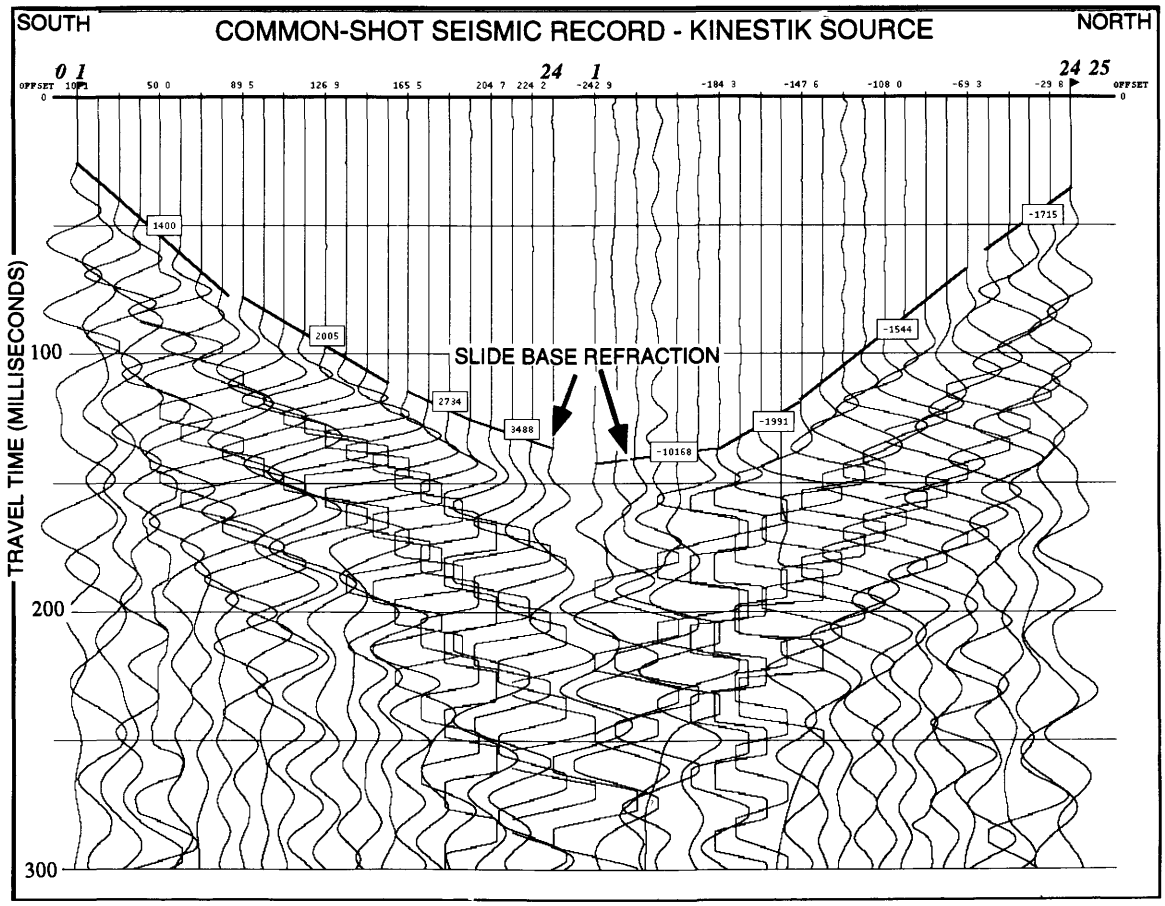

Figure 2. Two 24-channel seismic records acquired with Kinestik explosives for refraction interpretation. These data were acquired with geophones located at positions 1 through 24 (station 2+40 on figure 1) and the source at position 0 (left side of figure) and position 25 (right side of figure). Positions 0 through 25 are indicated on the seismic line shown in figure 1. Numbers in italics along the top are the ground stations. Numbers annotated at the top of each trace (below the italicized numbers) give the offset distance from the source in meters. Numbers inset in boxes adjacent to heavy lines indicate the apparent seismic velocities (m/s) interpreted from the first-arrival seismic waves. The 10,168 m/s and 3,488 m/s velocities for the long-offset refractions result from refracted waves traveling up- and down-dip, respectively.

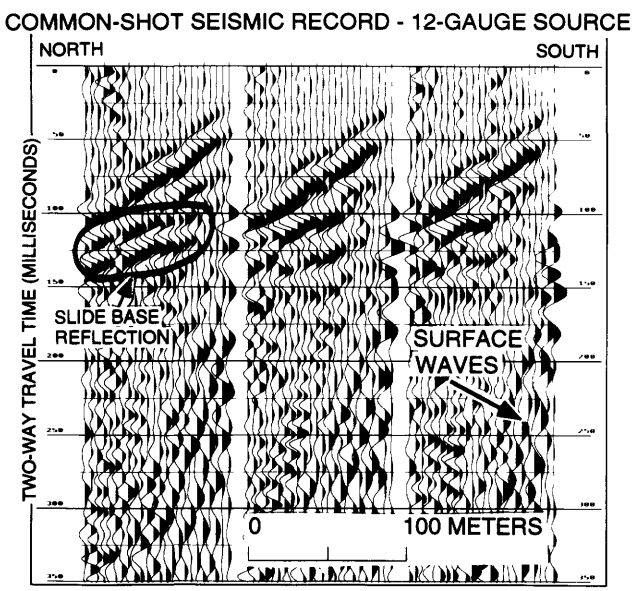

Figure 3 (facing column). Three 24-channel seismic records acquired with the 12-gauge shotgun source for reflection interpretation. These data were acquired between positions 22 and 32 (fig. 1). Seismic reflections and surface waves are annotated on the records.

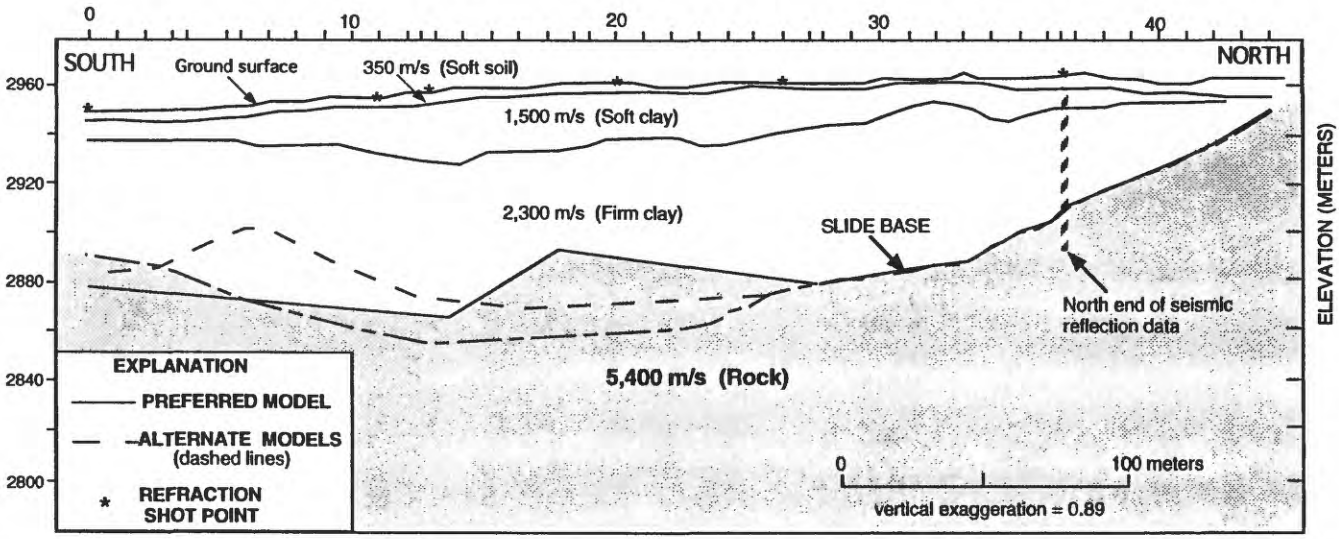

Figure 4. Refraction data interpretation showing the topography of the ground surface, the four distinct seismic-velocity layers, and the alternate refraction models. The vertical tic marks on the horizontal axis at the top of the figure show the true positions of the geophone stations and shotpoints. Asterisks mark the shotpoint positions on the ground surface.

that they underlie the slide. The seismic velocity of the rock underlying the slide is close to the value obtained by Gomberg and others (this volume) at a location about 1.5 km east of the seismic refraction/reflection site.

Previous studies of the pre-landslide topography of the Slumgullion landslide valley were conducted by projecting the slope of the existing valley walls (outside the boundaries of the slide) to a point of intersection under the flow (Parise and Guzzi, 1992). These projections, which assumed a V-shape pre-landslide topography, were made about 200 m west and 300 m east of the seismic profile locations and suggested a maximum depth of about 120 m.

From the refraction and reflection data, we interpret the pre-landslide valley topography to be generally U-shaped, with a 25° slope on the north end of the profile (position 28–44, figs. 4 and 5), a flat-to-undulating middle section (position 13–25), and 10°–20° slope on the south end of the profile (position 0–13). Projecting the interpreted slide base north of the seismic profiles suggests that bedrock reaches the surface 20 to 30 m north of position 44 (the rock is covered by surficial deposits in the field). The interpretation of the slide base south of position 13 is uncertain because the reflection data quality degrades and we are left to depend solely on the refraction data. Topographic constraints beyond the south end of the profile prevented acquiring longer offset refraction shots that would have reduced interpretation uncertainty. For the middle section of the slide, we rely on reflection data to show greater detail.

Beneath position 28, the reflection data show a V-shaped trough about 15 m deep and 100 m wide (fig. 5). South of the trough, the reflection and refraction data results diverge and, because of uncertainties in the refraction data, we present alternate interpretations. Also, out-of-plane reflections may complicate the reflection data and contribute to the mismatch of the reflection and refraction data at any point on the profile. We favor the refraction interpretation that coincides with the strong reflection between stations 14 and 20 (fig. 5). The reflection between positions 10 and 20 shows the base of the slide to be relatively flat-lying at 60- to 65-m depth over a distance of 100 m. South of position 10, the basal reflection weakens, but we infer from the refraction data that the base of the slide slopes up at 10°–20° (figs. 4 and 5). Projecting this slope south suggests that bedrock crops out in the vicinity of a small lake (beaver pond, fig. 1), which is in an area mapped as glacial moraine deposits (Lipman, 1976). Bedrock (rhyolite) is exposed off of the slide in the 22° slope near the lake (Lipman, 1976). An alternate, less certain refraction model shows a small hump in the slide base interface south of position 10 (fig. 4). We interpret no reflections below 110 m because the data are considered to be predominantly incoherent seismic noise below this depth (fig. 5).

The refraction data indicate three distinct P-wave seismic velocity layers within the slide: (1) a 1- to 3-m-thick surficial layer with a velocity of 350 m/s, 2) underlain by a 2- to 30-m-thick unit with a 1,500 m/s velocity, and (3) the basal 20- to 60-m-thick slide layer with a velocity of 2,300 m/s overlying bedrock (fig. 4). The seismic velocity and thickness of layer 1 suggest it is a loose, aerated (weathered) soil (Clark, 1966); the ease of planting geophones and digging shotholes in this layer confirmed its relatively loose texture. The seismic velocity of layer 2 suggests that it is a saturated, unconsolidated unit (Clark, 1966) whose top may represent the water-table surface. The velocity of layer 3 is consistent with that of a firm clay (Clark, 1966), and layer 3 could be a more consolidated form of layer 2 or a separate, older slide deposit. These internal layers were not detected by the reflection method.

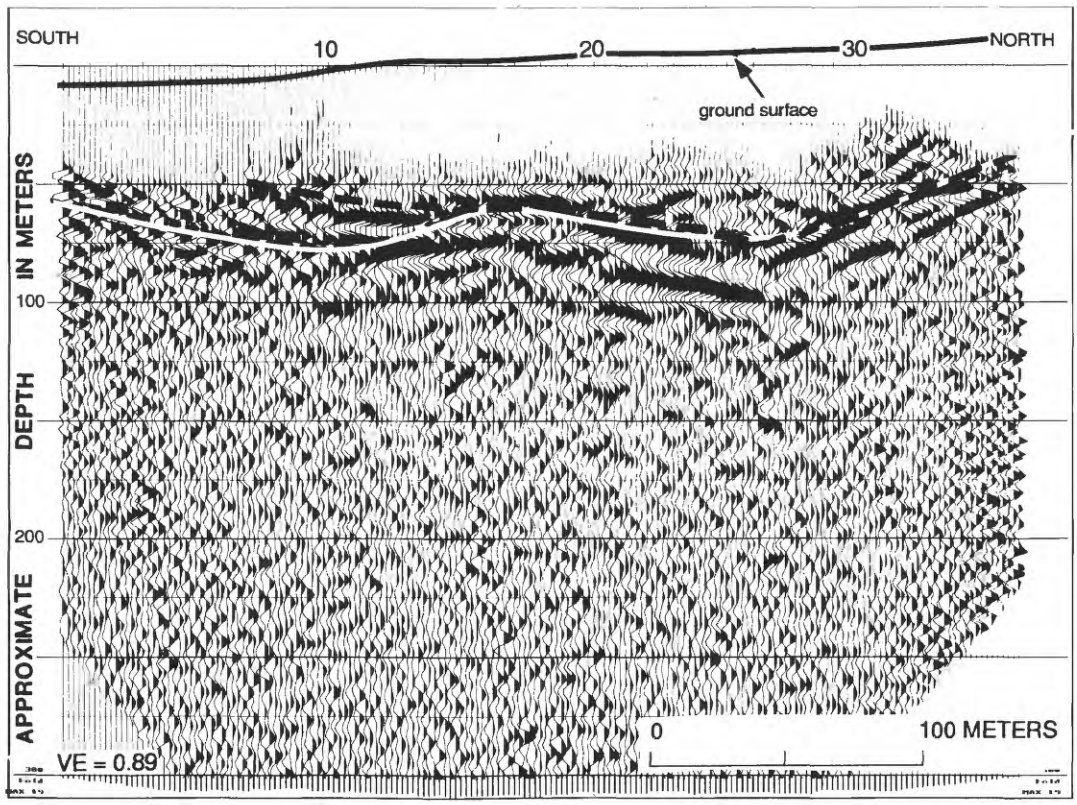

Figure 5. Stacked reflection profile depth section showing the main bedrock reflection (dashed horizon) and one overlying reflection. Position of preferred bedrock refraction model from figure 4 is shown as white line. Vertical exaggeration (VE) is 0.89.

We estimated S-wave (shear-wave) velocities, in a fashion similar to Nazarian and Stokoe (1984), from surface waves recorded on the P-wave seismic reflection records. Generally, the penetration depth of surface waves is about 1 or 2 wavelengths (Ballard, 1964). For the surface waves recorded in the refraction and reflection surveys, the penetration depth is as much as 25 m. The surface waves were identified on the P-wave common-shot records by their high-amplitude, dispersed wave train, and low speed (fig. 3). In this study, we have assumed the shear-wave velocity to be 10 percent greater than the surface-wave group velocity; empirical studies show that the surface wave velocity is generally 10 percent slower (Ballard, 1964; R. Williams, unpub. data, 1994). By this approach, we found two distinct S-wave velocity layers: from 0- to 5-m depth, surface waves recorded on the shotgun reflection data with a period of 0.03 s correspond to a S-wave velocity of 200 m/s, whereas surface waves recorded on the refraction data with a 0.05 s period correspond to a depth of 5–25 m with a S-wave velocity of 400 m/s.

CONCLUSIONS

The principal finding of this study is that the contact between slide and non-slide material is easily detectable by seismic reflection or refraction methods. The 5.4 km/s seismic velocity and the local geology suggest that the rock underlying the slide is a densely welded tuff. From the reflection and refraction data, the pre-landslide valley appears to be broadly U-shaped with a maximum depth of about 95 m. Three seismic velocity layers were detected within the slide by seismic refraction methods: a thin weathered layer at the surface, underlain by saturated unconsolidated material, and a more consolidated basal layer that makes up the majority of the slide. Shear-wave velocities calculated from recorded surface waves range from 200–400 m/s in the upper 25 m of the slide. Finally, the subsurface data described in this paper show how geotechnical sampling and testing of slide material at the surface would not be representative of the majority of the slide material.

ACKNOWLEDGMENTS

William Z. Savage and William K. Smith surveyed the seismic station locations and reduced that data. Philip S. Powers provided us with the map of our seismic line (used for fig. 1) on the base topography.

REFERENCES CITED

Ballard, R.F., 1964, Determination of soil shear modulus at depth by in situ vibratory techniques: U.S. Army Waterways Experiment Station, Miscellaneous Paper No. 4-691.

Clark, S., ed., 1966, Handbook of Physical Constants: Geological Society of America, Memoir 97, 587 p.

Dobrin, M.B., 1976, Introduction to Geophysical Prospecting: McGraw-Hill, 630 p.

Lipman, P.W., 1976, Geologic map of the Lake City caldera area, western San Juan Mountains, southwestern Colorado: U.S. Geological Survey Miscellaneous Investigations Series Map I–962.

Mayne, W.H., 1962, Common reflection point horizontal data stacking techniques: Geophysics, v. 27, no. 6, pt. 2 (supp.), p. 927–938.

Nazarian, S., and Stokoe, K.H., 1984, In situ shear wave velocities from spectral analysis of surface waves: Proceedings, 8th World Conference on Earthquake Engineering, v. 3, p. 31–38.

Pakiser, L.C., and Black, R.A., 1957, Exploring for ancient channels with the refraction seismograph: Geophysics, v. 22, no. 1, p. 32–47.

Parise, M., and Guzzi, R., 1992, Volume and shape of the active and inactive parts of the Slumgullion landslide, Hinsdale County, Colorado: U.S. Geological Survey Open-File Report 92-216.

Scott, J.H., Tibbets, B.L., and Burdick, R.G., 1972, Computer analysis of seismic refraction data: Geophysics, v. 38, no. 2, p. 271–284.

Widess, M.B., 1973, How thin is a thin bed?: Geophysics, v. 38, p. 1176–1180.

Yilmaz, O., 1987, Seismic Data Processing: S.M. Doherty, ed.: Tulsa, Oklahoma, Society of Exploration Geophysicists, 526 p.

CHAPTER 14

SLIDEQUAKES AND FAULT CREEP AT THE SLUMGULLION LANDSLIDE: AN ANALOG TO CRUSTAL TECTONICS

By Joan S. Gomberg, Paul W. Bodin, William Z. Savage, *and* Michael E. Jackson

INTRODUCTION

Fleming and Johnson (1989) noted that structures observed on certain types of landslides are strikingly similar to those associated with crustal-scale tectonics (fig. 1). This surficial similarity suggests the hypothesis that some landslides may provide useful analogs for the study of processes involved in crustal-scale tectonics, thus bridging the gap between laboratory experiments and regional field studies. We present observations of geomorphic and geophysical expressions of landslide faulting that support this hypothesis. The benefits of landslides as models are evident in the fact that much of the data presented was collected within a week on the Slumgullion landslide using conventional geophysical instrumentation from an area spanning less than 0.5 km^2. These results, in addition to further demonstrating the analogous behavior of landslide and crustal faulting, suggest several new opportunities for monitoring and evaluating landslide deformation and the hazards that landslides pose.

This experiment was designed to observe indicators of slide rheology and modes of deformation. In particular, we hoped to determine (1) if the displacement of landslide material, which had previously been observed to occur primarily along faults in and bounding the landslide (Crandell and Varnes, 1961), occurs along discrete or distributed shear zones; (2) whether landslide fault-slip occurs seismically or as aseismic fault creep; if slidequakes exist (indicating brittle failure), then (3) how does the rate and distribution of seismicity and creep correlate with the rate of fault slip?

To address these questions, during the period June 22–28, 1993, we deployed and operated a buried, digital, high-precision creepmeter and a portable seismic network in the vicinity of one of the major strike-slip faults bounding the Slumgullion landslide. Relative velocity vectors were also measured using Global Positioning System (GPS) methods. Measurements made over several months included creep observations from a modified tide-gauge used as a wire extensometer and from the displacement field in a grid of stakes placed across the fault. Both sets of measurements were made in the same region covered by the seismic network (fig. 2). Herein, the seismic, creep, and stake-grid measurements and their implications are summarized. GPS measurements and implications are summarized in chapter 15.

GEODETIC OBSERVATIONS

The displacement of the stake grid shows that deformation in the immediate vicinity of the slide-bounding strike-slip fault occurs as block motion (fig. 3*A*). Essentially rigid-block motion is also observed across segments of crustal strike-slip faults (fig. 3*B*), the San Andreas and Calaveras faults, which accommodate plate motions principally by continuous creep (fig. 4 in Savage and Burford, 1971; Lisowski and others, 1991).

SEISMIC OBSERVATIONS

Results of analyses of portable seismic network data suggest that slidequakes exist at the Slumgullion landslide and are detectable with conventional instruments. Slidequakes are evidenced by short duration, spatially and temporally clustered signals (fig. 4*A*), with sources that most probably occurred on the slide-bounding strike-slip faults (fig. 5). The seismic network that recorded these slidequakes included four analog seismographs and a phased digital micro-array. The analog seismographs operated with single-component sensors synchronized daily to radio-broadcasted time. Drift rates of the analog seismographs' internal clocks were insignificant relative to the precision with which seismic phases could be timed. Inside the analog network and crossing the slide-bounding fault, a phased digital micro-array contained three single-component sensors spaced at 50 m from a central three-component set of sensors (fig. 2). The digital signals were recorded on a single seismograph

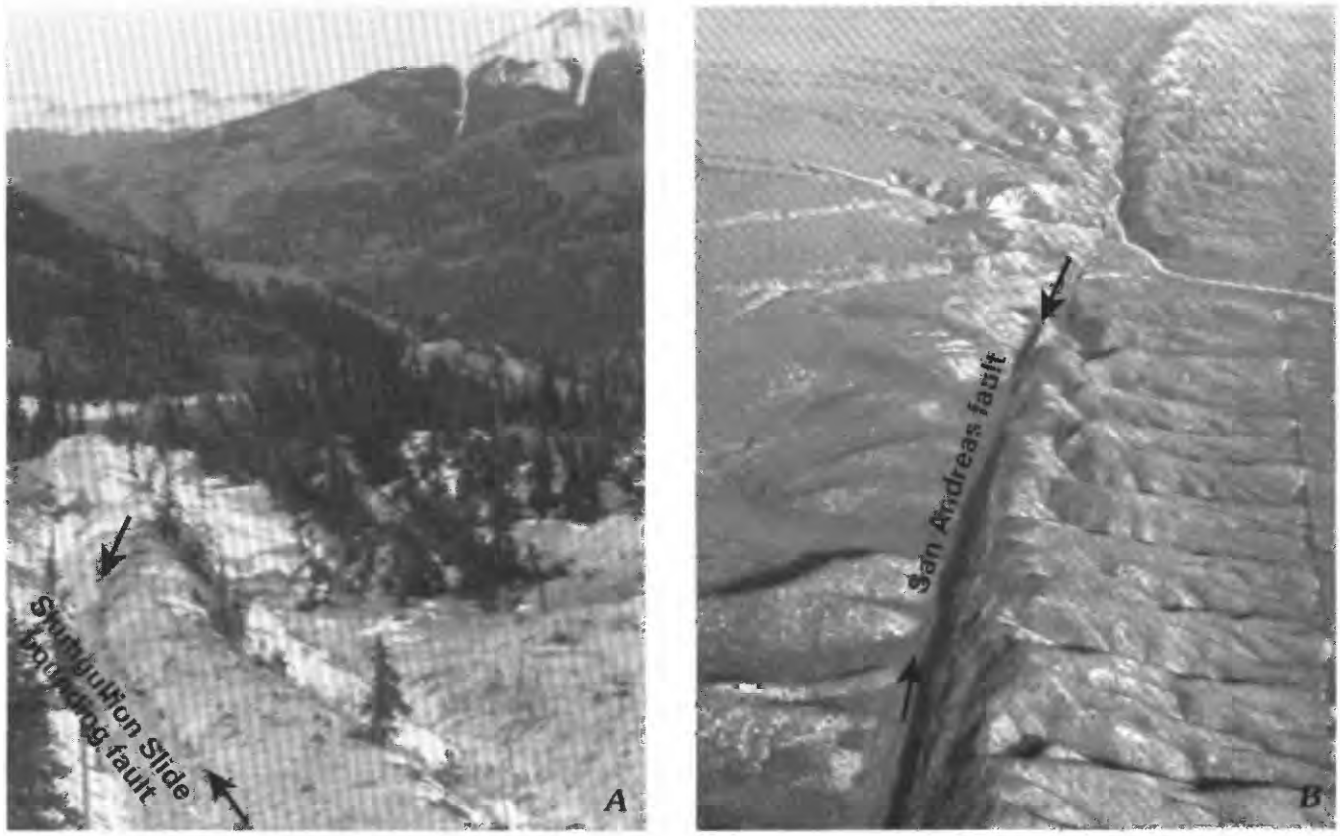

Figure 1. *A*, View looking along the trend (indicated by arrows) of a slide-bounding strike-slip fault on the Slumgullion landslide in Colorado. The ridges parallel and adjacent to the fault, often called levees, are composed of unconsolidated, highly dilated sandy soil. *B*, View along the trend of the strike-slip San Andreas fault in the Carizzo Plains of California. Note the similarity between the adjacent ridges, often attributed to differential erosion of fault and surrounding material, and the levees of the Slumgullion. We suggest that such structures are common to strike-slip faults of all scales, but, because of the slower slip rates along crustal faults, the levee formation is overtaken by more rapid erosion.

synchronized continuously to radio-broadcasted time. The relative arrival times at each station for 13 of the best recorded slidequakes show that they originated in essentially the same location. We were therefore able to treat them as one event, with little loss of information, and used the average relative arrival times to determine the approximate location of the events. The non-impulsive phase onsets and slightly dispersed wavetrains of these signals and ray-tracing analyses indicated that the observed signals were surface waves. Hypocenter estimation requires knowledge of the seismic velocity structure. Arrival times measured for P-waves and S-waves on seismograms of four explosions guided trial-and-error ray-tracing to estimate the velocity structure. The resultant P-wave and S-wave velocities indicate that the Poisson's ratio within the slide is approximately 0.49. Such a high value is consistent with models of slide deformation in which the slide material behaves plastically on some time scales (Savage and Smith, 1986).

Long duration, sinusoidal-like signals were also observed (fig. 4*B*). These signals may originate from slide-generated sources, but their generation by non-natural sources, such as traffic, cannot be ruled out. The very emergent onset of these signals makes timing of their onsets and estimating their hypocenters extremely difficult. Although they were observed most commonly at stations closest to traffic, in several instances the most distant stations recorded the largest amplitudes. The frequency of occurrence of these signals and time-of-day did not clearly correlate, and thus their association with traffic was ambiguous (traffic was relatively minimal during the night). Several sources may give rise to these monochromatic signals, some natural and from the slide and others man-made. Possible sources include slow rupture of faults or materials entrained within the faults (e.g., trees, boulders), or slow basal slip along the slide-bedrock interface.

Figure 5 shows a map-view distribution of seismic-source-location probability confidence levels at the ground surface. The most probable location of slidequakes is seen to occur in the vicinity of the southern slide-bounding strike-slip fault.

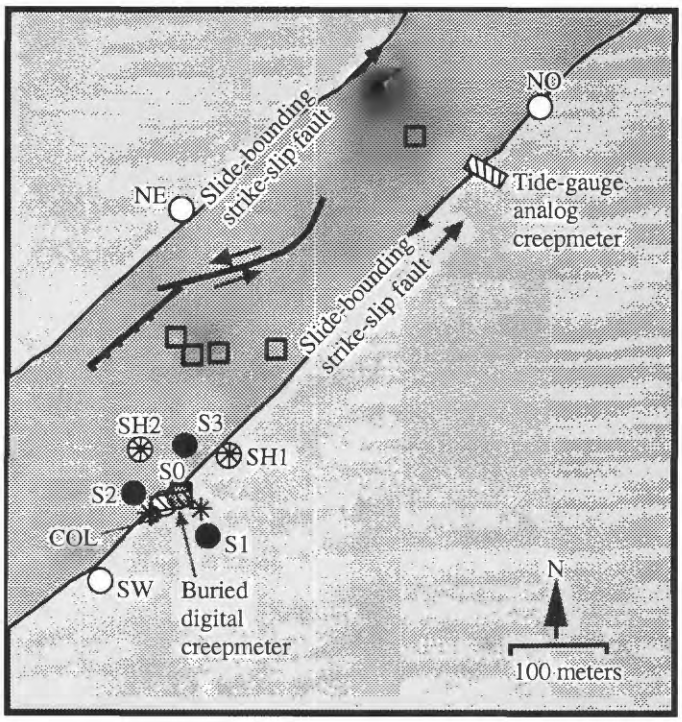

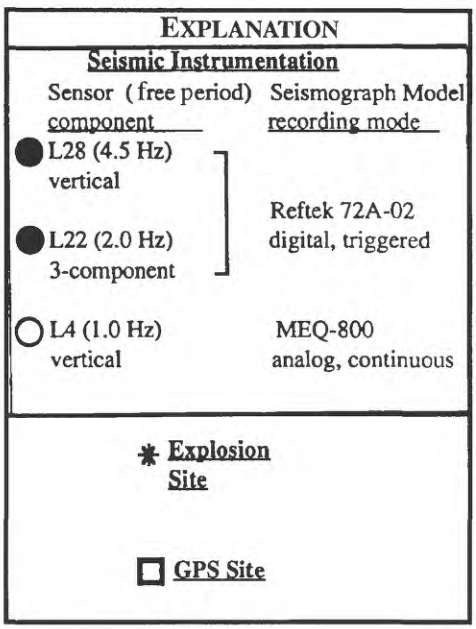

Figure 2. Schematic map of the central part of the Slumgullion landslide, the seismic network (station codes labeled), creepmeters, and GPS observation points (points near the main scarp and on the toe are not shown). These instruments were located to monitor one of the major slide-bounding strike-slip faults where the displacement rate of the slide mass is greatest (approximately 1.6 cm/day). Major mapped faults (normal = hatchured line, strike-slip = solid line with arrows) within the slide are also shown. Four explosions (asterisks) were made and recorded to constrain the velocity structure. The main scarp is to the upper right of the figure.

CREEP OBSERVATIONS

Creep observations presented by Savage and Fleming (this volume) for the Slumgullion landslide's south-bounding strike-slip fault show seasonal variations around a steady rate of approximately 1.5 cm/day (fig. 6*A*). We note that the creeping section of the San Andreas fault also exhibits seasonal variations (fig. 6*B*). The change in slope in both cases corresponds to increased climatic moisture: fall rains along the San Andreas fault and the spring snow melt on the Slumgullion landslide. Moreover, "creep events" were recorded that were triggered by explosions set off several tens of meters from the fault (fig. 6*D*). These explosions were used to calibrate the velocity structure for the seismic data analysis. It was not possible to assess whether these triggered creep events were seismogenic because their signals would be obscured by those generated by the explosions. Creep events triggered by earthquakes (fig. 6*C*) have been documented along the San Andreas fault but are not well understood (Bodin and others, 1994). The observation that creep events can actually be created along the landslide fault suggests future controlled experiments of triggered creep. Both the observation of slidequake signals and of triggered creep events implies that, at least on short time scales, the landslide material behaves elastically, storing and releasing elastic strain energy.

DISCUSSION

Our results illustrate that probable slidequakes can be recorded using conventional instrumentation and simple installations. Slidequakes may occur more frequently than our observations indicate because the small amplitudes of the slidequake signals were barely discernible above the background noise and only during periods of no wind (the roots of swaying trees and shrubs generate seismic signals). Their abundance could be more accurately characterized by use of sensors that have a broader frequency range (slidequakes may emit seismic waves with frequencies outside the range of the recording instruments) and that were buried deeper to reduce wind-generated noise.

Although the measurements only spanned a short time on a single landslide, analytical results suggest that landslide deformation occurring along the slide-bounding fault is analogous to creeping crustal faults. In particular, an analogy can be drawn to the San Andreas fault zone because it is the only fault in which both creep and seismicity are well documented. A segment of the San Andreas fault zone between San Juan Bautista and Cholame creeps at the fault's long-term slip rate (Savage and Burford, 1971), indicating that accumulating strain is continuously relieved almost completely by steady-state slip. In addition to a nearly constant

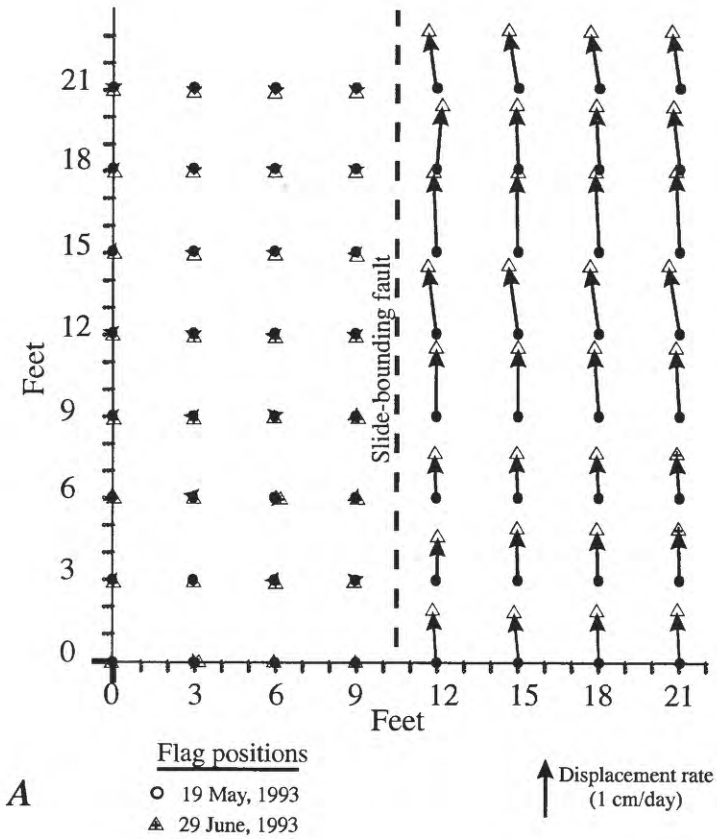

A

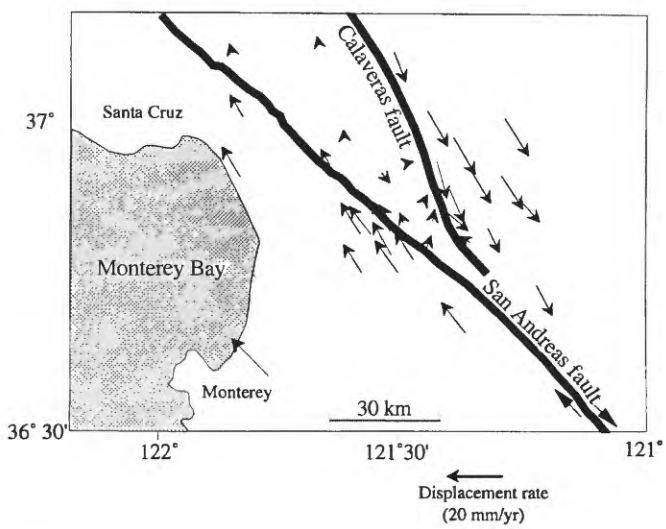

B

slip rate, this creeping section of the San Andreas also exhibits a high rate of small-magnitude seismicity. The relationship between the production of small earthquakes and creep is not well understood. Observations of creep and seismicity probably associated with slip along the landslide's strike-slip fault suggest that similar processes may be operative on both the Slumgullion and San Andreas faults. The accessibility in three dimensions and the potential to do controlled experiments (e.g., to create creep or seismic events) along the landslide fault make it an ideal natural laboratory for study of crustal faults. Moderate earthquakes have ruptured through creeping sections of the San Andreas fault, and the possibility that larger slidequakes may also occur and (or) that other sections of the landslide fault exhibit differing behaviors cannot be dismissed.

CONCLUSIONS

We have demonstrated that quantitative measures of landslide deformation, such as seismic, geodetic, and creep observations, can be made in a short time with readily available instrumentation. Comparison of these observations to those recorded near crustal faults that require more complex instrumentation deployed for much longer time periods, suggests that much could be learned from future studies of landslide faulting. Our results indicate that the displacement of landslide material appears to occur along discrete faults exhibiting a combination of brittle failure (evidenced by slidequakes and creep events) and stable sliding. The manner in which the rate and distribution of seismicity and creep correlate with fault-slip rate remains to be determined in future experiments.

Figure 3. *A*, Displacement vectors (relative to the point at 0,0) measured for a grid of stakes spanning a slide-bounding strike-slip fault of the Slumgullion landslide. Small differences in flag positions on the left are caused by measurement error. The grid was located several meters up the landslide from the digital creepmeter (fig. 2). *B*, Velocity vectors inferred from geodetic networks spanning the creeping segments of the San Andreas and Calaveras faults (from fig. 6 of Lisowski and others, 1991). The velocities indicate motion relative to the "center of mass" of the network (Lisowski and others, 1991).

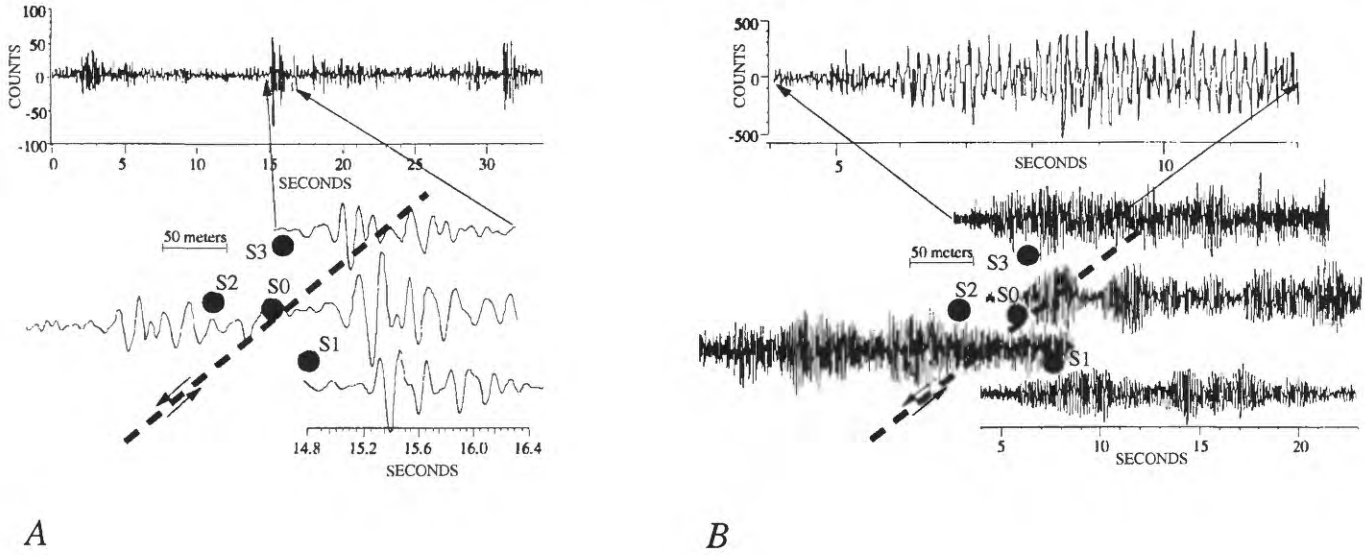

Figure 4. Seismic ground motions recorded on the Slumgullion landslide. All traces shown were recorded by the digital microarray and are plotted on the same amplitude and time scales. Only vertical-component seismograms are shown, each was recorded by the sensor denoted by the nearest corresponding shaded circle (sensors are shown in "map view" similar to that shown in fig. 2; 50-m scale bar refers to map view of sensors). The top trace spans a longer duration and includes the segment shown from sensor S3. *A*, Seismograms of probable slidequakes. *B*, Sinusoidal-like seismograms.

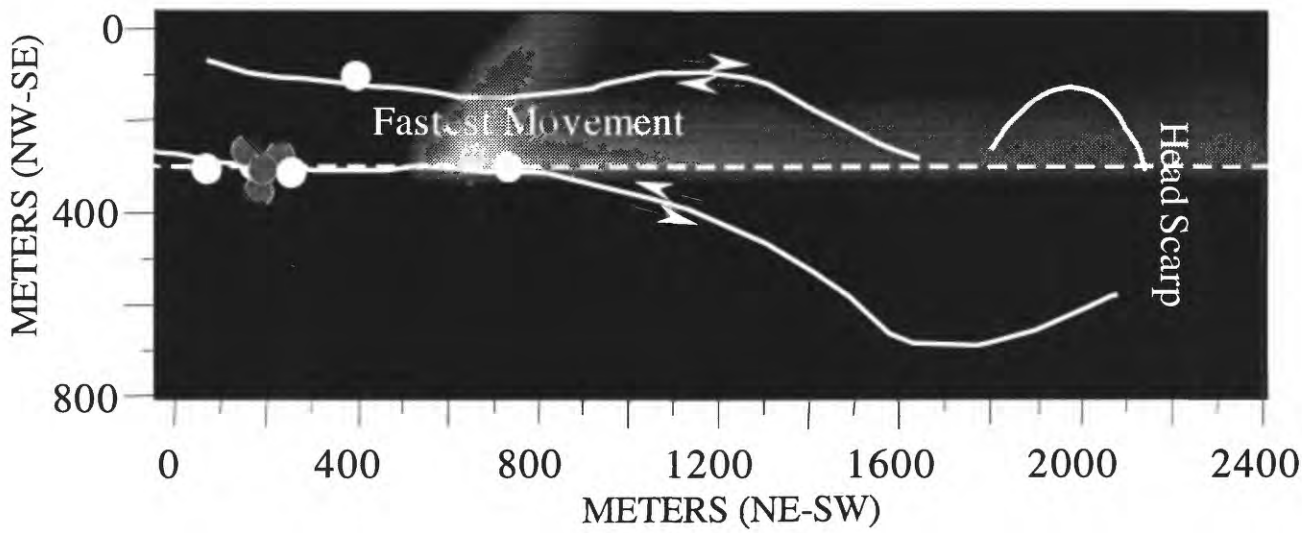

Figure 5. A map-view distribution of slidequake source location probability confidence levels at the ground surface (denoted by shading; the whitest shading indicates the most probable location). We assume a velocity structure that varies only in the lateral direction and that observed signals are surface waves traveling along straight-line trajectories between the source and seismic station. The shear (or group) velocity northwest of the dashed line is 0.286 km/sec and is 3.600 km/sec to the southeast. Circles indicate seismic stations (white, analog; gray, digital), and the white curved lines delineate the outline of the active slide. The distribution of probability confidence levels is calculated using a grid-search algorithm (Tarantola and Valette, 1982; Gomberg and others, 1989). The validity of the model and location algorithm is demonstrated by locating four explosions, and noting that their true locations are within their respective 90 percent confidence intervals, with the most probable locations being in error by <30 m. Results are insensitive to reasonable changes in model velocities.

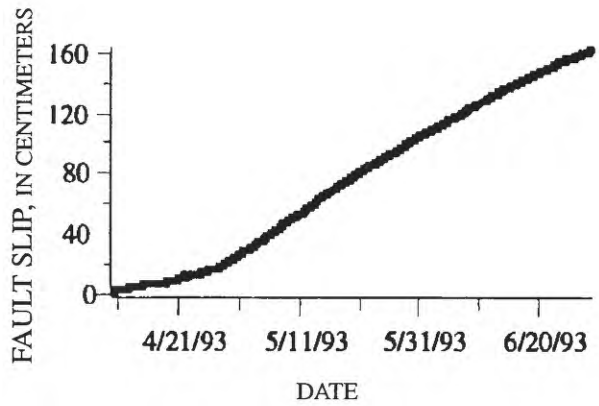

A

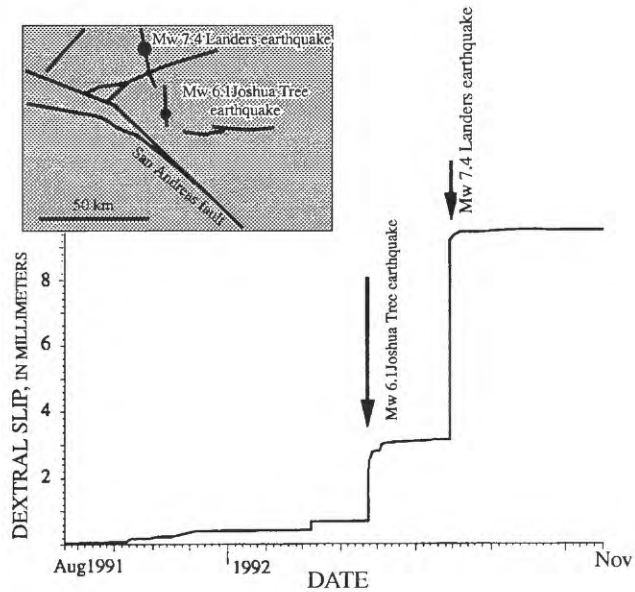

C

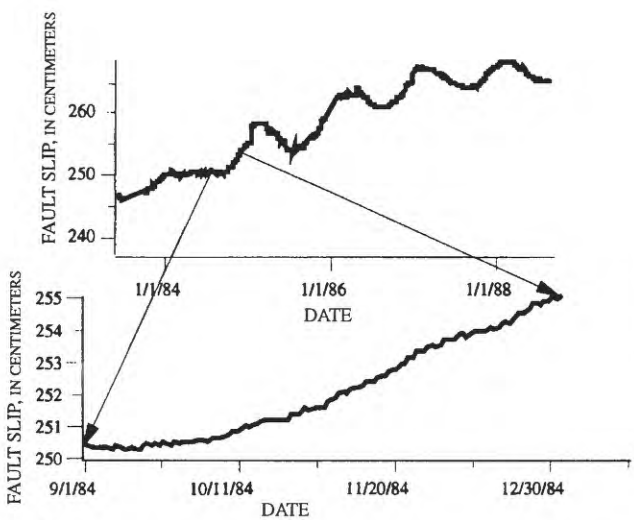

B

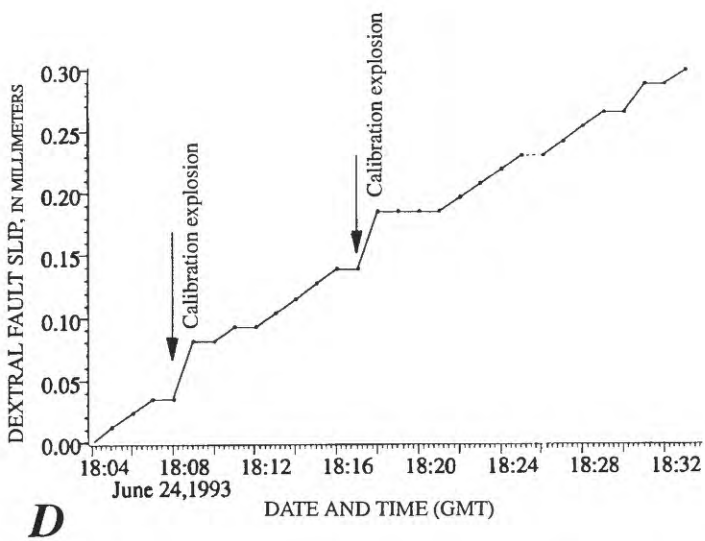

D

Figure 6. *A*, Seasonally varying creep measured on a slide-bounding strike-slip fault at the Slumgullion landslide. *B*, Seasonally varying creep measured across the San Andreas fault. *C*, Creep events induced by earthquakes near the San Andreas fault. *D*, Creep events on a slide-bounding strike-slip fault induced by explosions at the Slumgullion landslide.

ACKNOWLEDGMENTS

The authors thank M. Meremonte, E. Cranswick, T. Bice, D. Overturf, P. Powers, T. Pratt, R. Williams, and J. Savage for their assistance in the field experiment and B. Kindel for his help in analyzing the seismic data.

REFERENCES CITED

Bodin, P.W., Bilham, R., Behr, J., Gomberg, J.S., and Hudnut, K.W., 1994, Slip triggered on southern California faults by the 1992 Joshua Tree, Landers, and Big Bear earthquakes: Seismological Society of America Bulletin, v. 84, no. 3, p. 806–816.

Crandell, D.R., and Varnes, D.J. 1961, Movement of the Slumgullion earthflow near Lake City, Colorado, *in* Short Papers in the Geologic and Hydrologic Sciences: U.S. Geological Survey Professional Paper 424–B, p. B136–B139.

Fleming R.W., and Johnson, A.M., 1989, Structures associated with strike-slip faults that bound landslide elements: Engineering Geology, v. 27, p. 39–114.

Gomberg, J.S., Shedlock, K. M., and Roecker, S., 1989, The effect of S wave arrival times on the accuracy of hypocenter estimation: Seismological Society of America Bulletin, v. 80, p. 1605–1628.

Lisowski, M., Savage, J.C. and Prescott, W.H., 1991, The velocity field along the San Andreas fault in central and southern California: Journal of Geophysical Research, v. 96, p. 8369–8391.

Savage, J.C., and Burford, R.O., 1971, Discussion of paper by C.H. Scholz and T.J. Fitch, "Strain accumulation along the San Andreas Fault:" Journal of Geophysical Reearch, v. 76, p. 6469–6479.

Savage, W.Z., and Smith, W.K., 1986, A model for the plastic flow of landslides: U.S. Geological Survey Professional Paper 138–S, 32 p.

Tarantola, A., and Valette, B., 1982, Inverse problems = Quest for information: Journal of Geophysics, v. 50, p. 159–170.

CHAPTER 15

MEASUREMENT OF LOCAL HORIZONTAL VELOCITIES ON THE SLUMGULLION LANDSLIDE USING THE GLOBAL POSITIONING SYSTEM

By Michael E. Jackson, Paul W. Bodin, William Z. Savage, *and* Elizabeth M. Nel

INTRODUCTION

Determination of landslide velocity fields has traditionally relied on cadastral survey techniques, which require multi-year surveys (Varnes and others, 1993). A recent experiment on the Slumgullion landslide suggests that the rate of change of high precision Global Positioning System (GPS) coordinates can be used to determine slide velocities within 10 percent on a time scale of a few days.

The presently active part of the Slumgullion landslide has apparently been moving for the last 300 yr (Crandell and Varnes, 1961; Varnes and others, 1993). Traditional control surveys conducted during the past 35 yr suggest that the narrow middle part and toe of the active slide are moving at average velocities of approximately 1.6 cm/day, and 0.4 cm/day, respectively.

INTRODUCTION TO GPS GEODESY

The Global Positioning System is a constellation of 24 Department of Defense satellites orbiting at ≅ 21,000 km above the Earth. The satellites transmit precisely timed radio signals (pseudo-random codes called C/A and P-codes, and sine/cosine-shaped carrier phase signals called the L1 and L2 carrier) to ground-based receivers. In this study, both the L1 and L2 carrier phase data (L1 and L2 carrier phase are radio-frequency signals transmitted at 1,575.42 MHz, wavelength (λ) ≅ 20 cm; and 1,227.60 MHz, λ ≅ 25 cm, respectively) are used to attain the highest measurement precision possible. GPS satellites and receivers are equipped with precise clocks, and, by comparing the time of GPS signal reception with the time of transmission and multiplying this difference by the speed of light, the distance between the satellite and receiver is calculated. Simultaneous measurement to four satellites is required to solve for the receivers' latitude, longitude, and height. Repeating these measurements over discrete time intervals allows the change in station coordinates with time to be determined to a high degree of precision.

For high-precision work, the time of flight of the radio signals needs to be corrected for small offsets in the satellite and receiver clocks. This is accomplished by post-processing simultaneous GPS data from a minimum of two ground receivers. Satellite clock errors are removed by combining the data from two receivers that have the same satellites in view (this is called a single-difference calculation). Because the satellite clock error is common to both receivers, combining the data eliminates that error. Similarly, receiver clock errors are removed by combining two single-difference data files for two satellite pairs. In this case, the receiver clock errors are common in both single-difference files, and the combination removes the receiver clock error. Combinations of the L1 and L2 signals are, in turn, used to remove the distortion encountered as the GPS signal passes through the ionosphere. As previously mentioned, the L1 and L2 signals are each shaped like a continuous sine/cosine function. Therefore, any break in the continuous wave train impedes the ability to correctly calculate the distance between the satellite and the receiver. A further combination of the L1 and L2 carrier phase data, called the wide-lane combination, helps in recovering the distance using the carrier phase data.

GPS OBSERVATIONS

A GPS survey was initiated in June 1993 to determine if satellite geodesy can rapidly map the slide velocity field, describe the spatial and temporal distribution of velocity, and determine whether the inactive slide is moving relative to a stable bench mark well off the slide. A total of seven GPS stations (baselines < 5 km) were installed: five on the active slide, one on the inactive slide, and one on the stable portion near the slide main scarp (fig. 1).

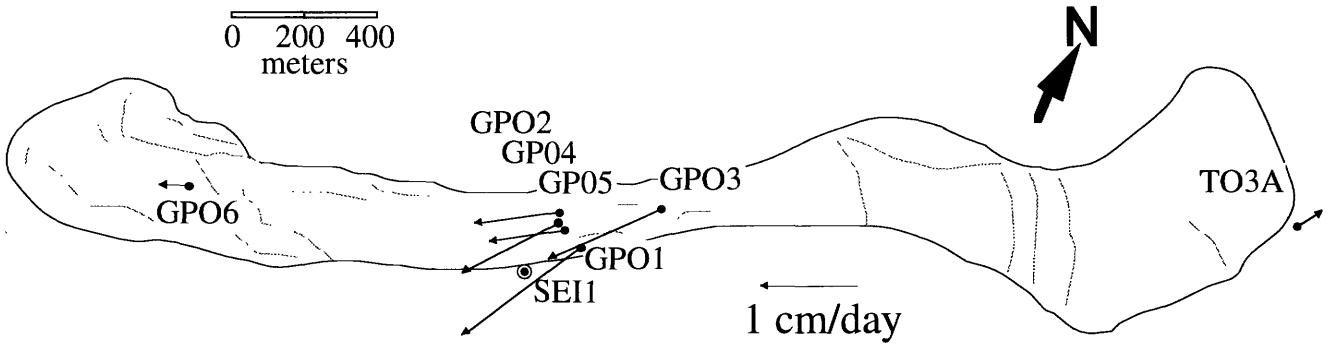

Figure 1. Location of GPS stations on the Slumgullion landslide and bench-mark velocities calculated during a 4-day measurement period. The coordinates of station SEI1 are held fixed relative to the rest of the network. Stations SEI1 and T03A are thought to be located on the inactive portion of the slide. Velocity measurement errors (table 1) suggest the motion of station T03A may be within the measurement noise. Dotted lines indicate the location of major structural elements on the landslide.

Station bench marks consist of 1-m sections of capped steel pipe driven flush with the landslide surface. The stations were occupied with Trimble 4000 SST, 8-channel, dual-frequency phase and C/A code receivers, which observed all satellites above a 15° horizon. Each station was measured for at least two, 4- to 6-hour sessions with most stations being occupied for four, 4- to 6-hour sessions. The baseline between stations SEI1, which is assumed to be stable, and GP01, located on the fastest moving portion of the active slide, was measured for a total of nine consecutive 4- to 6-hour sessions. Relative coordinates for the network were carried from the Pietown fiducial tracking site in northern New Mexico to a reference station (SEI1—lat 37°59′29.3392″N.; long 107°15′19.6388″ W., HAE (height above ellipsoid) 3,157.98 m) in the landslide network to a precision of 3, 3.5, and 5 cm in the north, east, and up components, respectively.

Table 1. Slumgullion bench-mark velocities.

[Displacement uncertainties based on repeatability studies on baselines of similar length]

Station	Velocity (cm/day)
SEI1	Fixed
GP01	1.5±0.3
GP02	0.9±0.4
GP03	1.3±0.2
GP05	1.2±0.3
TO3A	0.3±0.2
GP06	0.4±0.2

GPS DATA PROCESSING

The GPS data were analyzed with software designed for high-accuracy geodetic surveys. Precise GPS satellite orbits, with an estimated error of approximately 0.01 ppm, provided by Scripps Institute of Oceanography (Bock and others, 1993) were used to establish the Slumgullion GPS network within the geodetic reference frame. The coordinates of station SEI1 were held fixed, and single differences between network stations were formed to remove satellite and receiver clock errors. The single-difference files were preprocessed to fix carrier phase cycle slips or breaks in the carrier phase data caused by obstructions between satellites and receivers. Trees on the landslide often blocked the GPS signal, particularly at low satellite elevation angles (15°–30°) and caused frequent, but repairable, cycle slips. Double difference combinations were then formed to estimate phase integer ambiguities in the L1 and L2 signals. Once station ambiguities were resolved, station coordinates were estimated relative to station SEI1 using the L1, L2, and L3 (ionosphere-free) double-difference phase combinations. Because the baseline distances on the landslide were short, the ionosphere bias was negligible between stations and there was no significant difference between the L1 and L3 coordinate solutions within the measurement uncertainties. Landslide bench-mark displacements were calculated by comparing successive L1-frequency coordinate solutions for each station while assuming no movement of station SEI1. The cumulative displacements at each station and the time interval between measurements were used to calculate bench mark velocities.

RESULTS

Figure 1 shows velocities of bench marks determined during a 4-day measurement period. The motion of station T03A, which is in the inactive portion of the landslide and near the slide main scarp, may be caused by monument instability. Table 1 and figure 1 show that stations in the center of the active slide are moving at velocities of 1.2–1.5 cm/day.

These GPS-determined velocities are similar to slide velocities determined from traditional surveys (Crandell and Varnes, 1961), creepmeter measurements (Savage and Fleming, this volume; Bodin and others, 1993, Gomberg and others, this volume), and photogrammetric methods (Smith, 1993, this volume; Powers and Chiarle, this volume).

REFERENCES CITED

Bock, Y., Agnew, D. C., Fang, P., Genrich, J. F., Hagar, B. H., Herring, T. A., Hudnut, K.W., King, R.W., Larson, S. L., Minster, J. B. and others, 1993, Detection of crustal deformation from the Landers earthquake sequence using continuous geodetic measurements: Nature, v. 361, p. 337–340.

Bodin, P.W., Savage, W.Z., Gomberg, J.S., and Jackson, M.E., 1993, An analog to crustal-scale tectonics?: EOS, Transactions, American Geophysical Union, v. 43, p. 67.

Crandell, D.R. and Varnes, D.J., 1961, Movement of the Slumgullion earthflow near Lake City Colorado, U.S. Geological Survey Research: U.S. Geological Survey Professional Paper 424–B, p. 136–139.

Smith, W.K., 1993, Photogrammetric determination of movement on the Slumgullion Slide, Hinsdale County, Colorado 1985–1990: U.S. Geological Survey Open-File Report 93-597, 17 p., 2 pl.

Varnes, D.J., W.K. Smith, W.Z. Savage, and Varnes, K.L., 1993, Control and deformation surveys at the Slumgullion Slide, Hinsdale County, Colorado—A progress report: U.S. Geological Survey Open File Report, 93-577, 15 p., 1 plate.

Published in the Central Region, Denver, Colorado
Manuscript approved for publication May 2, 1995
Edited by Richard W. Scott, Jr.
Photocomposition and graphics preparation by
Carol A. Quesenberry; use made of author-drafted material

☆ U.S. GOVERNMENT PRINTING OFFICE: 1996 - 774-045 / 20039 REGION NO. 8

SELECTED SERIES OF U.S. GEOLOGICAL SURVEY PUBLICATIONS

Periodicals

Earthquakes & Volcanoes (issued bimonthly).
Preliminary Determination of Epicenters (issued monthly).

Technical Books and Reports

Professional Papers are mainly comprehensive scientific reports of wide and lasting interest and importance to professional scientists and engineers. Included are reports on the results of resource studies and of topographic, hydrologic, and geologic investigations. They also include collections of related papers addressing different aspects of a single scientific topic.

Bulletins contain significant data and interpretations that are of lasting scientific interest but are generally more limited in scope or geographic coverage than Professional Papers. They include the results of resource studies and of geologic and topographic investigations; as well as collections of short papers related to a specific topic.

Water-Supply Papers are comprehensive reports that present significant interpretive results of hydrologic investigations of wide interest to professional geologists, hydrologists, and engineers. The series covers investigations in all phases of hydrology, including hydrology, availability of water, quality of water, and use of water.

Circulars present administrative information or important scientific information of wide popular interest in a format designed for distribution at no cost to the public. Information is usually of short-term interest.

Water-Resources Investigations Reports are papers of an interpretive nature made available to the public outside the formal USGS publications series. Copies are reproduced on request unlike formal USGS publications, and they are also available for public inspection at depositories indicated in USGS catalogs.

Open-File Reports include unpublished manuscript reports, maps, and other material that are made available for public consultation at depositories. They are a nonpermanent form of publication that may be cited in other publications as sources of information.

Maps

Geologic Quadrangle Maps are multicolor geologic maps on topographic bases in 7 1/2- or 15-minute quadrangle formats (scales mainly 1:24,000 or 1:62,500) showing bedrock, surficial, or engineering geology. Maps generally include brief texts; some maps include structure and columnar sections only.

Geophysical Investigations Maps are on topographic or planimetric bases at various scales, they show results of surveys using geophysical techniques, such as gravity, magnetic, seismic, or radioactivity, which reflect subsurface structures that are of economic or geologic significance. Many maps include correlations with the geology.

Miscellaneous Investigations Series Maps are on planimetric or topographic bases of regular and irregular areas at various scales; they present a wide variety of format and subject matter. The series also includes 7 1/2-minute quadrangle photogeologic maps on planimetric bases which show geology as interpreted from aerial photographs. The series also includes maps of Mars and the Moon.

Coal Investigations Maps are geologic maps on topographic or planimetric bases at various scales showing bedrock or surficial geology, stratigraphy, and structural relations in certain coal-resource areas.

Oil and Gas Investigations Charts show stratigraphic information for certain oil and gas fields and other areas having petroleum potential.

Miscellaneous Field Studies Maps are multicolor or black-and-white maps on topographic or planimetric bases on quadrangle or irregular areas at various scales. Pre-1971 maps show bedrock geology in relation to specific mining or mineral-deposit problems; post-1971 maps are primarily black-and-white maps on various subjects such as environmental studies or wilderness mineral investigations.

Hydrologic Investigations Atlases are multicolored or black-and-white maps on topographic or planimetric bases presenting a wide range of geohydrologic data of both regular and irregular areas; the principal scale is 1:24,000, and regional studies are at 1:250,000 scale or smaller.

Catalogs

Permanent catalogs, as well as some others, giving comprehensive listings of U.S. Geological Survey publications are available under the conditions indicated below from USGS Map Distribution, Box 25286, Building 810, Denver Federal Center, Denver, CO 80225. (See latest Price and Availability List.)

"Publications of the Geological Survey, 1879-1961" may be purchased by mail and over the counter in paperback book form and as a set microfiche.

"Publications of the Geological Survey, 1962-1970" may be purchased by mail and over the counter in paperback book form and as a set of microfiche.

"Publications of the U.S. Geological Survey, 1971-1981" may be purchased by mail and over the counter in paperback book form (two volumes, publications listing and index) and as a set of microfiche.

Supplements for 1982, 1983, 1984, 1985, 1986, and for subsequent years since the last permanent catalog may be purchased by mail and over the counter in paperback book form.

State catalogs, "List of U.S. Geological Survey Geologic and Water-Supply Reports and Maps For (State)," may be purchased by mail and over the counter in paperback booklet form only.

"Price and Availability List of U.S. Geological Survey Publications," issued annually, is available free of charge in paperback booklet form only.

Selected copies of a monthly catalog "New Publications of the U.S. Geological Survey" is available free of charge by mail or may be obtained over the counter in paperback booklet form only. Those wishing a free subscription to the monthly catalog "New Publications of the U.S. Geological Survey" should write to the U.S. Geological Survey, 582 National Center, Reston, VA 22092.

Note.–Prices of Government publications listed in older catalogs, announcements, and publications may be incorrect. Therefore, the prices charged may differ from the prices in catalogs, announcements, and publications.